

Dissertation zur Erlangung des Doktorgrades der  
Naturwissenschaften der Fakultät für Biologie der  
Ludwig-Maximilians-Universität München

**Dasm1 - a molecule important for the development  
of inhibitory contacts**

vorgelegt von

Matthias H. Traut

München, den 15. Juli 2010





Erstgutachter: Prof. Dr. Rüdiger Klein

Zweitgutachter: PD Dr. Lars Kunz

Drittgutachter: Prof. Dr. Hans Straka

Viertgutachter: Prof. Dr. Andreas Herz

Fünftgutachter: Prof. Dr. Rainer Uhl

Sechstgutachter: Prof. Dr. Wilfried Gabriel

Tag der mündlichen Prüfung: 15.09.2010



*Dedicated to my family.*



Die vorliegende Arbeit wurde zwischen Dezember 2006 und Juli 2010 unter der Leitung von Prof. Dr. Rüdiger Klein und Dr. Valentin Stein am Max-Planck-Institut für Neurobiologie in Martinsried durchgeführt.



**Ehrenwörtliche Versicherung:**

Ich versichere hiermit ehrenwörtlich, dass ich die Dissertation mit dem Titel "Dasm1 - a molecule important for the development of inhibitory contacts" selbständig und ohne unerlaubte Beihilfe angefertigt habe. Ich habe mich dabei keiner anderen als der von mir ausdrücklich bezeichneten Hilfen und Quellen bedient.

**Erklärung:**

Hiermit erkläre ich, dass ich mich nicht anderweitig einer Doktorprüfung ohne Erfolg unterzogen habe. Die Dissertation wurde in ihrer jetzigen oder ähnlichen Form bei keiner anderen Hochschule eingereicht und hat noch keinen sonstigen Prüfungszwecken gedient.

München, den 15. Juli 2010

Matthias H. Traut



# Contents

<b>List of Figures</b>	<b>xiii</b>
<b>List of Tables</b>	<b>xv</b>
<b>1 Zusammenfassung</b>	<b>1</b>
<b>2 Synopsis</b>	<b>5</b>
<b>3 Abbreviations</b>	<b>7</b>
<b>4 Introduction</b>	<b>9</b>
4.1 Cell adhesion molecules . . . . .	10
4.1.1 Immunoglobulin superfamily . . . . .	10
4.1.2 Neurexins-neuroligins . . . . .	13
4.1.3 Cadherins and protocadherins . . . . .	14
4.1.4 Integrins . . . . .	14
4.2 Synaptic transmission and plasticity . . . . .	15
4.2.1 Presynaptic compartment . . . . .	15
4.2.2 Synaptic cleft . . . . .	16
4.2.3 Postsynaptic compartment . . . . .	16
4.2.4 Excitatory synaptic transmission . . . . .	16
4.2.5 Inhibitory synaptic transmission . . . . .	18
4.2.6 Miniature vesicle release . . . . .	19
4.2.7 Synaptic plasticity . . . . .	20
4.3 The hippocampus . . . . .	22
4.3.1 Pyramidal cells . . . . .	23
4.3.2 Granule cells . . . . .	24

4.3.3	Interneurons . . . . .	25
4.4	The immunoglobulin superfamily member 9 and turtle . . . . .	26
4.5	Aim of this study . . . . .	30
<b>5</b>	<b>Material and Methods</b>	<b>31</b>
5.1	Material . . . . .	31
5.1.1	Chemicals . . . . .	31
5.1.2	Media and solutions . . . . .	32
5.2	Methods . . . . .	34
5.2.1	Transgenic Mice . . . . .	34
5.2.2	Genotyping . . . . .	34
5.2.3	Preparation of acute hippocampal slices . . . . .	35
5.2.4	Electrophysiology . . . . .	35
5.2.5	Graphs and statistics . . . . .	41
<b>6</b>	<b>Results</b>	<b>43</b>
6.1	Field excitatory postsynaptic potentials (fEPSPs) . . . . .	43
6.2	Glutamatergic currents . . . . .	43
6.2.1	AMPA/NMDA ratio in <i>Dasm1<sup>-/-</sup></i> and <i>Dasm1<sup>ΔC/ΔC</sup></i> mice . . . . .	44
6.2.2	Miniature excitatory postsynaptic currents (mEPSCs) . . . . .	45
6.2.3	Paired pulse ratio (PPR) of evoked AMPA receptor mediated currents	48
6.2.4	Isolated NMDA receptor mediated fEPSPs . . . . .	48
6.2.5	Isolated decay time constant of NMDA receptors . . . . .	50
6.2.6	Current-voltage relationship (IV) and conductance (G) of the NMDA receptor . . . . .	50
6.3	Field Plasticity Paradigms . . . . .	50
6.3.1	Long term potentiation (LTP) . . . . .	51
6.3.2	Field paired pulse ratio . . . . .	52
6.4	GABAergic system . . . . .	53
6.4.1	Miniature inhibitory postsynaptic currents (mIPSCs) in <i>Dasm1<sup>-/-</sup></i> mice	53
6.4.2	mIPSCs in <i>Dasm1<sup>ΔC/ΔC</sup></i> mice . . . . .	55

6.4.3	Spontaneous inhibitory postsynaptic currents (sIPSCs) in <i>Dasm1</i> <sup>-/-</sup> mice	55
6.4.4	sIPSCs in <i>Dasm1</i> <sup>ΔC/ΔC</sup> mice . . . . .	56
6.4.5	<i>Dasm1</i> is present in hippocampal interneurons . . . . .	58
6.4.6	Number of inhibitory synapses in cultured neurons . . . . .	59
6.4.7	Homotypic interaction of <i>Dasm1</i> . . . . .	59
6.4.8	Evoked inhibitory postsynaptic currents (eIPSCs) in P15-20 mice . . .	60
6.4.9	Paired pulse ratio (PPR) of evoked IPSCs in P15-20 mice . . . . .	60
6.5	EPSP-spike (E-S) coupling . . . . .	62
6.6	Giant depolarizing potentials (GDPs) . . . . .	63
<b>7</b>	<b>Discussion</b>	<b>65</b>
7.1	<i>Dasm1</i> in dendrite arborization and synaptic transmission . . . . .	65
7.2	Excitatory currents . . . . .	68
7.3	Inhibitory currents . . . . .	70
7.4	GABA during development . . . . .	72
7.5	Extracellular versus intracellular domains of <i>Dasm1</i> . . . . .	73
7.6	Interneurons in hippocampus . . . . .	74
7.7	Synapse formation and network development . . . . .	76
<b>8</b>	<b>Outlook</b>	<b>79</b>
<b>9</b>	<b>Other projects during PhD</b>	<b>81</b>
9.1	Serine phosphorylation of ephrinB2 regulates trafficking of synaptic AMPA receptors . . . . .	81
9.2	Electrical activity suppresses axon growth through Ca <sub>v</sub> 1.2 channels in adult primary sensory neurons . . . . .	81
	<b>Bibliography</b>	<b>83</b>
<b>10</b>	<b>Acknowledgments</b>	<b>93</b>
<b>11</b>	<b>Curriculum vitae</b>	<b>95</b>



## List of Figures

4.1	Connectivity map by Ramón y Cajal . . . . .	9
4.2	Immunoglobulin-domain proteins . . . . .	11
4.3	The hippocampal network . . . . .	24
4.4	Interneuron diversity in the hippocampal CA1 area . . . . .	25
4.5	Complexity of dendrite arborization is not altered in <i>Dasm1</i> <sup>-/-</sup> mice in vivo . . . . .	28
4.6	Off-target effect of Dasm1-RNAi used by Shi et al. (2004b) . . . . .	29
5.1	Recording E-S-coupling . . . . .	37
5.2	Isolating NMDA receptor fEPSPs, AMPA, and NMDA receptor mediated currents . . . . .	40
6.1	Basal synaptic transmission is unaltered in <i>Dasm1</i> <sup>-/-</sup> mice . . . . .	43
6.2	AMPA/NMDA ratio is elevated in <i>Dasm1</i> <sup>-/-</sup> mice, but not in <i>Dasm1</i> <sup>ΔC/ΔC</sup> mice . . . . .	45
6.3	Decay kinetics of AMPA and NMDA receptor mediated currents are not altered . . . . .	46
6.4	Miniature excitatory postsynaptic currents (mEPSCs) are not different in P7-8 and P15-20 <i>Dasm1</i> <sup>-/-</sup> mice . . . . .	47
6.5	Paired pulse ratio for evoked AMPA receptor currents is not altered . . . . .	49
6.6	NMDA receptor fEPSPs are not altered . . . . .	49
6.7	NMDA receptor mediated synaptic transmission is not altered . . . . .	51
6.8	Plasticity is not altered in <i>Dasm1</i> <sup>-/-</sup> mice . . . . .	52
6.9	Frequencies, but not amplitudes of miniature inhibitory postsynaptic currents (mIPSCs) are significantly reduced in P5-6 and in P15-20 <i>Dasm1</i> <sup>-/-</sup> mice . . . . .	54
6.10	Neither frequencies, nor amplitudes of mIPSCs are different in <i>Dasm1</i> <sup>ΔC/ΔC</sup> mice (P5-6 and P15-20) . . . . .	56
6.11	Frequencies, but not amplitudes of spontaneous inhibitory postsynaptic currents (sIPSCs) are significantly reduced in P7-8 and P15-20 <i>Dasm1</i> <sup>-/-</sup> mice . . . . .	57

6.12	Neither frequencies, nor amplitudes of sIPSCs are different in <i>Dasm1</i> <sup>ΔC/ΔC</sup> mice (P7-8) . . . . .	58
6.13	RT-PCR on GAD65-GFP neurons suggests, that <i>Dasm1</i> is present in interneurons	58
6.14	Reduced gephyrin puncta in <i>Dasm1</i> <sup>-/-</sup> neurons . . . . .	59
6.15	<i>Dasm1</i> -EGFP as well as <i>Dasm1</i> -ΔC-EGFP are capable of homotypic adhesion in a cell aggregation assay . . . . .	60
6.16	Evoked inhibitory postsynaptic currents are not altered in <i>Dasm1</i> <sup>-/-</sup> mice . .	61
6.17	EPSP-spike (E-S) coupling is not altered in <i>Dasm1</i> <sup>-/-</sup> mice . . . . .	63
6.18	Giant depolarizing potentials are not altered in <i>Dasm1</i> <sup>-/-</sup> mice . . . . .	64
7.1	Fewer interneurons might be present in <i>Dasm1</i> <sup>-/-</sup> mice . . . . .	75
7.2	Excitatory neurons receive fewer inhibitory synapses in <i>Dasm1</i> <sup>-/-</sup> mice . . . .	77

## List of Tables

3.1	Abbreviations . . . . .	8
5.1	Chemicals . . . . .	32
5.2	Different ACSF solutions were used . . . . .	32
5.3	Internal recording solutions . . . . .	33
5.4	Thermopol buffer . . . . .	33
5.5	Primers . . . . .	34
5.6	PCR genotyping reaction . . . . .	34
5.7	PCR protocol . . . . .	35



## 1 Zusammenfassung

Das der Immunoglobulinfamilie zugehörige Protein IgSF9 (immunoglobulin superfamily member 9) wird im Hippocampus während der Embryonalentwicklung und der anschließenden nachgeburtlichen Reifung des Gehirns exprimiert. Es wurde gezeigt, dass akutes Supprimieren von IgSF9 mit RNA-Interferenz dazu führt, dass sowohl die dendritischen Verzweigungen, als auch die Synapsenreifung gestört sind. Deshalb wurde das Protein in Dendrite arborization and synapse maturation 1 (Dasm1) umbenannt (Shi et al., 2004a,b). Dasm1 ist ein 1179 Aminosäuren langes Transmembranprotein, das auf seinem extrazellulären N-terminalen Teil fünf Immunoglobulin-Domänen und zwei Fibronectin-Domänen besitzt. Auf der C-terminalen intrazellulären Seite befindet sich ein PDZ Motiv. Da Dasm1 strukturelle Ähnlichkeit mit dem neuronalen Zelladhäsionsmolekül NCAM (neural cell adhesion molecule) aufweist und darüber hinaus adhesive Immunoglobulin-Domänen besitzt, lässt sich vermuten, dass Dasm1 ein Zelladhäsionsmolekül ist.

Mit elektrophysiologischen Messungen habe ich an akuten Hirnschnitten untersucht, ob Dasm1 bei der Funktion von Synapsen eine Rolle spielt. Dazu untersuchte ich Mausmutanten, denen das Dasm1 Gen fehlt und verglich die Ergebnisse mit deren Wurfgeschwistern, denen das Gen nicht fehlt und die somit das Protein exprimieren. Erregende Feldpotentiale (field excitatory postsynaptic currents, fEPSPs) unterschieden sich in 15 bis 20 Tage alten Wurfgeschwistern nicht, was darauf hinweist, dass die Grundfunktionen der synaptischen Transmission in den Mausmutanten nicht gestört sind. Da in einer kontroversen Studie von Shi und Kollegen mittels RNA-Interferenz gezeigt wurde, dass die glutamaterge synaptische Transmission beeinträchtigt ist, wenn das Protein supprimiert wird (Shi et al., 2004b), habe ich die glutamatergen AMPA- und NMDA-Rezeptoren näher untersucht. Mit Ganzzelleableitungen konnte ich zeigen, dass das AMPA/NMDA-Verhältnis in den Mausmutanten signifikant erhöht ist. Da die, durch AMPA Rezeptoren hervorgerufenen, kleinen erregenden postsynaptischen Ströme (miniature excitatory postsynaptic currents, mEPSCs) sich weder in Amplituden,

noch Frequenzen unterschieden, untersuchte ich die NMDA Rezeptoren detaillierter. Jedoch waren weder isolierte NMDA Rezeptor Feldpotentiale, noch die Rezeptorkinetik, die Stromspannungskennlinie und die Leitfähigkeit des NMDA Rezeptors verändert.

Da neuronale Netze ein Gleichgewicht von Erregung und Hemmung benötigen, untersuchte ich zudem inhibitorische Ströme, die durch GABA Rezeptoren herbeigeführt werden. Erstaunlicherweise waren bei 15 bis 20 Tage alten Mausmutanten die Frequenzen, nicht aber die Amplituden von kleinen inhibitorischen postsynaptischen Strömen (miniature inhibitory postsynaptic currents, mIPSCs) und von spontanen inhibitorischen postsynaptischen Strömen (spontaneous IPSCs, sIPSCs) signifikant reduziert. Dies deutet auf eine Verringerung der Anzahl von Synapsen hin. Da die Proteinmenge von Dasm1 im Verlauf der Entwicklung abnimmt, habe ich mIPSCs und sIPSCs an jüngeren Tieren (5 bis 6 Tage alt) gemessen und fand eine noch größere Reduktion der Frequenz bei den Mausmutanten. Die Anzahl von inhibitorischen Synapsen war auch in dissoziierten Neuronen verringert, was mit morphologischen Färbungen von Gephyrin, einem Protein das nur in inhibitorischen Synapsen vorkommt, gezeigt werden konnte. Im Gegensatz zu den mIPSCs und den sIPSCs unterschieden sich evozierte inhibitorische postsynaptische Ströme (evoked IPSCs) in Wurfgeschwistern nicht. Da eine verringerte Inhibition Auswirkungen auf die Erregbarkeit nachgeschalteter Neurone haben kann, untersuchte ich das Feuerverhalten von CA1 Neuronen in Feldmessungen. Das Feld-zu-Feuerverhalten (fEPSP to spike, E-S) war in den Mausmutanten unverändert. In jungen Tieren war eine größere Reduktion der Frequenzen von mIPSCs und sIPSCs zu beobachten. Da in dieser Zeit Netzwerkoszillationen, wie z.B. die großen depolarisierenden Potentiale (giant depolarizing potentials, GDPs) auftreten, untersuchte ich diese. GDPs unterschieden sich nicht in Wurfgeschwistern, was darauf hindeutet, dass die frühe Hirnentwicklung nicht beeinträchtigt ist. Außerdem untersuchte ich Kurz- und Langzeitplastizität, die sich beide in Wurfgeschwistern nicht unterschieden.

Die Hypothese, dass Dasm1 ein Zelladhäsionsmolekül ist, wird durch Zellaggregationsexperimente unterstützt: Dasm1 Proteine können homophil miteinander interagieren. Um herauszufinden, welche Domänen von Dasm1 wichtig sind, untersuchte ich Tiere, die nur den N-terminalen Teil des Proteins und die Transmembrandomäne exprimieren (Dasm1- $\Delta$ C). Ich konnte zeigen, dass nur der N-terminale Teil des Proteins mit der Transmembrandomäne notwendig und hinreichend ist, um die beiden Phänotypen - das erhöhte AMPA/NMDA

---

Verhältnis und die reduzierte Frequenz von mIPSCs und sIPSCs - wiederherzustellen. Dies deutet darauf hin, dass der C-Terminus, obwohl dieser ein PDZ Motiv hat, für die beschriebenen Effekte nicht von Bedeutung ist.

Die vorliegende Studie legt nahe, dass Dasm1 ein Zelladhäsionsmolekül ist, das für die Entwicklung oder den Erhalt von inhibitorischen Synapsen wichtig ist. Wie der Phänotyp zustande kommt, muss abschließend noch geklärt werden: Entweder interagiert das Protein mit der Entwicklung oder Wanderung von Interneuronen und verursacht so die verringerte Anzahl von inhibitorischen Synapsen, oder Dasm1 wirkt direkt auf die Entwicklung von inhibitorischen Synapsen. Erste Ergebnisse von Co-Kultur-Experimenten konnten zeigen, dass Dasm1 bei der inhibitorischen Synaptogenese eine Rolle spielt.



## 2 Synopsis

The immunoglobulin superfamily member 9 (IgSF9) is highly expressed in hippocampus during embryonic development and postnatal maturation. Acute RNAi knockdown of IgSF9 in hippocampal neurons impaired dendrite arborization and synapse maturation, hence it was named Dasm1 (Shi et al., 2004a,b). Dasm1 is a 1179 amino acids long transmembrane protein with five extracellular immunoglobulin domains followed by two fibronectin domains and a PDZ motif located at the intracellular C-terminus. Structural similarity of Dasm1 to neural cell adhesion molecule (NCAM) as well as the presence of several adhesive Ig domains makes Dasm1 a candidate for a cell adhesion molecule.

To test whether loss of Dasm1 impairs synaptic function, I acquired electrophysiological recordings in acute hippocampal slices from *Dasm1<sup>+/+</sup>* and *Dasm1<sup>-/-</sup>* littermates. Field excitatory postsynaptic potentials (fEPSPs) were not different in P15-20 littermates, suggesting that basal synaptic transmission is not impaired. As a controversial study by Shi and colleagues, using RNAi to suppress Dasm1 expression levels, reported impaired glutamatergic synaptic transmission (Shi et al., 2004a), I focused on AMPA ( $\alpha$ -amino-3-hydroxyl-5-methyl-4-isoxazole-propionate) and NMDA (N-methyl-D-aspartic acid receptors) receptor mediated currents. Using whole cell patch clamp recordings I discovered a significantly elevated AMPA/NMDA-ratio in *Dasm1<sup>-/-</sup>* mice, without seeing any differences in frequencies or amplitudes of AMPA receptor mediated miniature excitatory postsynaptic currents (mEPSCs), pointing to alterations in NMDA receptor mediated synaptic transmission. However, neither isolated NMDA receptor fEPSPs, nor NMDA receptor kinetics, NMDA receptor current-voltage (I-V) relationship, and NMDA receptor conductance were altered.

As neural nets require a balance of excitation to inhibition I also recorded inhibitory currents mediated via GABA ( $\gamma$ -aminobutyric acid) receptors. Surprisingly, frequencies, but not amplitudes of miniature inhibitory postsynaptic currents (mIPSCs) as well as spontaneous inhibitory postsynaptic currents (sIPSCs) were significantly reduced in P15-20 *Dasm1<sup>-/-</sup>*

mice, which points to a loss of inhibitory synapses. Frequencies of P5-6 mIPSCs and P7-8 sIPSCs were reduced even more dramatically, suggesting a developmental phenotype which corresponds to declining protein levels during development. Stainings of cultured hippocampal neurons with the inhibitory-specific synapse marker gephyrin suggest that the number of inhibitory synapses is reduced in *Dasm1*<sup>-/-</sup> neurons. Further, I recorded evoked IPSCs, which were not altered in *Dasm1*<sup>-/-</sup> mice. As reduction of frequency of mIPSCs could increase excitability of CA1 neurons, I assessed the spike generation of CA1 neurons by fEPSP to spike (E-S) coupling, which was not altered. Proper wiring together with balanced excitation to inhibition is necessary for neural networks to mature. Dramatic reduction of mIPSCs was observed in the critical period of postnatal brain maturation. The giant depolarizing potentials (GDPs) are among the first network oscillations to occur in the developing brain. These early patterns of network activity were not altered in *Dasm1*<sup>-/-</sup> mice, suggesting that although mIPSCs and sIPSCs are significantly reduced, networks can still develop and mature. I also tested short and long term plasticity with paired pulse stimulation and long term potentiation, respectively. Neither presynaptic release probabilities nor the ability of adapting synaptic strength were altered.

The hypothesis, that Dasm1 is an adhesive molecule is supported by cell aggregation assay data which suggests that Dasm1 proteins interact with other Dasm1 proteins in a homophilic manner. To further elucidate which protein domains of Dasm1 are important, mice lacking only the intracellular C-terminus of Dasm1 were analyzed (*Dasm1*<sup>ΔC/ΔC</sup>). Studying these mice revealed that only the extracellular N-terminal part together with the transmembrane domain of the protein are necessary and sufficient for Dasm1 to function properly. Both phenotypes – the elevated AMPA/NMDA-ratio as well as the reduced miniature and spontaneous inhibitory postsynaptic currents – were rescued, strongly suggesting that the C-terminus is dispensable.

The present study suggests that Dasm1 is a cell adhesion molecule necessary for establishing and/or maintaining inhibitory synapses in the hippocampus. The way Dasm1 acts remains to be elucidated: either it interacts directly with the machinery necessary for the formation of inhibitory synapses, or the lack of the protein delays the maturation or migration of neurons and thereby impairs the required cell-specific connectivity. Preliminary results of a co-culture assay favor a role of Dasm1 in synapse formation.

### 3 Abbreviations

---

<b>aa</b>	amino acids
<b>ACSF</b>	artificial cerebro-spinal fluid
<b>APV</b>	amino-5-phosphonopentanoate
<b>AMPA</b>	$\alpha$ -amino-3-hydroxyl-5-methyl-4-isoxazole-propionate
<b>bp</b>	base pairs
<b>CA1</b>	cornu ammonis 1
<b>CA3</b>	cornu ammonis 3
<b>CB</b>	calbindin
<b>CCK</b>	cholecystokinin
<b>CNS</b>	central nervous system
<b><i>Dasm1</i><sup>+/+</sup></b>	Dendrite arborization and synapse maturation wildtype
<b><i>Dasm1</i><sup>-/-</sup></b>	Dendrite arborization and synapse maturation mutant
<b><i>Dasm1</i><sup><math>\Delta C/\Delta C</math></sup></b>	Dendrite arborization and synapse maturation Delta C mutant
<b>eIPSC</b>	evoked inhibitory postsynaptic current
<b><math>E_{Cl}</math></b>	equilibrium potential of chloride
<b>ECM</b>	extracellular matrix
<b>EPSC</b>	excitatory postsynaptic current
<b>EPSP</b>	excitatory postsynaptic potential
<b>E-S</b>	EPSP to spike coupling
<b>fEPSP</b>	field excitatory postsynaptic potential
<b>FN</b>	fibronectin type III domain
<b>FV</b>	fiber volley
<b>GABA</b>	$\gamma$ -aminobutyric acid
<b>GC</b>	granule cell

<b>GPI</b>	glycosyl-phosphatidylinositol
<b>GDP</b>	giant depolarizing potential
<b>GFP</b>	green fluorescent protein
<b>Ig</b>	immunoglobulin domain
<b>IgSF</b>	immunoglobulin superfamily
<b>ISI</b>	inter stimulus interval
<b>IV</b>	current voltage relationship
<b>KCC2</b>	$K^+$ - $Cl^-$ cotransporter 2
<b>K-S</b>	Kolmogorov-Smirnov test
<b>LTD</b>	long-term depression
<b>LTP</b>	long-term potentiation
<b>mEPSC</b>	miniature excitatory postsynaptic current
<b>mIPSC</b>	miniature inhibitory postsynaptic current
<b>NBQX</b>	1,2,3,4-Tetrahydro-6-nitro-2,3-dioxo-benzo[f]quinoxaline-7-sulfonamide
<b>NCAM</b>	neural cell adhesion molecule
<b>NKCC1</b>	$Na^+$ - $K^+$ - $Cl^-$ cotransporter 1
<b>NMDA</b>	N-methyl-D-aspartic acid
<b>O-LM</b>	oriens lacunosum moleculare
<b>P</b>	postnatal day
<b>PDZ</b>	PSD95 / disc large tumor suppressor DlgA / zonula occludens-1
<b>PPD</b>	paired pulse depression
<b>PPF</b>	paired pulse facilitation
<b>PPR</b>	paired pulse ratio
<b>PV</b>	parvalbumin
<b>sEPSC</b>	spontaneous excitatory postsynaptic current
<b>sIPSC</b>	spontaneous inhibitory postsynaptic current
<b>TCM</b>	trichlormethiazide
<b>TTX</b>	tetrodotoxin
<b>VGLUT3</b>	vesicular glutamate transporter 3
<b>VIP</b>	vasoactive intestinal peptide

---

Table 3.1: Abbreviations

## 4 Introduction

The human brain consists of approximately ten billion neurons of which each has the potential to establish thousands of contacts with other neurons. Different classes of neurons with diverse properties are needed to build neural circuits. To enable neural networks to process information properly, coordinated wiring of the neurons is required. During embryonic development and postnatal maturation of the brain neurons need to migrate to their exact destination place, and furthermore establish highly specific cell to cell connections. This cell-specific connectivity was already shown more than a century ago by neuroscientists such as Santiago Felipe Ramón y Cajal, who, amongst other things, proposed connectivity maps of brain structures (see Figure 4.1, taken from Piccolino et al., 1989).

Based on his work and the experiments of other groups, Nobel laureate Roger W. Sperry proposed already in 1939 that “[...] the cells and fibers of the brain and cord must carry some kind of individual identification tags, presumably cytochemical in nature, by which they are distinguished one from another almost, in many regions, to the level of the single neuron [...]” (reviewed by Sperry, 1963). And indeed, intense research during the last decades validated his chemoaffinity theory by demonstrating the existence of a variety of these hypothesized individual identification tags, which are necessary to build and maintain cell to cell contacts.

The specialized cell to cell contacts in the nervous system are called synapses and they are the essential building blocks of

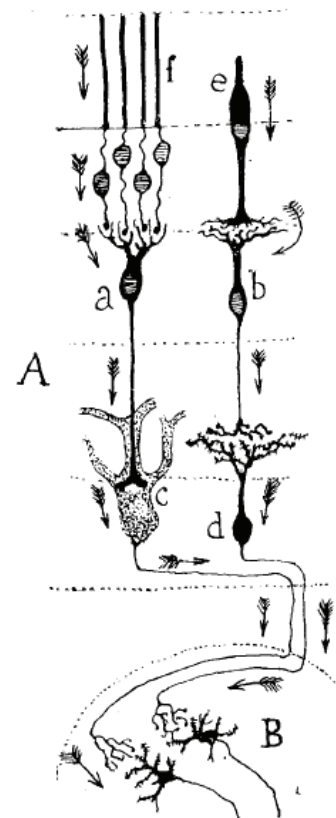


**Figure 4.1: Connectivity map by Ramón y Cajal.** Cells in the retina have to form appropriate contacts for building functional networks. Taken from Piccolino et al. (1989).

neural networks. Synapse formation is a process consisting of two distinct phases: first, nascent pre- and postsynaptic terminals need to find each other, then the synapse needs to mature. Today, cell adhesion molecules are thought to be responsible for both inducing initial contact formation and recruiting pre- and postsynaptic proteins necessary for a proper working synapse (for review see Dalva et al., 2007).

## 4.1 Cell adhesion molecules

More and more cell adhesion molecules involved in synaptogenesis have been discovered during the last years (Dalva et al., 2007; Yamagata et al., 2003). Cell adhesion molecules exist in several classes. Among them, the best-studied classes are the immunoglobulin (Ig) containing cell adhesion molecules, the neuroligins and neuroligins, the integrins, and the cadherins. In the following paragraphs, each of these classes will be discussed shortly to give an overview of how cell adhesion molecules can act on synaptic transmission.

### 4.1.1 Immunoglobulin superfamily

Members of the immunoglobulin superfamily (IgSF) have variable numbers of globular extracellular cysteine-looped domains (see Figure 4.2), that were first described in immunoglobulins. The immunoglobulin (Ig) domain contains about 100 amino acids and possesses a characteristic Ig-fold, formed by two sheets of antiparallel  $\beta$ -strands (Barclay, 2003). The majority of IgSF proteins are single-pass transmembrane proteins, but also soluble isoforms as well as glycosyl-phosphatidylinositol (GPI)-anchored members of this family exist. Often, fibronectin type III domains (FN), which are closely related to Ig domains, occur between the Ig domains and the transmembrane domain. Posttranslational modifications such as glycosylations or attachment of polysialic acid are often observed. Some of the IgSF proteins interact with the cytoskeleton via a common structural PDZ domain. It was named PDZ domain, as the consensus motif was first discovered in the postsynaptic density protein (PSD95), the *Drosophila melanogaster* septate junction protein disc large tumor suppressor (DlgA), and the tight junction protein zonula occludens-1 (zo-1).

IgSF proteins are expressed in different tissues and have a variety of functions ranging from being antigen receptors, antigen presenting molecules, adhesion molecules, and growth factor

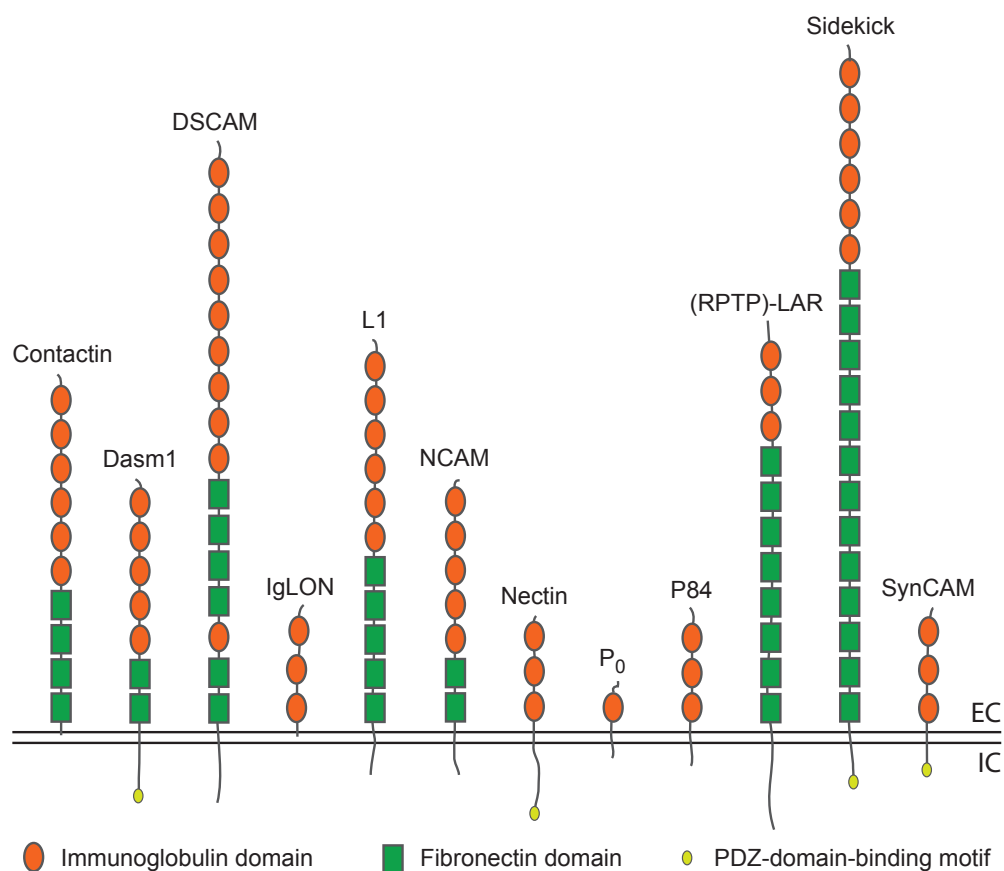


**Figure 4.2: Immunoglobulin-domain proteins.** Members of the immunoglobulin superfamily have variable numbers of Ig domains and often contain FN domains. The depicted members are either transmembrane proteins or GPI-anchored proteins. EC extracellular, IC intracellular side.

receptors. The adhesive function of Ig domain cell adhesion molecules can be modulated by secreted soluble Ig domain proteins, which are often produced via alternative splicing (Rougon and Hobert, 2003). The present study concerns the IgSF member Dendrite arborization and synapse maturation 1 (Dasm1), which will be discussed in detail in chapter 4.4.

Some members of the immunoglobulin superfamily will be mentioned in the following part to highlight the diverse effects of this large class of proteins. Within the brain, the most prominent member is the neural cell adhesion molecule (NCAM), which has in the extracellular part five Ig domains followed by two FN domains. NCAM, sharing extracellular domain structure with Dasm1, is posttranscriptionally modified by alternative splicing, that generates different isoforms (NCAM-120, -140, and -180, see Reyes et al., 1993). Moreover, NCAM can posttranslationally be modified by the attachment of polysialic acid (PSA) which alters its

properties dramatically. Removal of PSA from NCAM impairs memory formation and the formation of long term potentiation (LTP, see chapter about synaptic plasticity 4.2.7) *in vitro* (Becker et al., 1996). PSA attached to NCAM regulates plasticity by modulating NMDA receptor signaling (Kochlamazashvili et al., 2010) and application of PSA and PSA-NCAM in NCAM deficient mice restored LTP (Senkov et al., 2006). Contrary, absence of NCAM impairs LTP in gyrus dentatus but not absence of PSA alone (Stoenica et al., 2006).

IgSF member L1 is expressed in the central nervous system (CNS) and has been implicated in neuronal migration, neurite outgrowth and guidance, neuronal survival, and synaptic plasticity. LTP in CA1 neurons was reduced by application of L1 antibodies (Luthi et al., 1994), and frequencies of miniature inhibitory postsynaptic currents were also reduced in L1 deficient mice (Saghatelyan et al., 2004).

Synaptic cell adhesion molecules (SynCAM) are CNS-specific immunoglobulin superfamily proteins that interact with PDZ-domain proteins and function as homophilic cell adhesion molecules at the synapse (Fogel et al., 2007). Overexpression of SynCAM in heterologous cells induced synaptogenesis by co-cultured hippocampal neurons (Biederer et al., 2002).

The nectin family has four isoforms and co-localizes with the cadherin-catenin system. Inhibition of nectin-1 resulted in decreased synapse size and increased synapse number (Mizoguchi et al., 2002), pointing to a role of nectins in synapse formation.

Sidekicks, having six Ig domains followed by 13 FN domains, determine lamina-specific synaptic connectivity (Yamagata et al., 2002). The four members of the IgLON family (LAMP, OBCAM, neurotrimin, and kilon) are GPI-anchored Ig domain molecules (Miyata et al., 2003) and are involved in neurite outgrowth and synapse formation (Hashimoto et al., 2009). Other Ig domain molecules at synapses are the receptor protein tyrosine phosphatase (RPTP)-LAR (Wyszynski et al., 2002; Kaufmann et al., 2002) and P84/SHPS-1 (Mi et al., 2000).

Many other Ig domain proteins are not located at synapses, but still impair brain maturation. GPI-anchored TAG-1, a member of the contactin family (Murai et al., 2002), is involved in interneuron migration (Denaxa et al., 2001). The class of down syndrome cell adhesion molecules (DSCAM, Yamakawa et al., 1998) is required for neurite arborization and prevents self-fasciculation in mouse retina (Fuerst et al., 2008). P<sub>0</sub> mediates membrane adhesion in the spiral wraps of the myelin sheath, which influences conduction velocity in the peripheral

nervous system (Doyle and Colman, 1993; Shapiro et al., 1996). Cross talk of IgSF members with other cell adhesion molecules has been proposed, for example L1 and integrins cooperate in promoting migration and axogenesis of developing neurons (Silletti et al., 2000).

#### 4.1.2 Neurexins-neuroligins

Neurexins were discovered as receptors for  $\alpha$ -latrotoxin, a toxin found in the venom of the black-widow spider (Ushkaryov et al., 1992). Binding of  $\alpha$ -latrotoxin to presynaptically expressed neurexin induces massive release of neurotransmitter. Neurexins are encoded in the mammalian genome by three *NRXN* genes (*NRXN1-3*). Independent promoters transcribe two isoforms: the larger  $\alpha$  and the shorter  $\beta$  neurexins (Tabuchi and Sudhof, 2002), but potentially thousands of *NRXN* isoforms are generated by extensive alternative splicing (Ullrich et al., 1995). Neurexins are mainly located presynaptically, but can also be found postsynaptically (Taniguchi et al., 2007). Recently, it was shown that neurexins physically and functionally interact with postsynaptic GABA<sub>A</sub> receptors and suppress GABAergic synaptic transmission when overexpressed (Zhang et al., 2010).

The membrane spanning neuroligins (neuroligin-1, -2, -3, and -4) act as the endogenous neurexin ligands (Ichtchenko et al., 1995) and can modulate trans-synaptic activation of synaptic transmission (for review see Sudhof, 2008). Neuroligins are expressed postsynaptically and their extracellular domain has high homology to acetylcholinesterases, yet they do not exhibit esterase activity. Neuroligins are encoded in the mammalian genome by four genes (*NLGN1-4*) and undergo alternative splicing. Neurexins and neuroligins form trans-synaptic complexes together with PDZ-containing proteins. Overexpression of neuroligin-1 in neurons increases excitatory, but not inhibitory synaptic responses, whereas overexpression of neuroligin-2 selectively increases inhibitory synaptic responses (Chubykin et al., 2007; Chih et al., 2005). As neuroligins-1, -3, and -4 localize to glutamatergic synapses and neuroligin-2 localizes primarily to inhibitory synapses (Graf et al., 2004) they might be able to control the balance of excitatory to inhibitory synapses.

Varoquaux and colleagues reported that triple knockout mice lacking neuroligin-1, -2, and -3 die shortly after birth as a consequence of impaired GABAergic/glycinergic and glutamatergic transmission in brainstem centers controlling respiration (Varoquaux et al., 2006). Synapse

numbers of triple knockout mice were almost not impaired, suggesting that neuroligins are dispensable for synapse formation but crucial for synapse function.

Neurexins and neuroligins are involved in the pathogenesis of cognitive diseases, such as schizophrenia, autism spectrum disorders, Tourette's syndrome, and learning disabilities (Jamain et al., 2003; Walsh et al., 2008; Yan et al., 2005).

#### **4.1.3 Cadherins and protocadherins**

The calcium-dependent adhesion molecules cadherins are single-pass transmembrane molecules which mediate mainly homophilic adhesion at intercellular junctions. Cadherins are linked to the cytoskeleton via their intracellular binding sites for catenins, which can also act as mediators for downstream signaling (Yamagata et al., 2003). The specificity of the cadherin-cadherin binding is regulated by the outmost of five characteristic extracellular cadherin domains (EC1-5). Many cadherins are expressed by neurons and each cadherin shows a distinct and unique expression pattern (Redies, 2000). They help to establish the functional interconnectivity and are expressed by neurons already at stages preceding synapse formation (Benson and Tanaka, 1998). Different neurons can express different subtypes of cadherins during development (Matsunaga et al., 1988). N-cadherin which is initially expressed at all synaptic sites is restricted to glutamatergic synapses in adult brain, whereas another yet unidentified classical cadherin is associated to GABAergic synapses (Benson and Tanaka, 1998; Yamada and Nelson, 2007). Moreover, N-cadherin is required for regulating presynaptic function at glutamatergic synapses (Jungling et al., 2006).

Protocadherins, which lack cytoplasmic signaling functions, have 6-7 EC domains and are the largest subgroup of cadherins. In the genome, the roughly 80 different protocadherin genes are arranged in three clusters ( $\alpha$ ,  $\beta$ , and  $\gamma$ ). Upon deletion of the  $\gamma$  cluster, a dramatic loss of interneurons but not sensory and motor neurons from the spinal cord was observed (Wang et al., 2002), pointing to an interneuron-specific role of a subset of protocadherins.

#### **4.1.4 Integrins**

Integrins mediate interactions of cells with other cells or with the extracellular matrix (ECM) in different tissues, including the CNS (Hynes, 2002). They are  $\alpha$ - $\beta$  heterodimers of single-

pass transmembrane proteins with large ectodomains and short cytoplasmic tails. Vertebrates, having 18 different  $\alpha$  and eight different  $\beta$  subunits encoded in their genome, form at least 24 different heterodimer pairs. Some integrins have ligand binding domains that can recognize a large number of physiological ligands, for example ECM molecules such as fibronectin and laminin (Arnaout et al., 2005). Integrins are not only involved in cell adhesion, but also in migration, for which the ECM serves as a scaffold (Janik et al., 2010).

## 4.2 Synaptic transmission and plasticity

In the brain, information is encoded as electrical signals and transferred between neurons at specialized contact sites called synapses. These synapses are either electrical synapses or chemical synapses.

Electrical synapses are the simpler and evolutionarily more ancient form of synapses and occur at special sites called gap junctions. At these sites, the membranes of two adjacent neurons are separated by only three nanometers and proteins called connexins form a pore that allows for the transfer of electrical and chemical signals.

In the mature mammalian nervous system, synaptic transmission is mostly chemical and uni-directional. At chemical synapses, the arriving electrical signal is converted into a chemical signal, which is then able to regenerate the electrical signal in the postsynaptic neuron. Electrical signals arrive at specialized presynaptic structures, the presynaptic terminals or synaptic boutons, and trigger the release of synaptic vesicles that contain the neurotransmitter. The neurotransmitter is released into the synaptic cleft and diffuses to the juxtaposed postsynaptic membrane. Receptors in the postsynaptic membrane are activated by binding of their cognate neurotransmitter and allow ions to pass the membrane. Thereby, an electrical postsynaptic signal is generated.

### 4.2.1 Presynaptic compartment

The presynaptic bouton is an axonal expansion containing mitochondria, neurotransmitter-filled vesicles, and an active zone with voltage gated calcium channels. Synaptic vesicles form pools which are either in direct contact with the presynaptic membrane at active zones and ready to release (ready releasable pool) or they are found at more distant sites of the active

zone and serve as a reserve pool. Upon the arrival of an electrical signal, the voltage gated calcium channels open, and allow influx of calcium which triggers the fusion of vesicles docked at the presynaptic membrane, which requires a complex molecular machinery. Subsequently, calcium sensitive proteins can induce vesicle fusion with the membrane. After synaptic vesicles have emptied their vesicle content, they are recycled in the presynaptic terminal and refilled with neurotransmitter.

#### **4.2.2 Synaptic cleft**

The synaptic cleft is approximately 20-50 nm wide and is filled with a matrix of fibrous extracellular protein. The main function of this matrix is to make the pre- and postsynaptic membrane adhere to each other. Synaptic cell adhesion molecules are part of the matrix and help to establish or maintain these contacts as well as control synapse specificity during development. As the volume of the synaptic cleft is very small, neurotransmitter concentration can be raised and lowered rapidly. Some of the neurotransmitter rapidly diffuses out of the cleft, where it also can activate extrasynaptic receptors. Neurotransmitter is removed from the synaptic cleft either by reuptake through the presynaptic neuron or glia, or the neurotransmitter is chemically degraded by cleavage enzymes.

#### **4.2.3 Postsynaptic compartment**

The most important part of the postsynapse are the receptors which are located in the membrane opposite to the presynaptic active zone. The postsynapse also contains the machinery for the exo- and endocytosis of receptors as well as other proteins which modulate receptor properties. Scaffolding molecules help to maintain the position of the receptors, which are either ionotropic or metabotropic. As for the generation of postsynaptic electrical signals the ionotropic receptors play a more prominent role, these receptors will be discussed in more detail. Ionotropic receptors are ligand gated ion channels which after opening allow for the influx of positively or negatively charged ions, depending on whether the receptor is an excitatory or an inhibitory receptor.

#### 4.2.4 Excitatory synaptic transmission

Activation of excitatory postsynaptic receptors depolarizes the postsynaptic membrane due to the influx of positively charged ions into the postsynaptic cell. The postsynaptic cell starts firing, if temporal and spatial summation of excitation is powerful enough to reach the action potential threshold. Excitatory synaptic transmission thus increases the probability that the postsynaptic cell will fire an action potential.

Glutamate is the dominant excitatory neurotransmitter in the central nervous system and acts via specialized metabotropic and ionotropic glutamate receptors. Besides the G-protein coupled glutamate receptors (metabotropic, mGluR1-8), three classes of ionotropic glutamate receptors are known: the  $\alpha$ -amino-3-hydroxyl-5-methyl-4-isoxazole-propionate (AMPA) receptors (GluA1-4), the kainate receptors (GluK1-5), and the N-methyl-D-aspartic acid (NMDA) receptors (GluN1, N2A-D, N3A-B; for details of the new IUPHAR nomenclature see Collingridge et al., 2009).

AMPA receptors, activated by the eponymous artificial glutamate analog AMPA, mediate fast synaptic transmission in the central nervous system. They are heterotetrameric ionotropic receptors with conductances for sodium, potassium, and - depending on the subunit composition - also for calcium. The presence of the GluA2 subunit confers impermeability for calcium.

The less well understood KARs obtained their name by being selectively activated through kainate, and are thought to be involved in modulating synaptic transmission. NMDA receptors with their selective agonist NMDA are key players of synaptic plasticity. At negative membrane potentials they are blocked by extracellular magnesium and thus need a depolarization to open. Their nonselective conductance for cations allows for the influx of the second messenger calcium which can trigger signaling cascades resulting in the insertion of AMPA receptors into synapses during long term potentiation (LTP), as well as the removal of AMPA receptors during long term depression (LTD). For detailed description of plasticity see chapter 4.2.7.

NMDA receptors require the binding of the co-agonist glycine in addition to glutamate to open (Thomson, 1990). NMDA receptors are tetramers composed of the subunits NR1, NR2(A-D), and NR3. In hippocampus, the NMDA receptors are assembled as the heterodimers

NR1/NR2A and NR1/NR2B, and as the heterotrimer NR1/NR2A/NR2B. NMDA receptor decay kinetics are much slower than AMPA receptor decay kinetics and depend on the subunit composition of the receptor. NR2B containing receptors have slower decay kinetics compared to NR2A containing receptors.

Excitatory receptors are often found on so-called dendritic spines, which are small protrusions on the dendrites. Excitatory synapses are asymmetric: in electron micrographs the postsynaptic membrane appears thicker than the presynaptic membrane. This can be attributed to the densely packed postsynaptic scaffold in excitatory synapses.

#### 4.2.5 Inhibitory synaptic transmission

Inhibitory synaptic transmission in adult hippocampus is mainly mediated by  $\gamma$ -aminobutyric acid (GABA), acting on ligand gated ionotropic GABA<sub>A</sub> receptors as well as on G protein coupled GABA<sub>B</sub> receptors. In mammals, 19 different GABA receptor subunits ( $\alpha_{1-6}$ ,  $\beta_{1-3}$ ,  $\gamma_{1-3}$ ,  $\delta$ ,  $\epsilon$ ,  $\theta$ ,  $\pi$ ,  $\rho_{1-3}$ ) have been cloned so far (for review see Jentsch et al., 2002). Functional pentameric GABA<sub>A</sub> receptors are formed, if at least  $\alpha$  and  $\beta$  subunits are present (Mohler, 2006). The most common subunit composition in the brain comprises two  $\alpha$ , two  $\beta$ , and one  $\gamma$  subunit.

Inhibitory synaptic transmission controls in a spatiotemporal manner the net flow of excitability by various mechanisms, for example phasic and tonic modulation of the membrane potential, and shunting inhibition. Inhibition at synapses is called phasic inhibition, whereas inhibition occurring at extrasynaptic sites is called tonic. Action potential-driven GABA release acts predominantly on synaptic GABA receptors and prevents overexcitation of neurons. A low concentration of GABA in the extracellular space persists despite the activity of GABA uptake transporters in neurons as well as in glia. Ambient GABA activates high-affinity extrasynaptic GABA receptors and leads to a persistent chloride conductance (Farrant and Nusser, 2005).

GABA<sub>A</sub> receptors are, like most ionotropic inhibitory receptors, permeable to only one natural ion, which is chloride. Opening of the chloride channel allows chloride to cross the membrane and bring the resting membrane potential to the equilibrium potential of chloride ( $E_{Cl}$ ), which in mature neurons is about -65 mV. Inhibition largely depends on the membrane potential

as well as on the  $E_{Cl}$ . A more negative  $E_{Cl}$  compared to the resting membrane potential leads upon activation of GABA<sub>A</sub> receptors to an hyperpolarizing inhibitory postsynaptic potential (IPSP).  $E_{Cl}$  in mature neurons is mostly close to the resting membrane potential. Activation of an inhibitory synapse in this case acts as an electrical shunt and prevents the flow of positive charge to travel further. This type of inhibition is called shunting inhibition (Bear et al., 2001).

However, in immature neurons, the  $E_{Cl}$  is more positive than the resting membrane potential and activation of GABA<sub>A</sub> receptors therefore acts depolarizing (Ben-Ari, 2002). An elevated intracellular Cl<sup>-</sup> concentration shifts the  $E_{Cl}$  towards more positive values which is caused by different expression levels of the sodium-potassium-chloride cotransporter NKCC1 and the potassium-chloride cotransporter KCC2 (Ben-Ari, 2002; Blaesse et al., 2009) during early postnatal maturation. NKCC1, which typically raises intracellular Cl<sup>-</sup> concentration, shows decreasing expression levels during early postnatal brain maturation (Hubner et al., 2001a). In contrast, KCC2 which normally lowers intracellular Cl<sup>-</sup> concentration, shows increasing functional expression levels during development (Hubner et al., 2001b). The resulting high intracellular Cl<sup>-</sup> concentration during early hippocampal development renders GABAergic excitation, which is crucial for network maturation (Pfeffer et al., 2009).

Excitatory action of GABA is involved in the generation of giant depolarizing potentials (GDPs), one of the first electrical activity pattern of the developing brain (Ben-Ari et al., 2007), which disappear around the second postnatal week (Garaschuk et al., 1998). GDPs are only observed until the GABA shift from acting excitatory to inhibitory (Ben-Ari et al., 1989) occurring in mouse hippocampus at the end of the first postnatal week (Stein et al., 2004) and in rat around postnatal day 13.5 (Khazipov et al., 2004).

During early postnatal maturation, GABA provides the depolarization needed to relieve the voltage-dependent magnesium block of NMDA receptors and thus initiates excitatory network maturation (Ben-Ari et al., 1997; Wang and Kriegstein, 2008).

Inhibitory receptors are usually not found in spines but on the shaft of dendrites and at the soma. Inhibitory synapses in the central nervous system are also called symmetrical as they show similar thickness of the pre- and postsynaptic membrane in electron micrographs.

#### **4.2.6 Miniature vesicle release**

Vesicles in presynapses can not only fuse in a coordinated manner, initiated by the arriving electrical signal, but they can also fuse in a stochastic manner. The postsynaptic signal generated by such a spontaneous fusion event is called a miniature excitatory or inhibitory postsynaptic current (mEPSC or mIPSC). Miniature postsynaptic currents were first described by Fatt and Katz (1952) at the neuromuscular junction. Miniature postsynaptic currents might play important roles in dendritic protein synthesis (Sutton et al., 2004), maintenance of dendritic spines (McKinney et al., 1999), synaptic homeostasis (Frank et al., 2006), and modulation of interneuron firing (Carter and Regehr, 2002). Miniature EPSCs and IPSCs exhibit variations in amplitudes for which different mechanisms have been proposed. Multiquantal release (Ropert et al., 1990), variation in transmitter content of different vesicles (Frerking et al., 1995), and postsynaptic receptor number (Borst et al., 1994; De Koninck and Mody, 1994) could account for amplitude variations. Nusser et al. (1997) assessed mIPSCs amplitudes with electrophysiological recordings and the number of GABA<sub>A</sub> receptors with immunogold stainings; these authors suggest that differences in amplitudes reflect different numbers of postsynaptic GABA<sub>A</sub> receptors.

Alterations in frequencies of miniature excitatory or inhibitory postsynaptic currents reflect either alterations in the release probability, or in the number of release sites. Elevated presynaptic calcium concentrations, for instance, increase the frequency of these events. If unaltered presynaptic release probabilities are observed, the favored explanation for alterations of the frequency of miniature events is that the number of functional release sites is altered. Miniature EPSCs and IPSCs are recorded in conditions of suppressed activity to avoid contamination with action potential triggered vesicle exocytosis. In contrast to mEPSCs and mIPSCs, spontaneous excitatory or inhibitory postsynaptic currents (sEPSCs or sIPSCs) are recorded in the presence of activity and include action potential-driven events.

#### **4.2.7 Synaptic plasticity**

Synaptic plasticity is the ability of synapses to increase or decrease synaptic strength, which can last from a few milliseconds to the entire lifetime of the synapse. Short term plasticity is transient and the underlying mechanisms are different compared to the mechanisms

contributing to long lasting changes. Specific patterns of stimulation can evoke long lasting changes in synaptic strength which can either be a potentiation of the response (long term potentiation, LTP) or a depression of synaptic strength (long term depression, LTD). Both, LTP as well as LTD are believed to represent the molecular mechanisms of learning and memory (Malinow and Malenka, 2002; Kessels and Malinow, 2009). Homeostatic synaptic scaling is another form of plasticity which helps to keep the excitability of a neuron or a neuronal circuit in a constant range (Turrigiano and Nelson, 2004), although global activity is elevated or decreased. Stabilizing mechanisms prevent, that upon perturbations, such as changes in synapse number or strength, neural circuits become hyper- or hypoactive (Turrigiano, 2008).

#### 4.2.7.1 Short term plasticity

Short term plasticity lasts for at most a few minutes and is mainly attributed to presynaptic effects (Zucker and Regehr, 2002). Strengthening of the postsynaptic response is called facilitation, and results from an elevated calcium concentration which primes vesicles for fusion upon the next stimulus. Weakening of the postsynaptic response is called synaptic depression, and is believed to result from depletion of the readily releasable vesicle pool. Initial presynaptic release probability correlates with whether facilitation or depression occurs: facilitation is observed if initial release probability is low, and depression is observed if initial release probability is high.

Presynaptic release probability can be assessed by applying two consecutive pulses to the presynapse and is called paired pulse paradigm. The first of the two pulses only assesses the readily releasable pool and elevates the calcium concentration in the presynaptic terminal. The second pulse then either elicits a larger or a smaller postsynaptic response, which is called paired pulse facilitation (PPF) or paired pulse depression (PPD), respectively (Muller et al., 2010). Presynaptic calcium accumulation primes more vesicles to fuse with the membrane during the second pulse and hence is the cause for PPF (Neher and Sakaba, 2008; Katz and Miledi, 1968). Depletion of the ready releasable pool within the first pulse (Foster and Regehr, 2004), reduction of release probability (Wu and Borst, 1999), and postsynaptic receptor desensitization (Koike-Tani et al., 2008) have been proposed as being the mechanisms

underlying PPD. However, the most widely accepted hypothesis for PPD remains the first of the aforementioned alternatives.

#### **4.2.7.2 Long term plasticity**

Long term potentiation (LTP) and long term depression (LTD) are long lasting changes of synaptic strength, and are believed to be the molecular mechanisms underlying learning and memory. In 1973 it was discovered that high synaptic activity can result in LTP, a persistent increase of synaptic strength (Bliss and Gardner-Medwin, 1973). In 1977 the opposing counterpart, LTD, was discovered (Lynch et al., 1977). Changes in synaptic strength following specific stimulation patterns can be attributed to presynaptic or postsynaptic changes, depending on the synapse. At the mossy fiber – CA3 synapse in hippocampus (see chapter 4.3), a change of the probability of neurotransmitter release is thought to be responsible for long term plasticity (Nicoll and Schmitz, 2005; Malenka and Bear, 2004).

However, at the CA3–CA1 synapse, probably the best described synapse in the brain, long lasting changes in synaptic strength are mediated by postsynaptic mechanisms. Postsynaptic NMDA receptors have a critical role in long lasting synaptic plasticity which arises from several unique features of these excitatory receptors. NMDA receptors have a conductivity for the second messenger calcium, they are blocked at resting membrane potentials with extracellular magnesium, and they have slow current kinetics. Activation of AMPA receptors leads to a depolarization which activates the NMDA receptors and removes the magnesium block. Depending on the pattern of NMDA receptor activation, calcium enters the postsynapse and activates second messenger cascades, which either lead to the insertion (LTP) or the removal (LTD) of AMPA receptors. Short periods of synaptic activity thus can weaken or strengthen synaptic transmission. The number of AMPA receptors is regulated by endocytosis and exocytosis of vesicles containing receptors, as well as lateral diffusion of receptors into synapses. The favored view is that AMPA receptors are exocytosed or endocytosed at extrasynaptic sites and diffuse into (LTP) or out (LTD) of the synapse.

Besides the NMDA receptor dependent LTD, another form of LTD exists at the CA3–CA1 synapse: mGluR dependent LTD (Malenka and Bear, 2004), which can also be induced in the presence of NMDA receptor antagonists (Oliet et al., 1997). This form of LTD requires

a rise of the dendritic calcium concentration as well, but this rise is attributed to T-type calcium channels instead of NMDA receptors (Oliet et al., 1997).

Long lasting changes in synaptic transmission can be induced in acute slices with different stimulation protocols. The tetanic stimulation protocol is a common protocol for inducing LTP: therefore, two trains of 100 Hz of one second duration, separated by a 20 seconds break are delivered to the presynaptic axons. Immediately after the induction stimulus, the postsynaptic response is elevated, which is called post tetanic potentiation. After several minutes, the potentiation weakens and reaches a plateau, which is still higher than the initial postsynaptic response prior to the induction of LTP. A weaker protocol for inducing LTP is the theta burst protocol consisting of short trains of high frequency bursts interrupted by several seconds without stimulus.

LTD on the other hand is usually elicited by prolonged stimulation with low frequency, e.g. delivering 900 pulses with 1 Hz to Schaffer collaterals decreases synaptic strength at the CA3–CA1 synapse persistently.

### **4.3 The hippocampus**

The hippocampus is an ideal model system for neurophysiology, as it has a relatively simple laminar structure and principal cells with a well-described connectivity pattern. Belonging to the limbic system, the hippocampus is important for long-term episodic memory as well as for spatial navigation.

The famous case study of patient H.M. (Henry Gustav Molaison) revealed the importance of the hippocampus for long term, but not short term and procedural memories (Scoville and Milner, 1957). H.M. suffered from severe epilepsy and therefore underwent bilateral surgical resection of both temporal lobes including the hippocampus. After the surgery, H.M. suffered from severe anterograde amnesia - he could not commit new events to long term memory but was still able to recall what happened before the operation as well as what happened in recent past.

The two interconnected hippocampi are located inside the medial temporal lobe of each hemisphere. The hippocampus consists of several regions: cornu ammonis with its subdivisions (CA1, CA2, CA3, and CA4), gyrus dentatus, subiculum, and entorhinal cortex. Granule

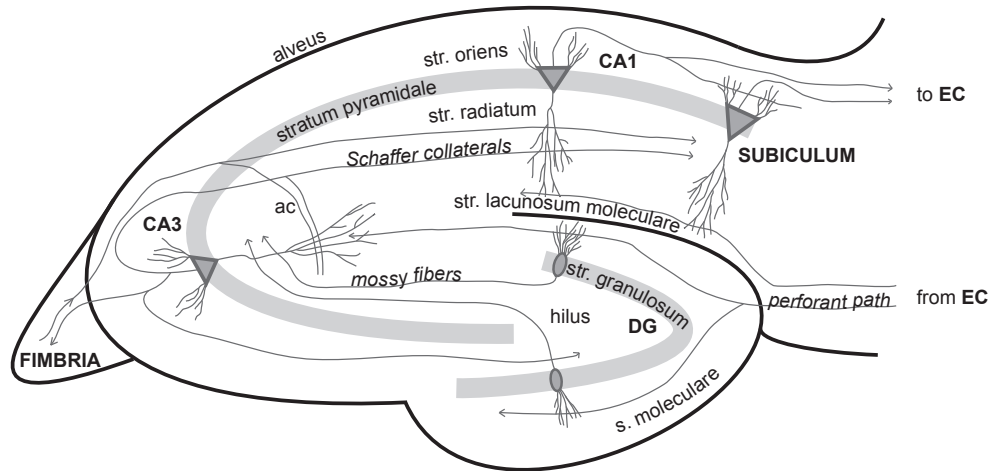


**Figure 4.3: The hippocampal network.** The entorhinal cortex (EC) projects via the medial and lateral perforant path to the gyrus dentatus (dentate gyrus, DG), CA3 (cornu ammonis region 3) and to distal dendrites of CA1. Granule cells in stratum granulosum (str. granulosum) send their mossy fiber axons to the CA3 region. CA3 neurons innervate ipsi- and contralateral CA1 neurons via the Schaffer collateral axons. In addition, they also project to ipsi- and contralateral CA3 neurons via the associational commissural (ac) pathway. CA1 neurons project to the subiculum and to the EC.

cells of the gyrus dentatus receive their major input from the entorhinal cortex and in turn project via mossy fiber axons to the CA3 field of hippocampus. The pyramidal cells of the CA3 region then project via Schaffer collateral axons to the CA1 region, as well as to CA1 cells in the contralateral hippocampus via the associational commissural pathway. The CA3–CA1 synapse is probably the best characterized synapse in the brain. CA1 pyramidal cells provide input to neurons situated in subiculum and in entorhinal cortex (see Figure 4.3). The entorhinal cortex closes the loop by receiving inputs from the CA1 region and projecting to the gyrus dentatus.

The term “trisynaptic pathway” entorhinal cortex – gyrus dentatus (via perforant path, first synapse) – CA3 (via mossy fibers, second synapse) – CA1 (via Schaffer collaterals, third synapse) was coined by Anderson and colleagues (Anderson et al., 1971).

#### 4.3.1 Pyramidal cells

Named after the triangular shape of their soma (20  $\mu\text{m}$  to 30  $\mu\text{m}$  in size), pyramidal cells are excitable cells which can be found not only in hippocampus, but also in cerebral cortex and amygdala. The axon of a pyramidal cell is long and often extensively branched, which

enables it to project over long distances. Pyramidal cell dendrites arise from the apex (apical dendrite), as well as the base of the soma (basal dendrites). In contrast to the apical dendrite, which is a single thick dendrite that branches, the basal dendritic tree consists of three to five primary dendrites.

Small protrusions called dendritic spines are located on the dendrites and represent the location of excitatory inputs of the neuron. Spines are extensively found in distal regions of the dendrites and are absent in proximal regions as well as at the soma. A CA1 pyramidal cell of the hippocampus receives between 1,000 to 30,000 synaptic inputs (Klausberger and Somogyi, 2008) via their dendrites.

The cell body and the axon-initial segment of a pyramidal cell receive only GABAergic synapses which do not form postsynaptic spines. As neurons integrate their excitatory and inhibitory inputs at the axon-initial segment, the influence of proximal inputs is in general larger than that of distal ones. However, a recent study suggests, that CA2 neurons are more excited by their distal inputs than by their more proximal inputs and inputs from the entorhinal cortex (Chevalayre and Siegelbaum, 2010).

#### **4.3.2 Granule cells**

In gyrus dentatus, elliptical granule cells with a width of approximately 10  $\mu\text{m}$  and a height of 20  $\mu\text{m}$  (Claiborne et al., 1990) are densely packed in stratum granulosum. Granule cells have a cone-shaped dendritic tree directed toward the superficial portion of the molecular layer and give rise to the mossy fiber axons which project to the CA3 region (see Figure 4.3). Granule cells in the suprapyramidal blade have longer dendrites and more spines per dendrite length compared to granule cells of the infrapyramidal blade (length 3500  $\mu\text{m}$  and 1.6 spines/ $\mu\text{m}$  versus 2800  $\mu\text{m}$  and 1.3 spines/ $\mu\text{m}$ , respectively). Mossy cells, a special class of cells in the gyrus dentatus, do not project to CA3 region, but instead to the gyrus dentatus of the other brain hemisphere.

#### **4.3.3 Interneurons**

In the central nervous system, interneurons are, with few exceptions, locally projecting inhibitory neurons that regulate pyramidal cell activity. Unlike the uniform pyramidal cells,

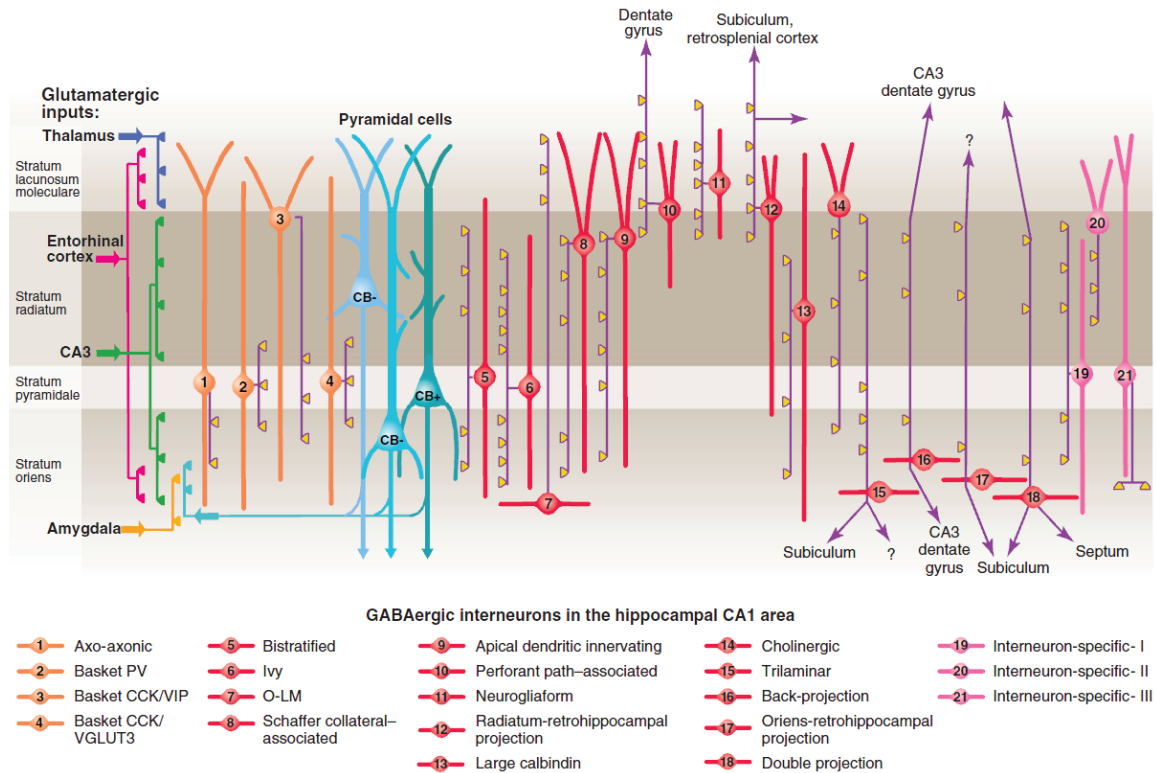


**Figure 4.4: Interneuron diversity in the hippocampal CA1 area.** Axo-axonic interneurons (1) and basket cells (2-4) innervate pyramidal cells (blue) at their axon and somata, respectively. Interneurons mainly innervating other interneurons are depicted in pink (19-21). Axons are purple and the main synaptic terminations are yellow. Glutamatergic inputs are indicated on the left. CB, calbindin; CCK, cholecystokinin; O-LM, oriens lacunosum moleculare; PV, parvalbumin; VIP, vasoactive intestinal peptide; VGLUT3, vesicular glutamate transporter 3. Adapted from Klausberger and Somogyi (2008).

they form a very diverse class of neurons that differs dramatically in innervation and firing patterns, as well as in molecular expression profiles. In the hippocampus, the prevailing inhibitory neurotransmitter released by interneurons is GABA.

Different classes of interneurons have varying firing profiles and presumably release GABA at different time points to distinct subcellular domains of pyramidal cells (Klausberger and Somogyi, 2008). The way interneurons influence pyramidal cells depends largely on their target zone: inhibition at the pyramidal cell somata regulates the generation of action potentials, whereas inhibition at dendrites impacts voltage-gated currents, regulates  $Ca^{2+}$ -dependent action potentials or shunts excitatory inputs (McBain and Fisahn, 2001).

Often, interneurons are classified based on the presence of singular neurochemicals, such as

calcium-binding proteins (parvalbumin, calretinin, and calbindin), neuropeptide Y, nitric oxide synthase, and vasoactive intestinal peptide.

Another attempt to classify the large number of different interneurons is based on their individual innervation pattern: basket cells project to somata and proximal dendrites, axo-axonic cells innervate exclusively the axon-initial segment of pyramidal cells, bistratified cells innervate basal and oblique dendrites (dendrites that branch from the main dendritic tree), and oriens-lacunosum moleculare interneurons have their somata in stratum oriens and project to the distal apical dendrites of pyramidal cells in stratum lacunosum moleculare. Klausberger and Somogyi suggest 21 different types of interneurons (see Figure 4.4, taken from Klausberger and Somogyi, 2008), whereas Parra and colleagues suggest that there is a very large but finite number of different subtypes or even that each hippocampal interneuron is different (Parra et al., 1998).

Interneurons are associated with several neurological disorders, such as schizophrenia, bipolar disorders, epilepsy, autism spectrum disorders, and Huntington's disease (Benes and Berretta, 2001; Rubenstein and Merzenich, 2003; Blum and Mann, 2002; Lewis, 2000).

#### **4.4 The immunoglobulin superfamily member 9 and turtle**

The present study suggests a novel role for the immunoglobulin superfamily member 9 (IgSF9) protein, being a cell adhesion molecule that acts on the number of inhibitory synapses in hippocampus.

Initially discovered in *Drosophila melanogaster*, it was named turtle, as flies lacking the protein are unable to regain an upright position after inverting (Bodily et al., 2001). The turtle protein consists of five immunoglobulin (Ig) domains followed by two fibronectin type III domains (FN) and a transmembrane domain. Through alternative splicing of the *tutl* gene, five isoforms of the protein are produced, two of which are diffusible (Al-Anzi and Wyman, 2009).

Mutations in the *tutl* gene cause movement defects such as abnormal responses to tactile stimulation and inability to fly in adulthood (Bodily et al., 2001). Later it was shown that turtle acts as a non-cell autonomous axonal attractant that promotes midline-crossing, axonal branching, and invasiveness (Al-Anzi and Wyman, 2009). Ferguson and colleagues suggested

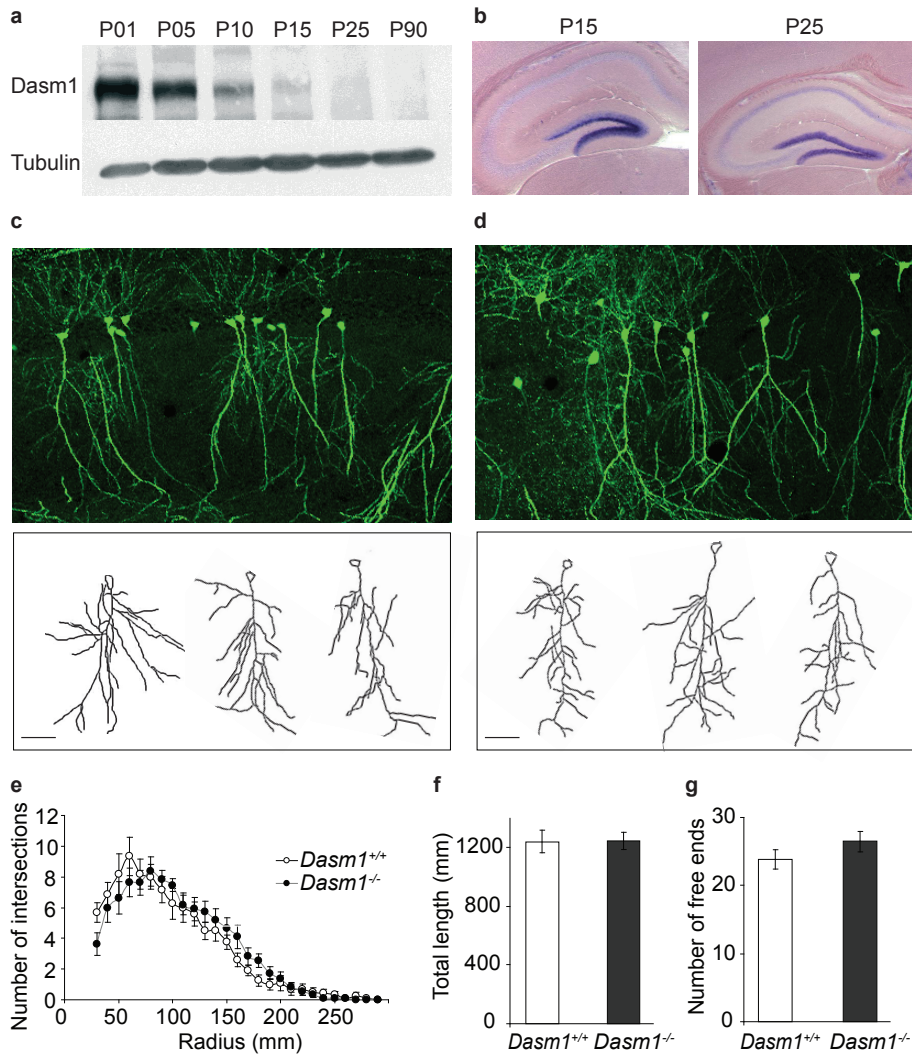
that turtle is involved in the regulation of the tiling pattern of R7 photoreceptor terminals, in that it prevents fusion of two adjacent R7 terminals, an effect which could be mediated by the ability of turtle proteins to interact in a homophilic manner (Ferguson et al., 2009). Long and colleagues propose that in neurons with simple arbors, turtle restrains dendrite branch formation, and that in neurons with complex arbors, turtle promotes self-avoidance (Long et al., 2009). Moreover, they suggest that the cytoplasmic tail is dispensable for the control of dendrite branching.

In mice, the 1179 amino acids immunoglobulin superfamily member 9 (IgSF9) was identified as being the most closely related protein to turtle, having in the extracellular part of the protein 31% identity and 50% similarity of the amino acid sequence and also having the same domain structure (Doudney et al., 2002). A type I PDZ domain-binding motif is located at the intracellular C-terminal tail (Shi et al., 2004b). Both, the structural similarity to the neural cell adhesion molecule (NCAM, 26% identity and 41% similarity, Doudney et al., 2002), which also has extracellularly five Ig domains followed by two FN domains, and the presence of several Ig domains itself, which have adhesive properties, makes IgSF9 a likely candidate for a cell adhesion molecule.

As RNAi knockdown of IgSF9 in rat and mouse hippocampal neurons impaired dendritic arborization and synapse maturation, it was named Dasm1 (Shi et al., 2004b). Furthermore, cell-specific knockdown of Dasm1 impaired AMPA but not NMDA receptor mediated synaptic transmission (Shi et al., 2004a).

Mishra and colleagues generated mice lacking the Dasm1 protein (Mishra et al., 2008). *Dasm1*<sup>-/-</sup> mice are viable and have no apparent phenotype. In *Dasm1*<sup>+/+</sup> mice, the Dasm1 protein is abundantly expressed in hippocampus (see Figure 4.5b). The complexity of dendrite arborization is not altered in hippocampal neurons of mice lacking Dasm1 *in vitro* and *in vivo* (see Figure 4.5c-g). Neither Sholl analysis, nor analysis of total length of dendrites and number of free ends were altered, indicating that either the protein does not interfere with hippocampal dendrite arborization or compensatory mechanisms substitute for the absent Dasm1 protein.

Knockdown of Dasm1 in *Dasm1*<sup>+/+</sup> mice with the RNAi constructs used by Shi and colleagues (Shi et al., 2004b) led to the reported impairment in dendritic arborization (see Figure 4.6a and c). Strikingly, this effect could also be observed with the same RNAi constructs in



*Dasm1*<sup>-/-</sup> mice (see Figure 4.6b and d), strongly suggesting that the reported phenotype arises from off-target effects. Not only the morphological experiments based on these RNAi constructs (Shi et al., 2004b), but also the electrophysiological experiments involving these RNAi constructs (Shi et al., 2004a) should therefore be considered as invalid.

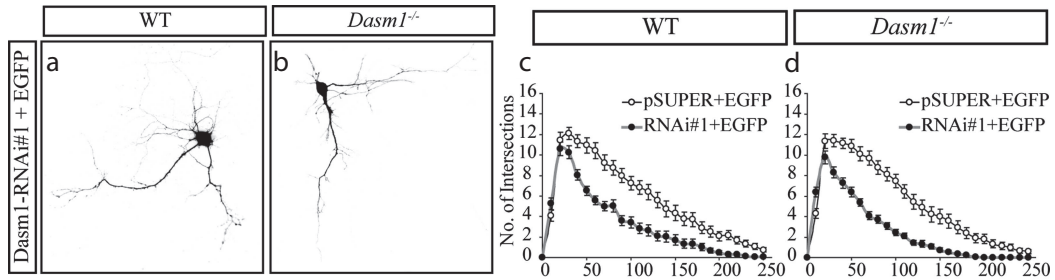


**Figure 4.6: Off-target effect of Dasm1-RNAi used by Shi et al. (2004b).** The Dasm1-RNAi used by Shi et al. (2004b) reduces dendrite complexity not only in *Dasm1*<sup>+/+</sup> neurons (a and c), but also in *Dasm1*<sup>-/-</sup> neurons (b and d), strongly suggesting an off-target effect. Left side: *Dasm1*<sup>+/+</sup> and *Dasm1*<sup>-/-</sup> neurons transfected with Shi-Dasm1-RNAi; right side: Sholl analysis. Adapted from Mishra et al. (2008).

#### 4.5 Aim of this study

The high expression level of Dasm1 in hippocampus, structural similarity to NCAM and the publications concerning Dasm1 (Shi et al., 2004a,b) and turtle (Bodily et al., 2001) motivated me to examine potential functions of Dasm1 in synaptic transmission. I addressed potential roles of Dasm1 in synaptic transmission in acute hippocampal slices of *Dasm1*<sup>+/+</sup> and *Dasm1*<sup>-/-</sup> mice with electrophysiological recordings. First, I studied basal synaptic transmission and plasticity with field recordings and focused then on excitatory and inhibitory currents of CA1 pyramidal neurons. Excitatory synaptic transmission was assessed by recording AMPA and NMDA receptor mediated currents as well as isolated NMDA receptor currents. As GABA is the main inhibitory neurotransmitter in the brain, playing a pivotal role during brain maturation, I studied GABA receptor mediated synaptic transmission.

To unravel whether the extracellular N-terminal part of the protein, containing five Ig and two FN domains, or whether the intracellular C-terminal part of the protein, containing a PDZ domain-binding motif, has more importance, mice lacking the C-terminus of Dasm1 (*Dasm1*<sup>ΔC/ΔC</sup>) were analyzed. If the *Dasm1*<sup>ΔC/ΔC</sup> mice displayed the same phenotypes as *Dasm1*<sup>-/-</sup> mice, the C-terminus would mediate the observed effect. Otherwise, if *Dasm1*<sup>ΔC/ΔC</sup> mice did not have the phenotypes observed in *Dasm1*<sup>-/-</sup> mice, the N-terminus would be necessary and sufficient for the observed effects of the protein. Electrophysiological recordings of these mice thus provide information for understanding the function of individual Dasm1 subdomains.

## 5 Material and Methods

### 5.1 Material

The following table lists all chemicals used in this study. Chemicals were dissolved in aqua bidest or in dimethylsulfoxid (DMSO) to obtain stock solutions. Stock solutions were dissolved in aqua bidest to get the concentration used in the experiment.

#### 5.1.1 Chemicals

Chemical	Supplier
1,2,3,4-Tetrahydro-6-nitro-2,3-dioxo-benzo[f]quinoxaline-7-sulfonamide (NBQX)	Sigma
(2R)-amino-5-phosphonopentanoate (APV)	BioTrend
6x gel loading buffer	Fermentas
Adenosine 5'-triphosphate magnesium salt (MgATP)	Sigma
Agarose	Inivitrogen
Calcium chloride dihydrate (CaCl <sub>2</sub> )	Merck
Cesium chloride (CsCl)	Sigma
Cesium methane-sulfonate (CsMeSO <sub>4</sub> )	Sigma
D(+)-Glucose monohydrate	Merck
Dimethylsulfoxid (DMSO)	Sigma
Ethidiumbromide Solution	Fluka Chemie
GeneRuler 1kb DNA-ladder	Fermentas
Magnesium chloride hexahydrate (MgCl <sub>2</sub> )	Merck
Magnesium sulfate heptahydrate (MgSO <sub>4</sub> )	Merck
N-(2,6-Dimethylphenylcarbamoylmethyl)triethylammonium-chloride (QX314)	Alomone labs
N-2-Hydroxyethylpiperazine-N'-2-ethane sulfonic acid (HEPES)	Biomol

Picrotoxin (PTX)	Sigma
Potassium chloride (KCl)	Merck
Restriction enzymes	Fermentas
Potassium dihydrogen phosphate (KH <sub>2</sub> PO <sub>4</sub> )	Merck
Sodium chloride (NaCl)	Merck
Sodium dihydrogen phosphate monohydrate (NaH <sub>2</sub> PO <sub>4</sub> )	Merck
Sodium hydrogen carbonate (NaHCO <sub>3</sub> )	Merck
Tetrodotoxin citrate (TTX)	BioTrend
Titriplex II (EDTA)	Merck
Titriplex VI (EGTA)	Merck
Trichlormethiazide (TCM)	Sigma

**Table 5.1:** List of chemicals.

### 5.1.2 Media and solutions

Depending on the experiment, different artificial cerebrospinal fluids (ACSF) were used (see Table 5.2). ACSF was carbogenated with 95% O<sub>2</sub> and 5% CO<sub>2</sub> to saturate the solution with oxygen and to adjust the pH to 7.2. Five-fold stock solution without glucose and calcium were prepared and stored at room temperature for up to two weeks. Prior to the experiment, the stock solution was diluted and glucose was added. Calcium was added after carbogenating the solution for 10 minutes, to prevent precipitation.

Chemical	Standard ACSF	ACSF for GDPs
NaCl	119 mM	117 mM
KCl	2.5 mM	4.5 mM
MgSO <sub>4</sub>	1.3 mM	1.3 mM
NaH <sub>2</sub> PO <sub>4</sub>	1 mM	1 mM
NaHCO <sub>3</sub>	26.2 mM	26.2 mM
CaCl <sub>2</sub>	2.5 mM	2.5 mM
Glucose	11 mM	11 mM

**Table 5.2:** Different ACSF solutions were used.

Different internal solutions were prepared for recording excitatory currents, and inhibitory currents, respectively (see Table 5.3). Internal solutions were prepared on ice and after adjusting osmolarity to 290 mOsm/kg and pH to 7.2, solutions were aliquoted and stored at -20°C.

Name	Chemical	Molarity
Excitatory internal recording solution	CsGluc	150 mM
	HEPES	10 mM
	NaCl	8 mM
	MgATP	2 mM
	EGTA	0.2 mM
	QX314	5 mM
Inhibitory internal recording solution	CsCl	90 mM
	CsGlc	20 mM
	HEPES	10 mM
	NaCl	8 mM
	MgCl <sub>2</sub>	2 mM
	EGTA	1 mM
	QX314	2 mM

**Table 5.3:** Internal recording solutions.

For the genotyping polymerase chain reactions (PCR), the thermopol buffer was used (see Table 5.4). After this buffer was prepared, aliquots were stored at -20°C prior to use it for PCR reactions.

Chemical	Molarity
Tris-HCl (pH 8.8)	200 mM
(NH <sub>4</sub> ) <sub>2</sub> SO <sub>4</sub>	100 mM
KCl	100 mM
20 MgSO <sub>4</sub>	20 mM
Triton X-100	0.1%

**Table 5.4:** Thermopol buffer

## 5.2 Methods

### 5.2.1 Transgenic Mice

*Dasm1*<sup>-/-</sup> mice were generated by A. Mishra as previously published (Mishra et al., 2008). The same cloning strategy was used for the *Dasm1*<sup>ΔC/ΔC</sup> mice and will be published soon.

### 5.2.2 Genotyping

The genotypes of the *Dasm1*<sup>+/+</sup> and *Dasm1*<sup>-/-</sup> mice as well as the *Dasm1*<sup>+/+</sup> and *Dasm1*<sup>ΔC/ΔC</sup> mice were tested with polymerase chain reaction (PCR) with the primers listed in the following table.

Primer	Sequence
Dasm fwd	act act gtt tgt cac ctg gac caa aga cgg
Dasm rev	caa tca act cgg aat gag gtc atg tta agc
Dasm neo	tta tta ggt ccc tgc acc tgc agc cca agc
Dasm-ΔC fwd	aag gga aag agc agc cta ggc aag gcg
Dasm-ΔC rev	cct tgc ctg ata gct acg tca gtg acc c
Dasm-ΔC neo	ttg aaa acc aca ctg ctc gat ccg gaa ccc

**Table 5.5:** List of primers for genotyping.

DNA lysates for PCR were obtained by boiling tail biopsies at 94°C in 50 mM NaOH for one hour. All three primers necessary for genotyping wildtype, heterozygous, and mutant of a mouse strain were put in one 50 μl PCR reaction (see Table 5.6).

Amount	Chemical
1.5 μl	DNA lysate
5 μl	TP buffer (10x)
1 μl	dNTPs (100 mM)
1 μl	primer-1
1 μl	primer-2
1 μl	primer-3
0.5 μl	Taq polymerase
39 μl	water
<hr/>	
50 μl	

**Table 5.6:** PCR genotyping reaction.

The PCR protocol used for all genotyping reactions is shown in Table 5.7.

Temperature	Time	Cycles
94°C	3 min	1
94°C	30 sec	30
61°C	30 sec	
72°C	40 sec	
72°C	10 min	1
4°C	for ever	1

**Table 5.7:** PCR protocol.

PCR reactions were visualized with standard ethidium bromide gel electrophoresis. Gels with 1% agarose in TAE buffer complemented with 3  $\mu$ l ethidium bromide per 100 ml TAE were used. PCR products were loaded together with loading buffer (10:1) and separated with electrophoresis (30 min at 90 V). DNA-bands were visualized under UV light using a gel documentation system (Bio-Rad). Expected bands for the *Dasm1* breeding were *Dasm1*<sup>+/+</sup> (582 bp), *Dasm1*<sup>-/-</sup> (450 bp), and for the *Dasm1*- $\Delta$ C breeding *Dasm1*<sup>+/+</sup> (358 bp), and *Dasm1* <sup>$\Delta$ C/ $\Delta$ C</sup> (426 bp).

### 5.2.3 Preparation of acute hippocampal slices

Acute hippocampal slices were prepared from littermates of the *Dasm1*<sup>+/+</sup>-*Dasm1*<sup>-/-</sup> breeding, as well as from the *Dasm1*<sup>+/+</sup>-*Dasm1* <sup>$\Delta$ C/ $\Delta$ C</sup> breeding at different ages, depending on the experiment. Mice were decapitated and brains were chilled in ice cold ACSF for two minutes. Hippocampi were isolated and subsequently placed on an agarose block which then was transferred to a Leica VT 1200S Vibratome. 400  $\mu$ m thick slices were cut and afterwards incubated in 32°C ACSF for 30 minutes before storing them in ACSF at room temperature prior to use them within the following six to eight hours. Coverslips for transferring slices to the recording chamber were coated with poly-D-lysine to prevent detaching.

### 5.2.4 Electrophysiology

Hippocampal slices were visualized using differential interference contrast (DIC) with an infrared charge coupled device (IR CCD) camera (VX55, Till Photonics) on a fixed-stage upright microscope (BX51WI, Olympus). Glass electrodes (GB150TF-8P, Science Products

GmbH) for stimulation and recording were pulled with a micropipette puller (P-97, Sutter Instruments) and had resistances of 2-3 M $\Omega$ . Data were collected using a MultiClamp 700 B amplifier and digitized at 5 kHz with a Digidata 1440A controlled by Clampex 10.2 Software (all Axon Instruments). Data were analyzed using Clampfit 10.2 (Axon Instruments) and in house written matlab routines. If not otherwise stated, experiments were performed at room temperature with acute hippocampal slices of *Dasm1*<sup>+/+</sup>/*Dasm1*<sup>-/-</sup> and *Dasm1*<sup>+/+</sup>/*Dasm1* <sup>$\Delta C/\Delta C$</sup>  littermates of defined ages (postnatal day x is referred to as Px) with standard artificial cerebrospinal fluid (ACSF). Slices were transferred to the recording chamber on poly-D-lysine coated coverslips. To prevent epileptiform activity of slices in field recordings, the Schaffer collateral bundles were cut next to the CA3 region.

For whole cell recordings, pipettes were filled with the internal solution according to the currents to be measured. To avoid contamination of the pipette on the approach to neurons, a small pressure was put on the pipette to allow for the efflux of internal solution. Cell attached configuration was established when the pipette contacted the cell. Immediately after contacting the cell, the membrane resistance increased, and the holding potential was set to the resting membrane potential. Whole cell configuration was applied by a brief suction. Cell parameters as e.g. membrane and access resistance were monitored by applying -5 mV test pulses. Access and membrane resistances had to be constant over recording time and lower than 20 M $\Omega$  and bigger than 100 M $\Omega$ , respectively.

#### **5.2.4.1 Basal synaptic transmission**

Schaffer collaterals were stimulated with 0.2 ms pulses of varying intensity and synaptic responses were recorded in the dendritic tree of CA1 neurons. For E-S coupling experiments an additional recording electrode was placed next to the somas of the CA1 neurons to record their excitability. Standard electrodes with a resistance of approximately 2.5 M $\Omega$  were filled with ACSF and used for stimulation and recording.

#### **Field excitatory postsynaptic potentials (fEPSPs)**

Field EPSPs were recorded in ACSF, complemented with 100  $\mu$ M picrotoxin (PTX) to block GABAergic inhibition. Input-output curves were plotted after calculating amplitudes of fiber volley and slopes of corresponding fEPSPs (see Figure 5.1). Isolated NMDA receptor mediated

field excitatory postsynaptic potentials (fEPSPs) were recorded in the presence of 0.1 mM  $Mg^{2+}$  to relieve the extracellular magnesium block and 10  $\mu$ M NBQX (2,3-Dioxo-6-nitro-1,2,3,4-tetrahydrobenzo(f)quinoxaline-7-sulfonamide) was added to block AMPA receptors. Isolated NMDA receptor fEPSP were smaller and slower compared to fEPSPs including AMPA receptor mediated synaptic transmission (see Figure 5.2a).

### E-S-coupling

Field EPSPs were recorded as described previously, a second recording electrode was placed next to the somas of CA1 neurons to record their excitability (see Figure 5.1). Slope of the fEPSP was plotted against spike height.

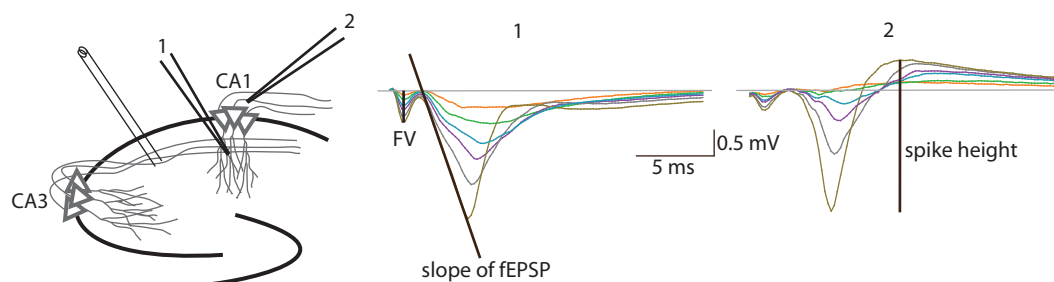


**Figure 5.1: E-S-coupling** Schematic drawing of the hippocampus with placement of electrodes and example traces of fEPSPs (recorded at electrode #1) and the spike (electrode #2). Same colors represent same stimulus strengths.

### Long term potentiation

After recording baseline fEPSPs with half-maximal stimulation for 30 minutes, LTP was induced with the tetanic stimulation protocol. Therefore, a stimulus of 100 Hz with the duration of one second was applied twice to the Schaffer collaterals with a break inbetween the two stimuli trains of 20 seconds. LTP was recorded for one more hour after induction and the average slope of the last ten minutes (minute 50 to 60 after induction) was compared to the last ten minutes prior to induction (minutes 20 to 30 of baseline).

### Paired pulse stimulation in field recordings

Two consecutive pulses were applied to the Schaffer collaterals with an inter stimulus interval of 40 ms, 80 ms, and 120 ms. After averaging 10 sweeps, the slope of the second pulse was

divided by the slope of the first pulse to obtain the paired pulse ratio.

### **Giant depolarizing potentials**

Giant depolarizing potentials (GDPs) were recorded at 32°C with an ACSF-filled electrode placed into stratum pyramidale of the CA3 region. GDPs could only be observed if excitability was increased by elevating KCl to 4.5 mM. GDPs were manually detected using a threshold search. As initial frequency was low, minutes 20 to 30 of the recording were analyzed.

#### **5.2.4.2 Excitatory whole cell recordings**

Patch pipettes were filled with excitatory internal solution. Excitatory synaptic currents were recorded in the presence of 100  $\mu$ M PTX to block inhibition.

### **Miniature excitatory currents**

For miniature excitatory currents, ACSF was supplemented with tetrodotoxin (TTX). TTX blocks the voltage dependent sodium channel and thus avoids action potential-driven events. Additionally, 250  $\mu$ M trichlormethiazide (TCM) was added to prevent AMPA receptor desensitization when recording mEPSCs. 50 mM sucrose was added in mEPSCs of young mice (P7-8) to increase frequency. Miniature EPSCs were analyzed with a matlab routine written by Valentin Stein. Briefly, after calculating the first derivative of the original trace, a threshold search identifies time points with defined steepnesses. After testing for several other parameters, the proposed event is manually accepted or denied as a miniature postsynaptic current. Only cells with more than 100 accepted events and stable cell parameters were taken into consideration. Recordings were grouped and tested for significance with Kolmogorov-Smirnov test for cumulative probability distributions.

### **AMPA/NMDA ratio**

AMPA and NMDA receptor mediated currents were evoked at -70 mV and +40 mV, respectively, by stimulating Schaffer collateral axons approximately 200  $\mu$ m to 400  $\mu$ m away from the soma. AMPA receptor mediated currents, which are fast glutamatergic currents, are presented as downward currents (see Figure 5.2b). The slower NMDA receptor mediated

currents are depicted as upward currents. For calculating the AMPA/NMDA ratio, the amplitude of the AMPA receptor peak current was divided by the NMDA receptor mediated current 75 ms after the stimulus artifact. This was done to avoid contamination of NMDA receptor currents with AMPA receptor currents, as AMPA receptors are also active at positive potentials.

### Decay kinetic parameters

The decay weighted time constant ( $\tau$  decay) was calculated from the integral of the current normalized to the peak current, according to Cathala et al. (2005):

$$\tau = \left( \int_{t_{peak}}^{t_{baseline}} I(t) dt \right) / I_{peak}$$

where  $t_{peak}$  is the time of the EPSC peak,  $t_{baseline}$  is the time at which the current had returned to preevent baseline, and  $I_{peak}$  is EPSC peak amplitude (see also Figure 5.2c).

### Paired pulse stimulation for excitatory synapses

Two consecutive pulses were applied to the Schaffer collaterals with an inter stimulus interval of 20 ms or 40 ms. Recording conditions were as for AMPA receptor mediated currents at a holding potential of -70 mV. After averaging 10 sweeps of an inter stimulus interval, the amplitude of the second peak was divided by the amplitude of the first peak to get the paired pulse ratio.

### Isolated NMDA receptor mediated currents

NMDA receptor mediated currents were isolated by adding 10  $\mu$ M NBQX to block AMPA receptor mediated currents. Decay parameters were calculated as described previously.

### NMDA receptor current voltage (IV) relationship

Peak currents at different holding potentials were calculated with Clampfit 10.2 (Axon Instruments). Holding potentials were corrected for the liquid junction potential ( $V_m = V_p - 15.4$  mV, see Barry and Lynch, 1991). After normalizing currents of a cell to the biggest current at +40 mV, IV was plotted (see Figure 5.2d).

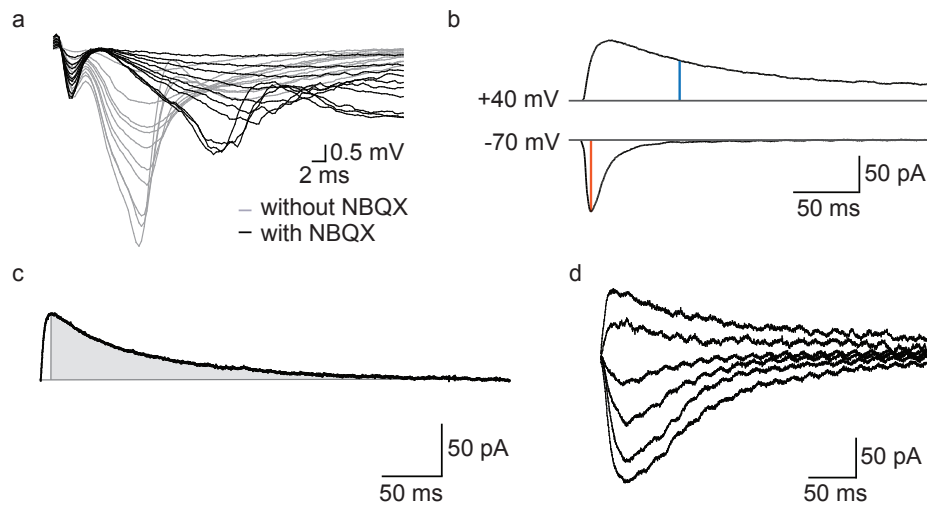


**Figure 5.2: NMDA receptor fEPSPs, AMPA and NMDA receptor mediated currents.** (a) NMDA receptor fEPSPs were isolated by blocking AMPA receptors with NBQX and reducing extracellular  $Mg^{2+}$  to 0.1 mM. Note: isolated NMDA receptor fEPSPs are smaller and slower than compound fEPSPs. (b) AMPA and NMDA receptor mediated currents were recorded at -70 mV and +40 mV, respectively. AMPA/NMDA ratio was calculated by dividing the AMPA peak current (orange) by the NMDA current 75 ms after stimulation (blue). (c) Decay kinetic parameters were calculated as described in the text. (d) Isolated NMDA receptor mediated currents at different holding potentials.

#### 5.2.4.3 Inhibitory whole cell recordings

Patch pipettes were filled with inhibitory internal solution. Inhibitory synaptic currents were recorded in the presence of 10  $\mu$ M NBQX and 100  $\mu$ M (2R)-amino-5-phosphonopentanoate (APV) to block AMPA and NMDA currents, respectively.

#### Miniature inhibitory currents

Miniature inhibitory postsynaptic currents (mIPSCs) were recorded in ACSF supplemented with 10  $\mu$ M NBQX and 100  $\mu$ M APV and in addition with 200 nM TTX to block action potential-driven events. Miniature IPSCs were analyzed with the same routines as mEPSCs.

#### Spontaneous inhibitory currents

Spontaneous inhibitory postsynaptic currents (sIPSCs) were recorded in ACSF containing 10  $\mu$ M NBQX and 100  $\mu$ M APV but without TTX to allow for activity driven events.

Spontaneous IPSCs were also analyzed using matlab routines.

### **Evoked inhibitory currents**

Inhibitory currents were evoked close to the soma (100  $\mu\text{m}$ ). The stimulus place was chosen such, that the smallest of the five stimuli (5  $\mu\text{A}$ , 10  $\mu\text{A}$ , 20  $\mu\text{A}$ , 30  $\mu\text{A}$ , and 50  $\mu\text{A}$ ) elicited only a current smaller than 20 pA. Only cells with responses to all five stimulus strengths were evaluated. Peak currents were analyzed and plotted versus stimulus input. Decay parameters of evoked IPSCs were calculated as described previously

### **Paired pulse stimulation for inhibitory synapses**

Two consecutive stimuli with an inter stimulus interval of 40 ms were applied at the same place where the electrode was placed for the evoked IPSCs. Stimulus strength for paired pulse stimulation was 10  $\mu\text{A}$ . After averaging ten sweeps the paired pulse ratio was calculated by dividing the amplitude of the second peak by the amplitude of the first peak.

#### **5.2.5 Graphs and statistics**

Graphs and statistics were done using Prism 5 (Graph Pad Software Inc.). Data are represented as mean  $\pm$  standard error of mean (SEM),  $n$  represents the number of cells examined. Differences between groups were tested using the Student's  $t$  test, when normally distributed. For mini-analysis, 150-200 events per cell were analyzed. To compare cumulative distributions, Kolmogorov-Smirnov (K-S) test was used. The K-S test is only appropriate for testing data against a continuous distribution. Therefore, 25 events were randomly chosen from each cell, and a continuous cumulative probability function was calculated from these events with a matlab routine. Significant levels were  $p < 0.05$  (\*),  $p < 0.01$  (\*\*), and  $p < 0.001$  (\*\*\*)



## 6 Results

### 6.1 Field excitatory postsynaptic potentials (fEPSPs)

I first assessed whether basal synaptic transmission is impaired in *Dasm1*<sup>-/-</sup> mice by recording field excitatory postsynaptic potentials (fEPSP). fEPSPs were recorded in the dendritic tree of CA1 neurons by stimulating Schaffer collateral axons in stratum radiatum. By increasing stimulus strength, the fiber volley (FV) as well as the fEPSP are increasing (see Figure 6.1a). Plotting the input (FV) against the output (slope of the fEPSP) did not reveal any differences between *Dasm1*<sup>+/+</sup> and *Dasm1*<sup>-/-</sup> mice (Figure 6.1b), indicating normal basal synaptic transmission.

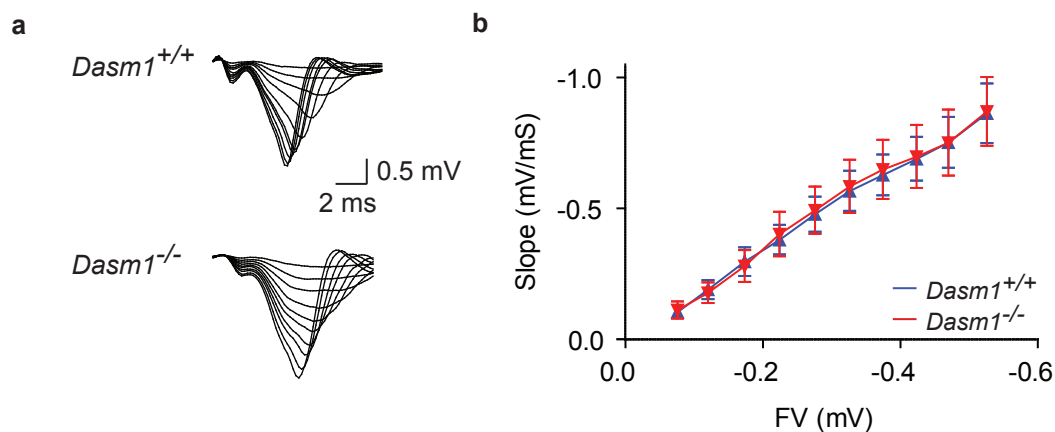


**Figure 6.1: Basal synaptic transmission is unaltered in *Dasm1*<sup>-/-</sup> mice.** (a) Example traces of field excitatory postsynaptic potentials (fEPSPs) of *Dasm1*<sup>+/+</sup> and *Dasm1*<sup>-/-</sup> mice. (b) Input-output curve of fEPSPs showed no significant differences between *Dasm1*<sup>+/+</sup> and *Dasm1*<sup>-/-</sup> mice. Shown is the fiber volley (FV) plotted against the slope of the fEPSP (blue: *Dasm1*<sup>+/+</sup>,  $n = 12$  and red: *Dasm1*<sup>-/-</sup>,  $n = 12$ ). Error bars represent SEM.

### 6.2 Glutamatergic currents

To further characterize whether synaptic transmission in *Dasm1*<sup>-/-</sup> mice is altered, whole cell recordings of CA1 neurons in acute hippocampal slices were performed. The main excitatory currents in hippocampus are mediated by the two glutamate receptors AMPA and NMDA

receptors. Basic parameters of these two receptors were examined.

### 6.2.1 AMPA/NMDA ratio in *Dasm1*<sup>-/-</sup> and *Dasm1*<sup>ΔC/ΔC</sup> mice

The ratio of AMPA to NMDA receptors at synapses influences synaptic transmission as well as plasticity. Therefore, AMPA and NMDA receptor mediated currents were recorded in CA1 pyramidal neurons by stimulating Schaffer collateral axons and blocking inhibitory currents with 100 μM picrotoxin (PTX). AMPA/NMDA-ratios were calculated as described in the methods section.

The AMPA/NMDA-ratio is mildly, but significantly elevated in *Dasm1*<sup>-/-</sup> mice (Figure 6.2a and c, mean ± SEM for *Dasm1*<sup>+/+</sup> 2.1 ± 0.2, *n* = 24, compared to *Dasm1*<sup>-/-</sup> 2.7 ± 0.2, *n* = 28, two-tailed unpaired t test *p* < 0.05), pointing to subtle alterations of either AMPA or NMDA receptor mediated currents, or both.

No alterations were observed when comparing *Dasm1*<sup>+/+</sup> mice (1.7 ± 0.3, *n* = 10) with *Dasm1*<sup>ΔC/ΔC</sup> mice (1.8 ± 0.3, *n* = 12, *p* > 0.05, see Figure 6.2b and d), suggesting that the C-terminus is not responsible for *Dasm1* induced alterations of the AMPA/NMDA ratio.

#### 6.2.1.1 AMPA and NMDA receptor decay time constants in *Dasm1*<sup>-/-</sup> and *Dasm1*<sup>ΔC/ΔC</sup> mice

The observed alterations in the AMPA/NMDA ratio could be caused by different numbers or properties of AMPA and/or NMDA receptors. To assess the kinetic properties of the receptors, decay time constants  $\tau$  were calculated as described in the methods section. For AMPA receptors the  $\tau$  value was 18.5 ms (± 1.4 ms, *n* = 19) for *Dasm1*<sup>+/+</sup> mice and did not significantly differ from *Dasm1*<sup>-/-</sup> mice with a  $\tau$  value of 16.2 ms (± 1.0 ms, *n* = 23, *p* > 0.05; see Figure 6.3a). NMDA receptor decay time constants were also not significantly altered in *Dasm1*<sup>-/-</sup> mice (101.2 ms ± 2.8 ms, *n* = 20), when compared to *Dasm1*<sup>+/+</sup> mice (109.5 ms ± 3.2 ms, *n* = 12, *p* > 0.05, see 6.3c). This suggests that other receptor properties are altered in *Dasm1*<sup>-/-</sup> mice causing the elevated AMPA/NMDA ratio.

Decay time constants of AMPA and NMDA receptors in *Dasm1*<sup>+/+</sup> and *Dasm1*<sup>ΔC/ΔC</sup> mice were as expected not different (Figure 6.3b, d;  $\tau$  ± SEM for AMPA receptors: *Dasm1*<sup>+/+</sup>, 19.1 ± 1.3, *n* = 11; *Dasm1*<sup>ΔC/ΔC</sup>, 18.7 ± 1.9, *n* = 12, *p* > 0.05; for NMDA receptors: *Dasm1*<sup>+/+</sup>, 115.1 ms ± 5.1 ms, *n* = 11; *Dasm1*<sup>ΔC/ΔC</sup>, 110.2 ms ± 3.9 ms, *n* = 12, *p* > 0.05).

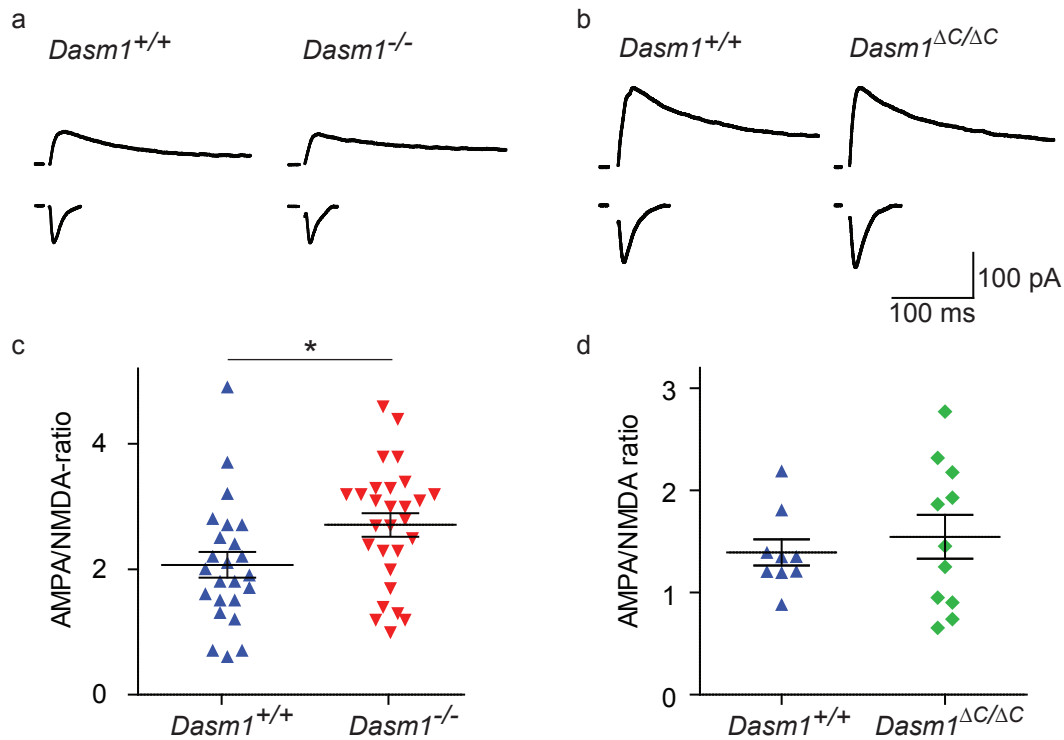


**Figure 6.2:** AMPA/NMDA ratio is elevated in *Dasm1*<sup>-/-</sup> mice, but not in *Dasm1*<sup>ΔC/ΔC</sup> mice. (a and b) Example traces of AMPA and NMDA receptor mediated currents in *Dasm1*<sup>+/+</sup> *Dasm1*<sup>-/-</sup> mice and *Dasm1*<sup>+/+</sup> *Dasm1*<sup>ΔC/ΔC</sup> mice, respectively. (c) AMPA/NMDA ratio from *Dasm1*<sup>-/-</sup> mice ( $n = 28$  cells) was significantly elevated compared to *Dasm1*<sup>+/+</sup> mice ( $n = 24$ ). Unpaired t-test  $p < 0.05$ . (d) In contrast, AMPA/NMDA ratio from *Dasm1*<sup>ΔC/ΔC</sup> mice ( $n = 12$ ) was not different compared to *Dasm1*<sup>+/+</sup> mice ( $n = 10$ ). Error bars represent SEM in all graphs.

### 6.2.2 Miniature excitatory postsynaptic currents (mEPSCs)

As the elevated AMPA/NMDA ratio can not be explained by alterations of the decay time constants of the receptors, I asked whether the number or size of AMPA receptor containing synapses was altered. Therefore, miniature excitatory postsynaptic currents (mEPSCs) were recorded at the resting membrane potential of -70 mV and in the presence of 1.3 mM MgCl<sub>2</sub>, 100 μM PTX and 200 nM tetrodotoxin (TTX). The main active receptor in these recording conditions is the AMPA receptor, because magnesium blocks NMDA receptors at the resting membrane potential and PTX avoids inhibitory currents. TTX is added to block action-potential driven release and thus only spontaneous fusion events of presynaptic vesicles can occur. Alterations in the frequency of AMPA receptor mediated miniature excitatory postsynaptic currents (EPSCs) are generally believed to reflect changes in the number of

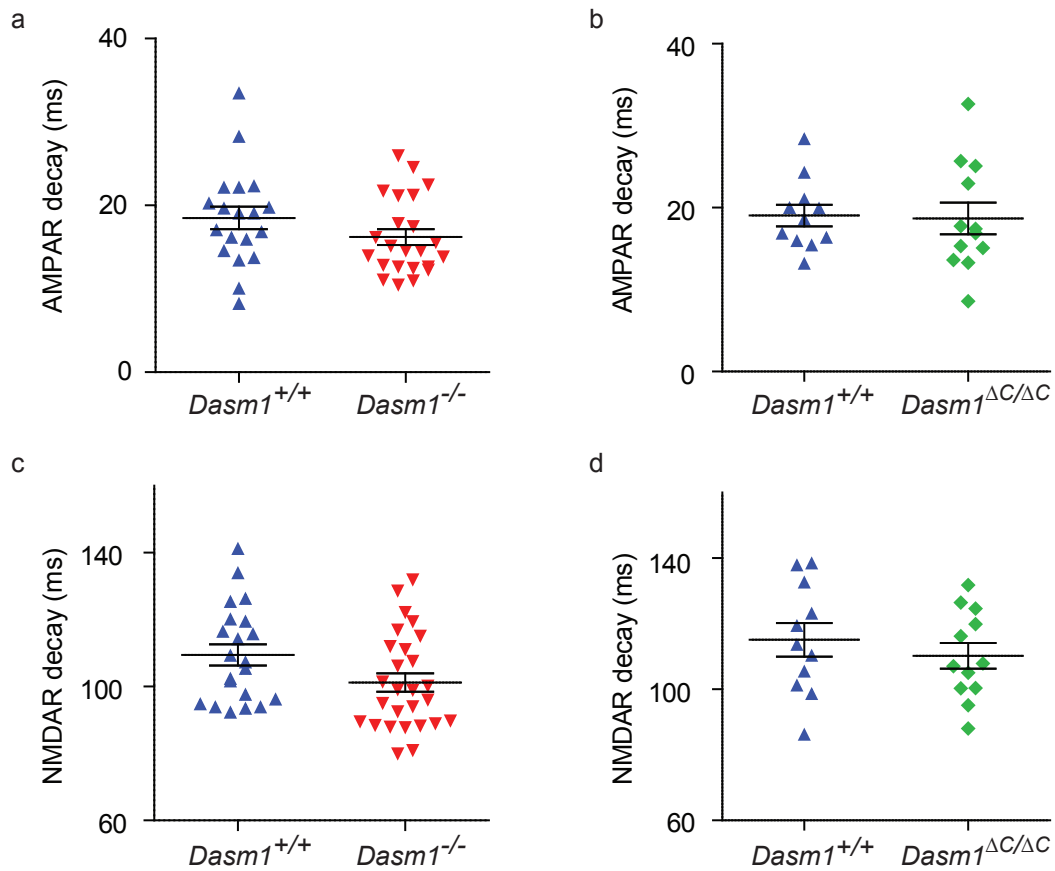


**Figure 6.3: Decay kinetics of AMPA and NMDA receptor mediated currents are not altered. (a and b)** AMPA receptor decay time constants of *Dasm1*<sup>+/+</sup>/*Dasm1*<sup>-/-</sup> mice and *Dasm1*<sup>+/+</sup>/*Dasm1*<sup>ΔC/ΔC</sup> mice, respectively. **(c and d)** NMDA receptor decay time constants of *Dasm1*<sup>+/+</sup>/*Dasm1*<sup>-/-</sup> mice and *Dasm1*<sup>+/+</sup>/*Dasm1*<sup>ΔC/ΔC</sup> mice, respectively. Error bars represent SEM in all graphs.

synapses, whereas alterations in the amplitudes suggest different quantity of receptors per synapse.

Miniature EPSCs were recorded in young (P7-8, Figure 6.4a, c, e) and juvenile mice (P15-20, Figure 6.4b, d, f). Neither amplitudes, nor frequencies of mEPSCs were different in *Dasm1*<sup>-/-</sup> mice compared to *Dasm1*<sup>+/+</sup> littermates (P7-8, mean frequency  $\pm$  SEM: *Dasm1*<sup>+/+</sup>,  $0.4 \pm 0.1$  Hz,  $n = 23$ ; *Dasm1*<sup>-/-</sup>,  $0.4 \pm 0.0$  Hz,  $n = 16$ ,  $p = 1$ ; mean amplitude  $\pm$  SEM: *Dasm1*<sup>+/+</sup>,  $14.3 \pm 3.8$  pA,  $n = 23$ ; *Dasm1*<sup>-/-</sup>,  $14.0 \pm 0.5$  pA,  $n = 16$ ,  $p = 1$ ; P15-20, mean frequency  $\pm$  SEM: *Dasm1*<sup>+/+</sup>,  $0.7 \pm 0.1$  Hz,  $n = 11$ ; *Dasm1*<sup>-/-</sup>,  $0.7 \pm 0.1$  Hz,  $n = 17$ ,  $p = 1$ ; mean amplitude  $\pm$  SEM: *Dasm1*<sup>+/+</sup>,  $13.8 \pm 0.7$  pA,  $n = 11$ ; *Dasm1*<sup>-/-</sup>,  $13.2 \pm 0.3$  pA,  $n = 17$ ,  $p = 1$ , K-S test), suggesting unaltered number and size of AMPA receptor containing synapses.

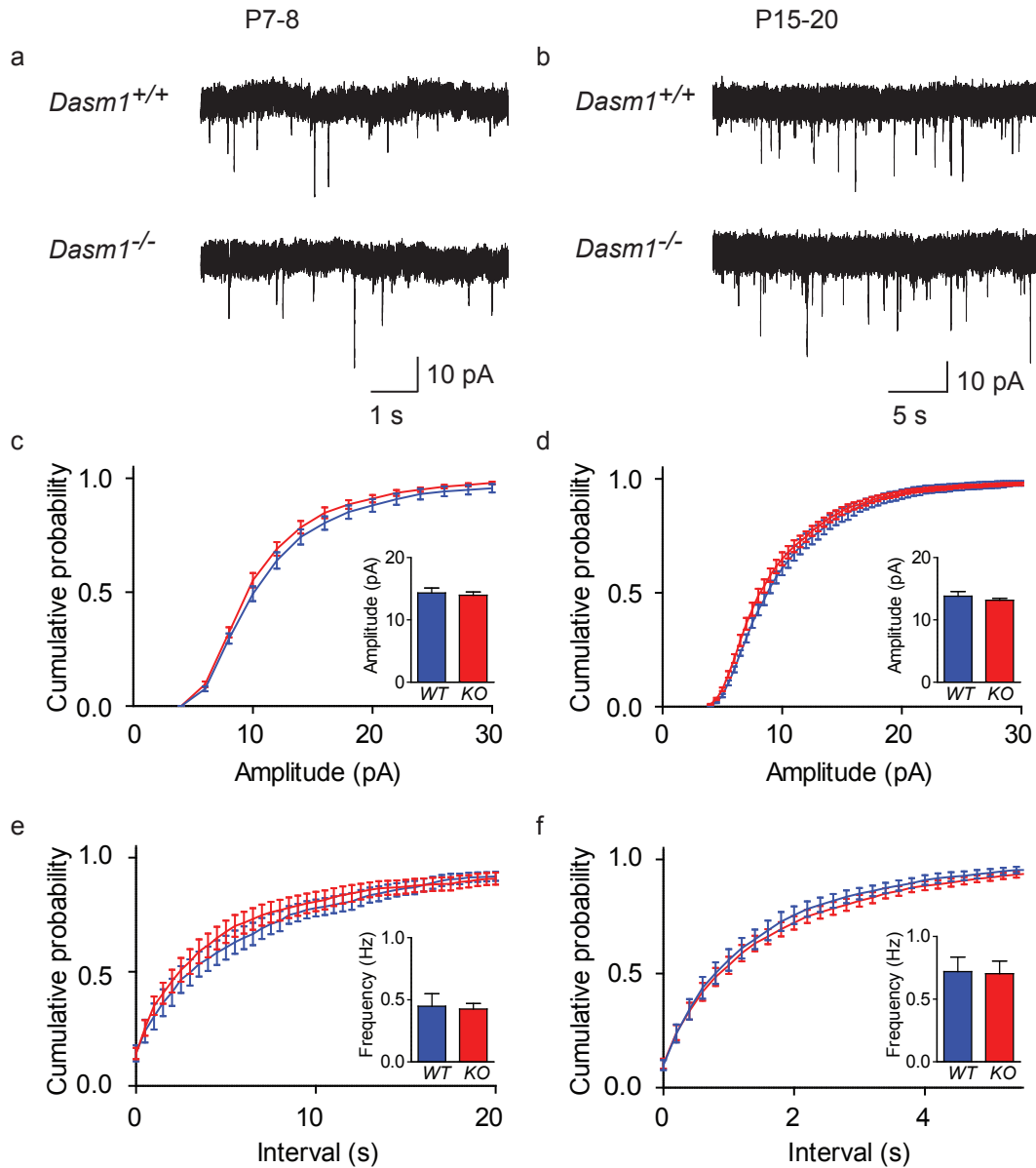


**Figure 6.4: Miniature excitatory postsynaptic currents (mEPSCs) are not different in P7-8 and P15-20 *Dasm1*<sup>+/+</sup> and *Dasm1*<sup>-/-</sup> littermates.** (a and b) Example traces of mEPSCs of P7-8 and P15-20 mice, respectively. (c and e) Cumulative distribution plots for amplitudes (c), and frequencies (e) of P7-8 mice (blue: *Dasm1*<sup>+/+</sup>  $n = 23$  and red: *Dasm1*<sup>-/-</sup>  $n = 16$ ). Insets show mean amplitude or frequency. (d and f) Cumulative distribution plots for amplitudes (d), and frequencies (f) of P15-20 mice (blue: *Dasm1*<sup>+/+</sup>  $n = 11$  and red: *Dasm1*<sup>-/-</sup>  $n = 17$ ). Insets show mean amplitude or frequency. Error bars represent SEM in all graphs.

### 6.2.3 Paired pulse ratio (PPR) of evoked AMPA receptor mediated currents

Alterations in the AMPA/NMDA ratio might also be attributed to presynaptic changes. Presynaptic release probability is commonly tested with the so-called paired pulse stimulation paradigm. Applying two consecutive pulses with a short inter stimulus interval leads upon the second pulse either to an elevated response (paired pulse facilitation, PPF) or a decreased response (paired pulse depression, PPD). PPF is caused by presynaptic calcium accumulation, which primes more vesicles to fuse upon the second pulse (Neher and Sakaba, 2008; Katz and Miledi, 1968). Depletion of the ready releasable pool within the first pulse causes PPD (Foster and Regehr, 2004). I tested, whether the presynaptic release machinery functions properly by applying two consecutive stimuli with different inter stimulus intervals (ISI of 20 ms, and 40 ms; see example traces in Figure 6.5a, and c, respectively). To calculate the paired pulse ratio (PPR), the amplitude of the second peak was divided by the amplitude of the first peak.

The PPR with the ISI of 20 ms (mean  $\pm$  SEM, *Dasm1*<sup>+/+</sup>,  $1.2 \pm 0.1$ ,  $n = 12$ ; *Dasm1*<sup>-/-</sup>,  $1.4 \pm 0.1$ ,  $n = 15$ ) as well as the ISI of 40 ms (*Dasm1*<sup>+/+</sup>,  $2.0 \pm 0.1$ ,  $n = 25$ ; *Dasm1*<sup>-/-</sup>,  $2.0 \pm 0.1$ ,  $n = 28$ ,  $p > 0.05$ ) was not altered (see Figure 6.5), suggesting that the presynaptic glutamate release machinery is not influenced by *Dasm1*.

### 6.2.4 Isolated NMDA receptor mediated fEPSPs

As the elevated AMPA/NMDA ratio cannot be explained by alterations of the AMPA receptor mediated currents, the NMDA receptor mediated currents were examined in more detail. Blocking the AMPA receptor with its specific antagonist NBQX (1,2,3,4-Tetrahydro-6-nitro-2,3-dioxo-benzo[f]quinoxaline-7-sulfonamide) reduces fEPSPs massively (see Figure 5.2a in material and methods section). NMDA receptor fEPSP are slower compared to compound fEPSP which consist of AMPA and NMDA receptor mediated currents.

Plotting the isolated NMDA receptor fEPSPs input-output curves (FV against slope) of *Dasm1*<sup>+/+</sup> and *Dasm1*<sup>-/-</sup> mice revealed no difference (see Figure 6.6), suggesting normal NMDA receptor transmission. However, as the resolution of fEPSPs is limited, isolated NMDA receptor mediated currents were recorded.

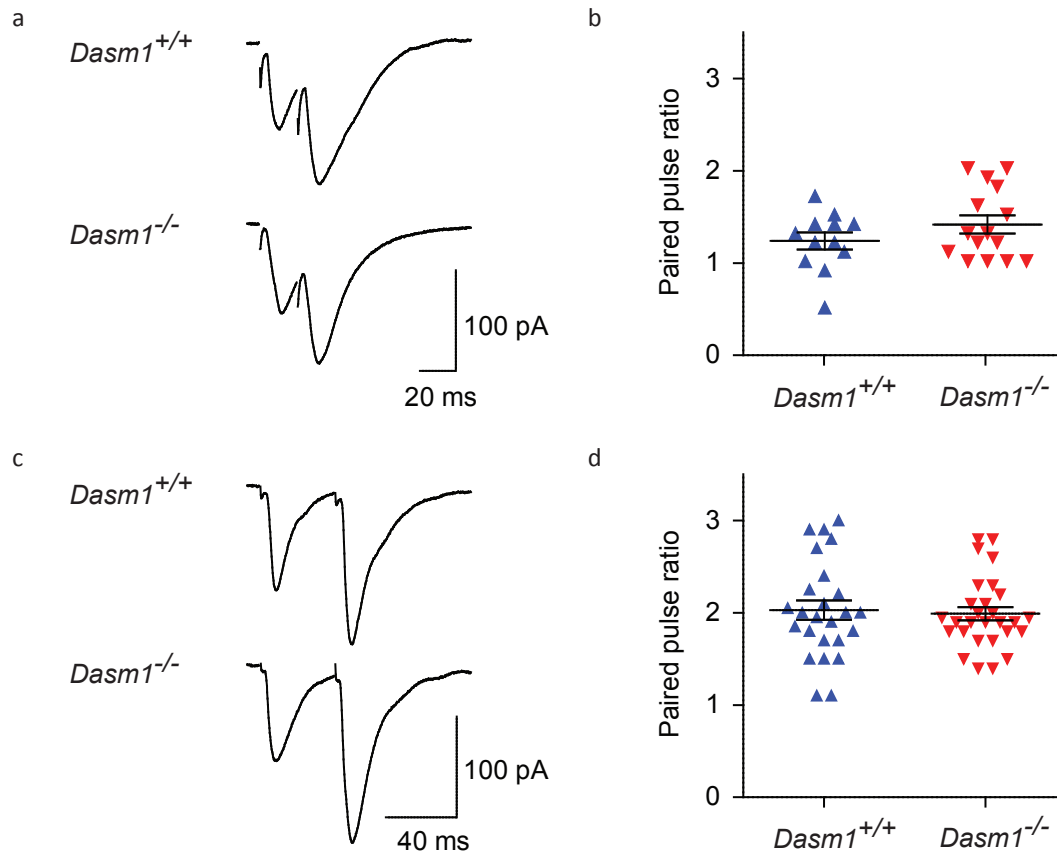


**Figure 6.5: Paired pulse ratio for evoked AMPA receptor currents is not altered.** (a and c) Example traces of paired pulse stimulation with an inter event interval of 20 ms and 40 ms in  $Dasm1^{+/+}$  and  $Dasm1^{-/-}$  mice. (b and d) Quantification of the paired pulse stimulation for the 20 ms and 40 ms interval, respectively. Error bars represent SEM.

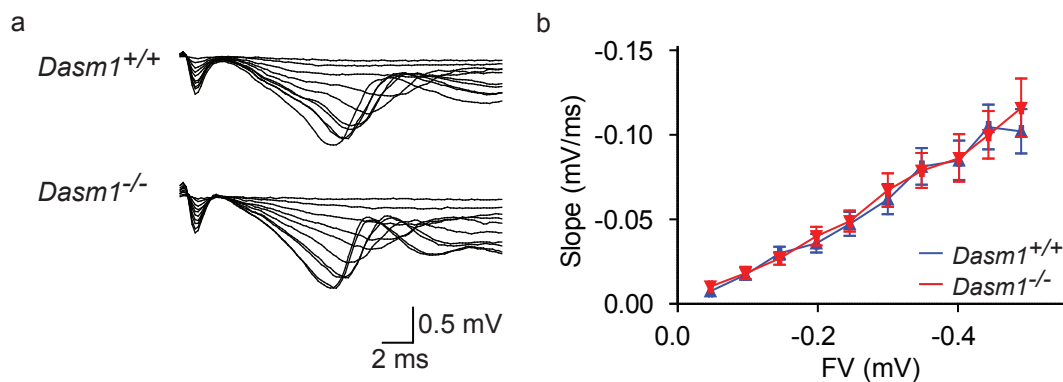


**Figure 6.6: NMDA receptor fEPSPs are not altered.** (a) NMDA receptor fEPSPs example traces of  $Dasm1^{+/+}$  and  $Dasm1^{-/-}$  mice. (b) Input-output curves of isolated NMDA receptor fEPSPs. Shown is the fiber volley plotted against the slope of the NMDA receptor fEPSP ( $Dasm1^{+/+}$   $n = 23$ ;  $Dasm1^{-/-}$   $n = 24$ ). Error bars represent SEM.

### 6.2.5 Isolated decay time constant of NMDA receptors

To analyze NMDA receptor kinetics in more detail, I decided to single out NMDA receptor currents pharmacologically, in order to circumvent contamination by AMPA receptor mediated currents. NMDA receptor currents were isolated by recording at a holding potential of +40 mV in the presence of 10  $\mu$ M NBQX to block AMPA receptors and in the presence of low MgCl<sub>2</sub> (0.1 mM) to avoid the magnesium block of NMDA receptors. Previous recordings of NMDA receptor mediated currents were performed in the absence of AMPA receptor blockers and normal MgCl<sub>2</sub> concentration (see Figure 6.2e and f).

The mean  $\tau$  value for *Dasm1*<sup>+/+</sup> was 254.0 ms  $\pm$  9.8 ms ( $n = 12$ ) and did not significantly differ from *Dasm1*<sup>-/-</sup> mice (278.1 ms  $\pm$  13.5 ms,  $n = 20$ ,  $p > 0.05$ ) as shown in Figure 6.7d. This suggests, that NMDA receptor subunit composition, which is responsible for decay time constant, is unaltered.

### 6.2.6 Current-voltage relationship (IV) and conductance (G) of the NMDA receptor

Reduced NMDA receptor mediated currents could also be caused by different conductances of the NMDA receptors. To evaluate these alternatives, the current-voltage (IV) relationship was examined. For this purpose, NMDA receptor mediated currents were evoked at different holding potentials (see Figure 6.7c).

Plotting the current-voltage relationship (Figure 6.7d) and the conductance  $G (= 1/R)$  (Figure 6.7e) of the NMDA receptor did not reveal any difference between *Dasm1*<sup>+/+</sup> mice ( $n = 8$ ) and *Dasm1*<sup>-/-</sup> mice ( $n = 14$ ), suggesting normal functions of NMDA receptors. The reason for the significantly elevated AMPA/NMDA ratio therefore remains elusive, but might be caused by the number of receptors per synapse.

## 6.3 Field Plasticity Paradigms

Disturbances in glutamatergic synaptic transmission can alter the ability of synapses to adapt its strength, which is called synaptic plasticity. As the NMDA receptor plays a pivotal role in plasticity, I asked, whether long term potentiation (LTP) was impaired. To assess short term plasticity, paired pulse stimulation testing for presynaptic release probabilities was examined.

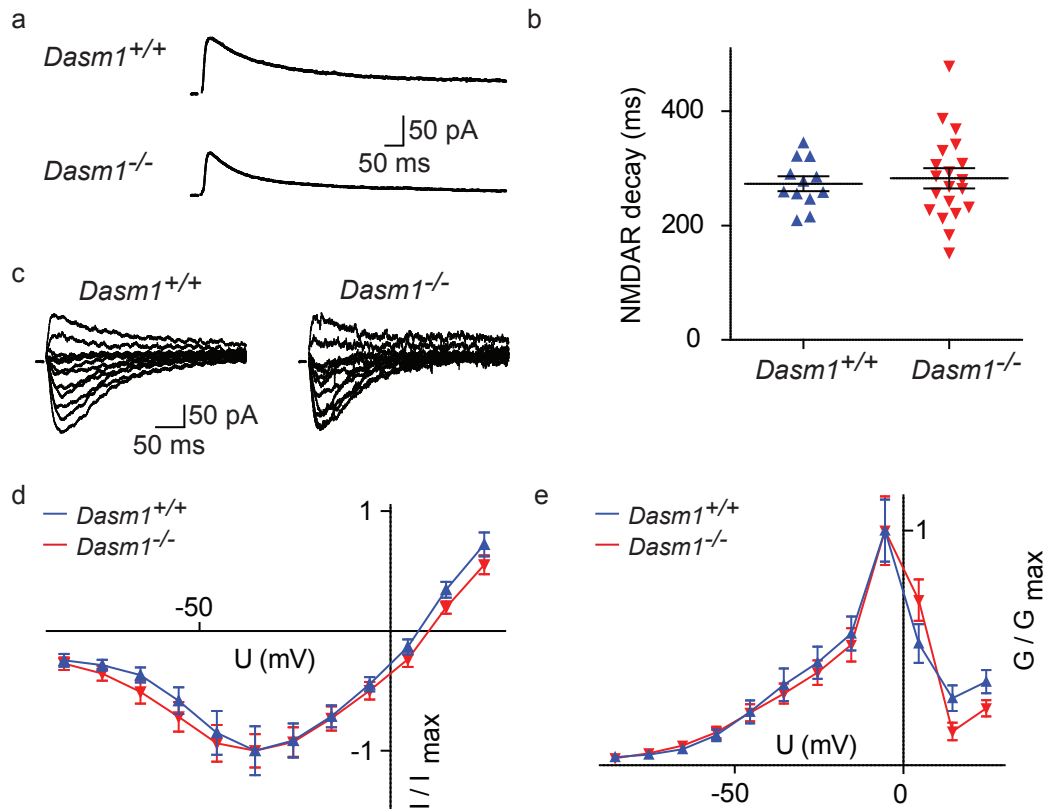


**Figure 6.7: NMDA receptor mediated synaptic transmission is not altered in *Dasm1*<sup>-/-</sup> mice.** (a) Example traces of isolated NMDA receptor mediated currents. (b) Quantification of the decay time constant of evoked isolated NMDA receptor currents. (c) Example traces of isolated NMDA receptor currents at different holding potentials. (d) Quantification of the current-voltage relationship (IV) of NMDA receptor currents. Data were normalized to the NMDA receptor current at -40 mV and corrected with the liquid junction potential. (e) Quantification of the conductance of the NMDA receptor currents from Figure 6.7d. Error bars represent SEM in all graphs.

### 6.3.1 Long term potentiation (LTP)

Stimulating synapses with strong stimuli leads to long lasting changes in synaptic strength by incorporating additional receptors into the synapses. This phenomenon is called long term potentiation and is believed to be the basis for learning and memory. Brief tetanic stimuli are able to induce long lasting higher field responses as prior to induction (see Figure 6.8a). The pre-stimulus strength was chosen such that the fEPSP was half-maximal. After recording the pre-stimulus condition for 20 minutes, two trains of 100 Hz stimuli separated by 20 seconds were applied to Schaffer collateral axons. The average slope of the fEPSP during the last ten minutes prior to induction was compared to the average fEPSP slope 50 minutes to 60

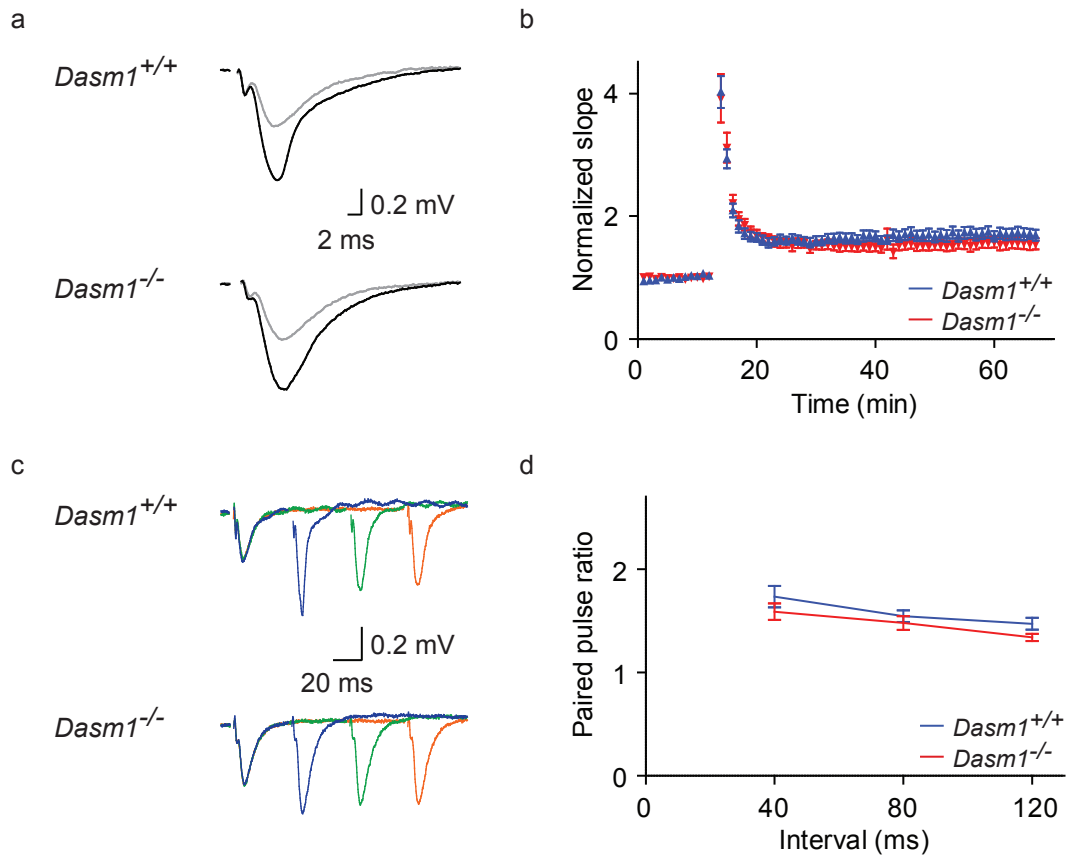


**Figure 6.8: Plasticity is not altered in *Dasm1*<sup>-/-</sup> mice.** (a) Example traces of a fEPSP before (gray) and after (black) induction of long term potentiation (LTP) with tetanic stimulation in acute P15-20 hippocampal slices. (b) Quantification of LTP, normalized to the last ten minutes before tetanic induction of LTP (blue: *Dasm1*<sup>+/+</sup>  $n = 16$  and red: *Dasm1*<sup>-/-</sup>  $n = 14$ ) (c) Example traces of field paired pulse stimulation with different inter stimulus intervals (blue: 40 ms, green: 80 ms, and orange: 120 ms). (d) To quantify the paired pulse ratio, the slope of the second peak was divided by the slope of the first peak (blue: *Dasm1*<sup>+/+</sup>  $n = 19$  and red: *Dasm1*<sup>-/-</sup>  $n = 14$ ). Error bars represent SEM in all graphs.

minutes after induction.

No difference in tetanic LTP was observed when comparing *Dasm1*<sup>-/-</sup> with *Dasm1*<sup>+/+</sup> mice (see Figure 6.8b), suggesting normal synaptic plasticity.

### 6.3.2 Field paired pulse ratio

Paired pulse stimulation is a protocol for testing short term plasticity. Two consecutive stimuli with a short inter stimulus interval (40 ms, 80 ms, and 120 ms) were delivered to Schaffer collateral axons and the postsynaptic response was compared afterwards. It is believed, that mainly presynaptic mechanisms such as the release probability and the size of the readily

releasable pool contribute to this form of short term plasticity. Paired pulse stimulation was tested with various inter stimulus intervals in P15-20 mice (see Figure 6.8c). The field paired pulse ratio (PPR) is calculated by dividing the slope of the second fEPSP by the first fEPSP. The PPR was always above one, pointing to a paired pulse facilitation (Figure 6.8d) and was not different in *Dasm1*<sup>-/-</sup> mice when compared to *Dasm1*<sup>+/+</sup> littermates, suggesting normal presynaptic release properties.

## 6.4 GABAergic system

Normal brain function requires a balance of excitation to inhibition, hence, I examined  $\gamma$ -aminobutyric acid (GABAergic) synapses, which make up the bulk of inhibitory synapses in hippocampus.

### 6.4.1 Miniature inhibitory postsynaptic currents (mIPSCs) in *Dasm1*<sup>-/-</sup> mice

GABAergic miniature inhibitory postsynaptic currents (mIPSCs) were pharmacologically isolated by blocking glutamatergic synaptic transmission with NBQX and (2R)-amino-5-phosphonopentanoate (APV) to block AMPA and NMDA receptors, respectively. TTX was added to block action potential-driven events.

Surprisingly, frequencies, but not amplitudes of mIPSCs were markedly reduced in P15-20 *Dasm1*<sup>-/-</sup> mice compared to *Dasm1*<sup>+/+</sup> mice (Figure 6.9b, d and f, mean frequency  $\pm$  SEM: *Dasm1*<sup>+/+</sup>,  $7.4 \pm 0.3$  Hz,  $n = 20$ ; *Dasm1*<sup>-/-</sup>,  $6.4 \pm 0.2$  Hz,  $n = 36$ ,  $p = 0.01$ ; mean amplitude  $\pm$  SEM: *Dasm1*<sup>+/+</sup>,  $38.1 \pm 2.2$  pA,  $n = 20$ ; *Dasm1*<sup>-/-</sup>,  $40.2 \pm 1.5$  pA,  $n = 36$ ,  $p = 1$ , Kolmogorov-Smirnov (K-S) test).

As protein levels of Dasm1 typically decline during early postnatal maturation of the brain (see Figure 4.5), I asked whether the observed phenotype might be more pronounced in younger mice.

Indeed, frequencies of mIPSCs were dramatically reduced in P5-6 mice, whereas the amplitudes were again not altered (Figure 6.9a, c and e, mean frequency  $\pm$  SEM: *Dasm1*<sup>+/+</sup>,  $0.6 \pm 0.1$  Hz,  $n = 31$ ; *Dasm1*<sup>-/-</sup>,  $0.2 \pm 0.0$  Hz,  $n = 30$ ,  $p < 0.001$ ; mean amplitude  $\pm$  SEM: *Dasm1*<sup>+/+</sup>,  $30.5 \pm 1.3$  pA,  $n = 31$ ; *Dasm1*<sup>-/-</sup>,  $30.3 \pm 1.9$  pA,  $n = 30$ ,  $p = 1$ , K-S test). Reduced frequency of mIPSCs points to a loss of GABAergic inhibitory synapses. However, to exclude that altered presynaptic release probabilities cause the observed phenotype, paired pulse

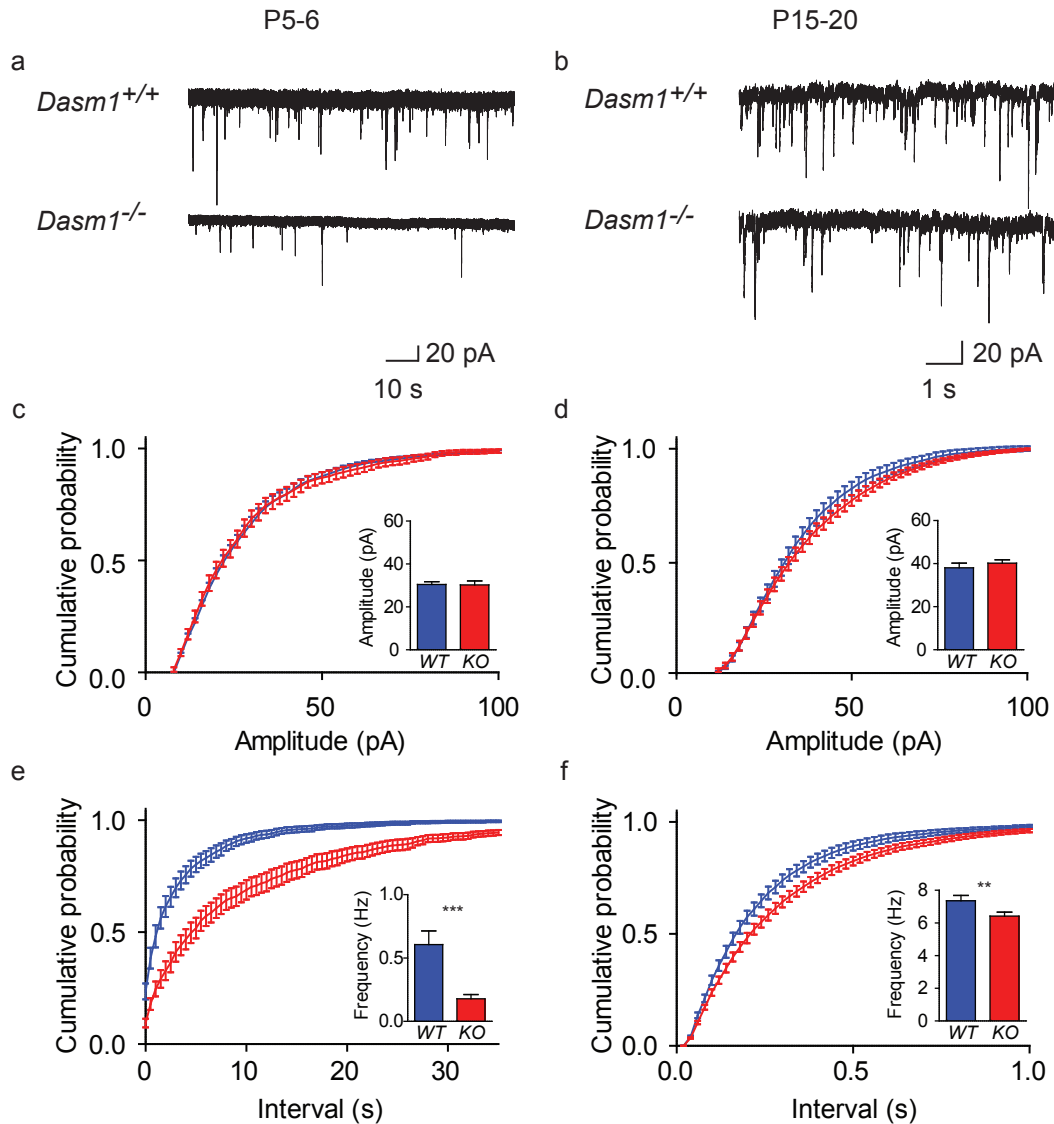


**Figure 6.9: Frequencies but not amplitudes of miniature inhibitory postsynaptic currents (mIPSCs) are significantly reduced in P5-6 as well as in P15-20 *Dasm1*<sup>-/-</sup> mice. (a and b) Example traces of mIPSCs of P5-6 mice and P15-10 mice, respectively. (c and e) Cumulative distribution plots of frequencies (e), but not amplitudes (c) of P5-6 mice (*Dasm1*<sup>+/+</sup>  $n = 31$  and *Dasm1*<sup>-/-</sup>  $n = 30$ ) were significantly reduced (Kolmogorov-Smirnov  $n < 0.001$ ). Insets show mean amplitude or frequency. (d and f) Also in P15-20 mice (*Dasm1*<sup>+/+</sup>  $n = 20$  and *Dasm1*<sup>-/-</sup>  $n = 36$ ) frequencies (f), but not amplitudes (d) were significantly reduced (Kolmogorov-Smirnov  $p < 0.01$ ). Insets show mean amplitude or frequency. Error bars represent SEM in all graphs. Note the different scaling of the x-axis in e and f.**

stimulation experiments of evoked inhibitory postsynaptic currents were also assessed (see chapter 6.4.9).

### 6.4.2 mIPSCs in *Dasm1*<sup>ΔC/ΔC</sup> mice

I could show that the intracellular C-terminus is not responsible for the elevated AMPA/NMDA ratio in *Dasm1*<sup>-/-</sup> mice (see Figure 6.2). I next assessed, whether the N-terminus is also necessary and sufficient to rescue the diminished frequencies of mIPSCs.

Indeed, neither frequencies, nor amplitudes of both young (P5-6) and juvenile (P15-20) mice were altered when comparing *Dasm1*<sup>+/+</sup> with *Dasm1*<sup>ΔC/ΔC</sup> littermates (Figure 6.10, P5-6, mean frequency ± SEM: *Dasm1*<sup>+/+</sup>, 0.1 ± 0.0 Hz, *n* = 12; *Dasm1*<sup>ΔC/ΔC</sup>, 0.2 ± 0.1 Hz, *n* = 14, *p* = 1; mean amplitude ± SEM: *Dasm1*<sup>+/+</sup>, 30.5 ± 1.9 pA, *n* = 12; *Dasm1*<sup>ΔC/ΔC</sup>, 32.5 ± 1.3 pA, *n* = 14, *p* = 1; P15-20, mean frequency ± SEM: *Dasm1*<sup>+/+</sup>, 4.7 ± 0.4 Hz, *n* = 11; *Dasm1*<sup>ΔC/ΔC</sup>, 5.1 ± 0.6 Hz, *n* = 11, *p* = 1; mean amplitude ± SEM: *Dasm1*<sup>+/+</sup>, 32.3 ± 2.1 pA, *n* = 11; *Dasm1*<sup>ΔC/ΔC</sup>, 31.7 ± 1.3 pA, *n* = 11, *p* = 1; K-S test), suggesting that only the absence of the N-terminal extracellular part of the protein is responsible for the reduced mIPSC frequencies.

### 6.4.3 Spontaneous inhibitory postsynaptic currents (sIPSCs) in *Dasm1*<sup>-/-</sup> mice

Miniature IPSCs reflect the non-activity driven fusion of presynaptic vesicles with the presynaptic membrane which occurs spontaneously. I asked whether the observed phenotype is also present when activity driven events are included. These spontaneous IPSCs are recorded in the absence of TTX.

Also sIPSCs had significantly reduced frequencies, whereas the amplitudes were again not altered in P15-20 mice (Figure 6.11b, d, and f, mean frequency ± SEM: *Dasm1*<sup>+/+</sup>, 7.1 ± 0.5 Hz, *n* = 27; *Dasm1*<sup>-/-</sup>, 4.9 ± 0.3 Hz, *n* = 22, *p* < 0.01; mean amplitude ± SEM: *Dasm1*<sup>+/+</sup>, 42.2 ± 6.2 pA, *n* = 27; *Dasm1*<sup>-/-</sup>, 37.6 ± 5.0 pA, *n* = 22, *p* = 1, K-S test).

The developmental phenotype of reduced mIPSCs led me hypothesize, that also sIPSCs of young mice would exhibit a reduced frequency. These experiments were performed with P7-8 mice, because at earlier developmental stages the neuronal network is not mature enough to have sufficient events within several minutes to statistically proof the hypothesis.

Again frequencies, but not amplitudes of sIPSCs in P7-8 mice were significantly reduced (Figure 6.11a, c, and e, mean frequency ± SEM: *Dasm1*<sup>+/+</sup>, 1.4 ± 0.1 Hz, *n* = 18; *Dasm1*<sup>-/-</sup>, 0.9 ± 0.1 Hz, *n* = 17, *p* < 0.01; mean amplitude ± SEM: *Dasm1*<sup>+/+</sup>, 40.7 ± 2.6 pA, *n* = 18;

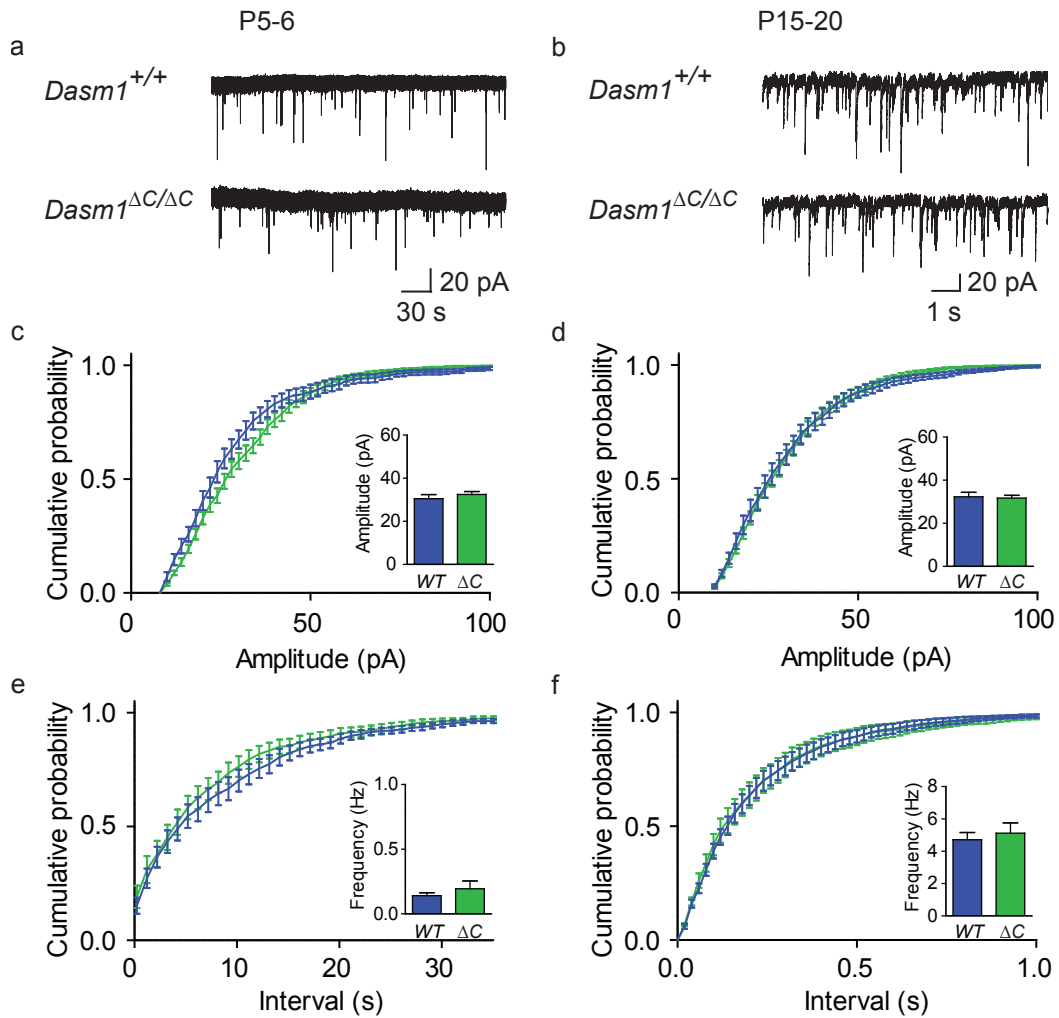


**Figure 6.10: Neither frequencies, nor amplitudes of mIPSCs are different in *Dasm1*<sup>ΔC/ΔC</sup> mice (P5-6 and P15-20).** (a and b) Example traces of mIPSCs of P5-6 mice, and P15-20 mice, respectively. (c and e) Cumulative distribution plots of the amplitudes (c), and frequencies (e) of P5-6 mice (blue: *Dasm1*<sup>+/+</sup> *n* = 12 and green: *Dasm1*<sup>ΔC/ΔC</sup> *n* = 14; K-S *p* values for amplitudes: *p* = 1 and intervals: *p* > 0.1). Insets show mean amplitude or frequency. (d and f) Cumulative distribution plots of the amplitudes (d), and frequencies (f) of P15-20 mice (blue: *Dasm1*<sup>+/+</sup> *n* = 11 and green: *Dasm1*<sup>ΔC/ΔC</sup> *n* = 11; K-S test for amplitudes and intervals: *p* = 1). Insets show mean amplitude or frequency. Error bars represent SEM in all graphs.

*Dasm1*<sup>-/-</sup>, 49.0 ± 4.2 pA, *n* = 17, *p* = 1, K-S test).

#### 6.4.4 sIPSCs in *Dasm1*<sup>ΔC/ΔC</sup> mice

To elucidate, whether the extracellular N-terminus is responsible for the observed reduction of frequency, I recorded spontaneous IPSCs in *Dasm1*<sup>ΔC/ΔC</sup> mice.

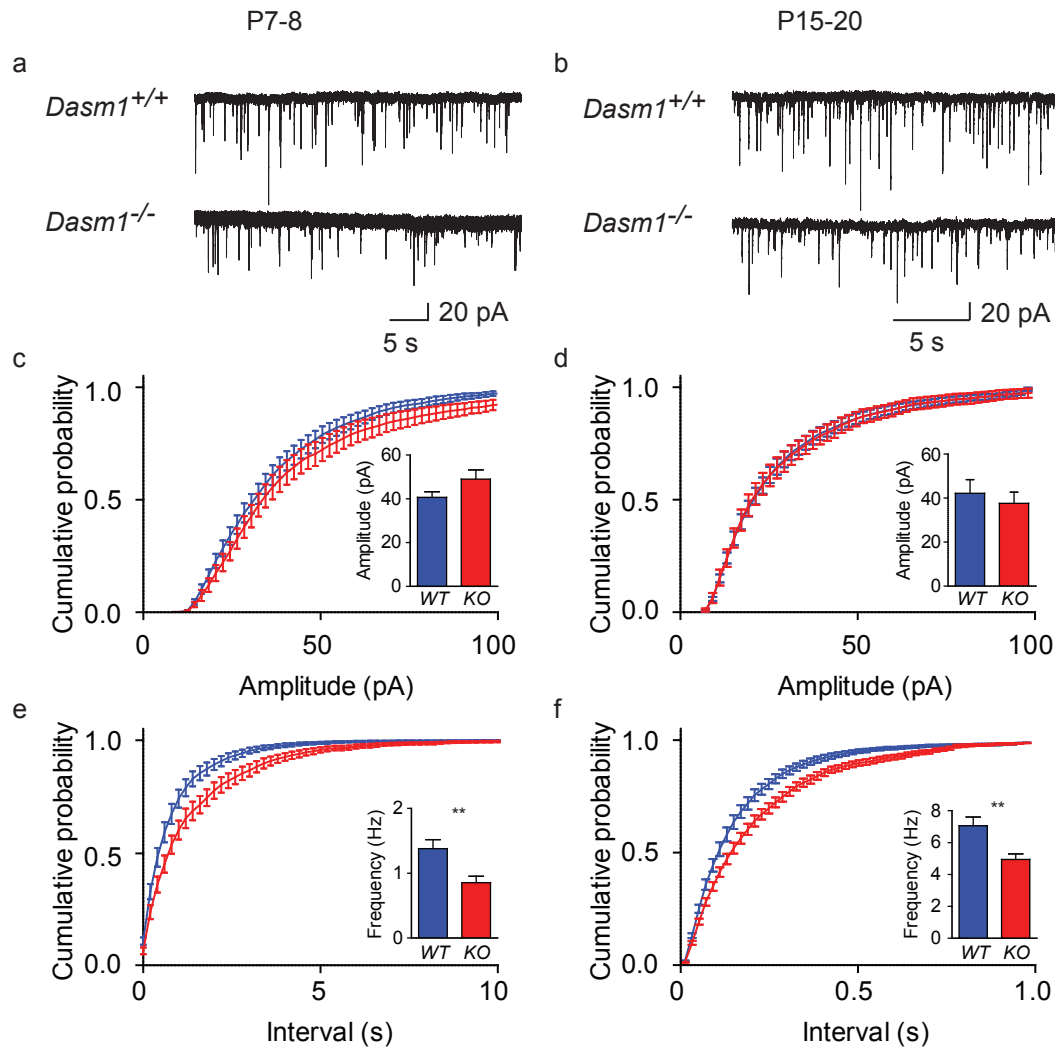


**Figure 6.11: Frequencies but not amplitudes of spontaneous inhibitory postsynaptic currents (sIPSCs) are significantly reduced in P7-8 as well as in P15-20 *Dasm1*<sup>-/-</sup> mice.** (a and b) Example traces of sIPSCs of P7-8, and P15-20, respectively. (c and e) Cumulative distribution plots of frequencies (e), but not amplitudes (c) of P7-8 mice (*Dasm1*<sup>+/+</sup>  $n = 18$  and *Dasm1*<sup>-/-</sup>  $n = 17$ ) were significantly reduced (Kolmogorov-Smirnov  $p < 0.01$ ). Insets show mean amplitude or frequency. (d and f) Also in P15-20 mice (*Dasm1*<sup>+/+</sup>  $n = 27$  and *Dasm1*<sup>-/-</sup>  $n = 22$ ) frequencies (f) but not amplitudes (d) were significantly different (Kolmogorov-Smirnov  $p < 0.01$ ). Note the different scaling of the x-axis in e and f. Insets show mean amplitude or frequency. Error bars represent SEM in all graphs.

Again, only the N-terminal part of *Dasm1* including the transmembrane domain is necessary to rescue decreased frequency of sIPSCs (Figure 6.12, mean frequency  $\pm$  SEM: *Dasm1*<sup>+/+</sup>,  $0.5 \pm 0.1$  Hz,  $n = 22$ ; *Dasm1* <sup>$\Delta C/\Delta C$</sup> ,  $0.7 \pm 0.1$  Hz,  $n = 18$ ,  $p = 1$ ; mean amplitude  $\pm$  SEM: *Dasm1*<sup>+/+</sup>,  $37.0 \pm 2.5$  pA,  $n = 22$ ; *Dasm1* <sup>$\Delta C/\Delta C$</sup> ,  $39.9 \pm 5.0$  pA,  $n = 18$ ,  $p = 1$ ; K-S test).

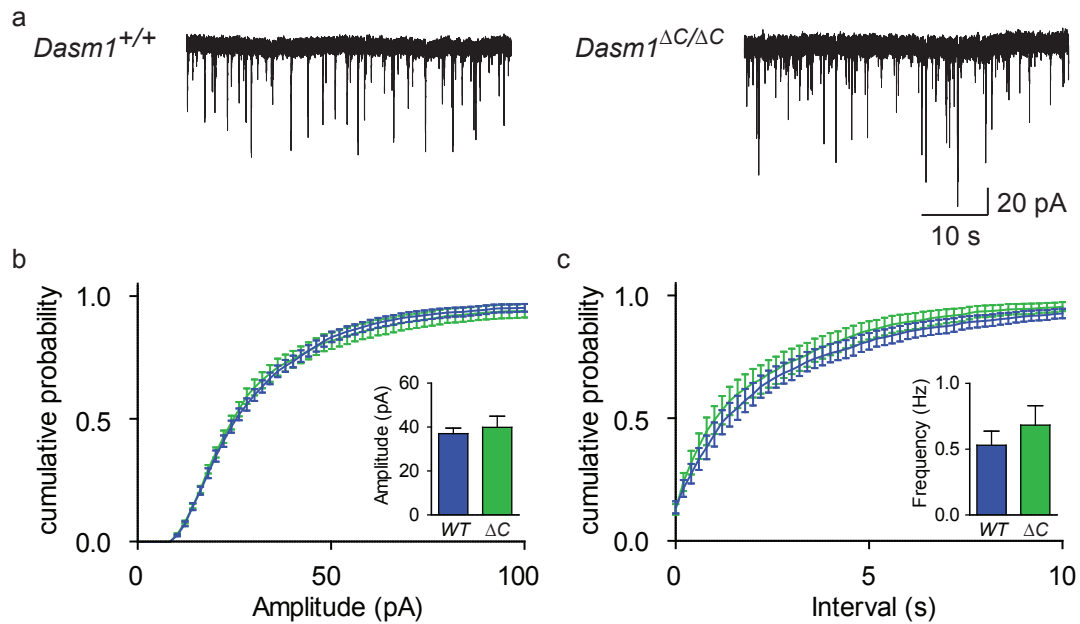


**Figure 6.12: Neither frequencies, nor amplitudes of sIPSCs are different in *Dasm1*<sup>ΔC/ΔC</sup> mice (P7-8).** (a) Example traces of sIPSCs of P7-8 mice. (b and c) Cumulative distribution plots of the amplitudes (b), and frequencies (c) of P7-8 mice (blue: *Dasm1*<sup>+/+</sup>  $n = 22$  and green: *Dasm1*<sup>ΔC/ΔC</sup>  $n = 18$ ; K-S values for amplitudes ( $p = 1$ ) and intervals ( $p = 1$ ) were not significantly different). Insets show mean amplitude or frequency. Error bars represent SEM in all graphs.

#### 6.4.5 *Dasm1* is present in hippocampal interneurons

We next asked whether *Dasm1* is present in interneurons, as this seems the place where *Dasm1* acts. Therefore, hippocampal neurons of GAD65-GFP mice (Lopez-Bendito et al., 2004) expressing green fluorescent protein (GFP) under the control of glutamic acid decarboxylase 65 (GAD65) were isolated. GAD65 is the enzyme that produces the inhibitory neurotransmitter GABA and therefore is only present in interneurons and hence, GFP positive cells of these mice are interneurons. Isolated

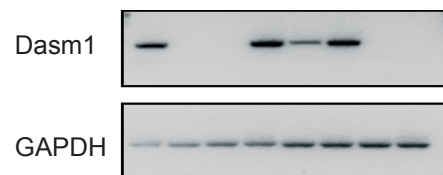


**Figure 6.13: RT-PCR on GAD65-GFP-positive neurons suggests, that *Dasm1* is present in interneurons.** *Dasm1* (upper lane) is expressed in a subset of GAD65-GFP interneurons (GAPDH control in lower lane). Experiments were performed by A. Mishra.

cells were tested with reverse transcriptase polymerase chain reaction (RT-PCR) for expression of *Dasm1*-mRNA and as a control for Glyceraldehyde-3-phosphate-dehydrogenase (GAPDH). At least a subset of these GFP-positive GABAergic interneurons expressed mRNA necessary for producing the *Dasm1* protein. Experiments were performed by A. Mishra.

#### 6.4.6 Number of inhibitory synapses in cultured neurons

Reduced frequencies of mIPSCs point to a reduced number of inhibitory synapses. For that reason, we examined their number on a morphological level in cultured hippocampal neurons with a gephyrin staining. Gephyrin is a postsynaptic scaffolding molecule of inhibitory synapses and serves as a marker for inhibitory synapses (Kneussel et al., 1999).

We could show that in cultured hippocampal neurons from *Dasm1*<sup>-/-</sup> mice the number of inhibitory synapses is significantly reduced by 16% (see Figure 6.14). Experiments were performed by A. Mishra.

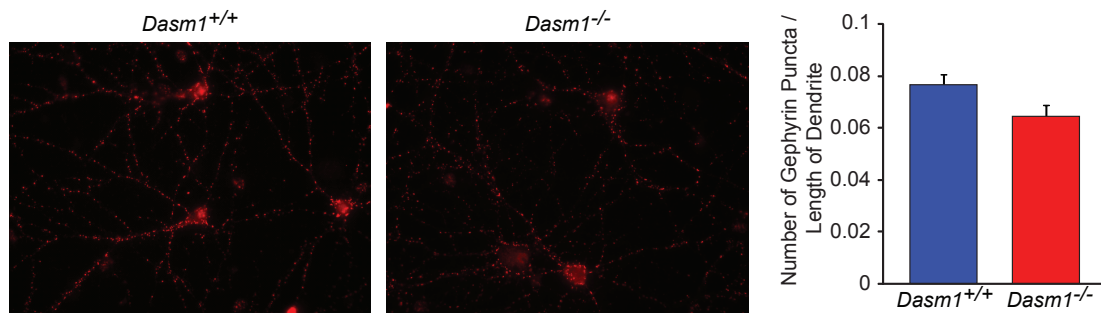


**Figure 6.14: Reduced gephyrin puncta in *Dasm1*<sup>-/-</sup> neurons.** Cultured hippocampal neurons display reduced numbers of gephyrin puncta, indicating a loss of inhibitory synapses. Experiments were performed by A. Mishra.

#### 6.4.7 Homotypic interaction of Dasm1

Based on the structural similarity of Dasm1 to NCAM, we hypothesized, that Dasm1 is a cell adhesion molecule. We asked whether Dasm1 is capable of binding to other Dasm1 molecules in a homotypic manner. In a cell aggregation assay, Dasm1 and Dasm1 lacking the intracellular C-terminus (*Dasm1*- $\Delta$ C) were fused to EGFP and overexpressed in HEK293 cells and transferred to a shaker. Cell aggregates typically only form if the proteins expressed at the surface have adhesive properties. To quantify the aggregation potential of different constructs the number of aggregates was divided by the size of the biggest aggregate (= aggregation index; the lower the number, the more adhesive properties are observed).

*Dasm1*-EGFP as well as *Dasm1*- $\Delta$ C-EGFP are able to induce homotypic aggregates, suggesting that the N-terminal extracellular part of the protein has adhesive properties (see Figure

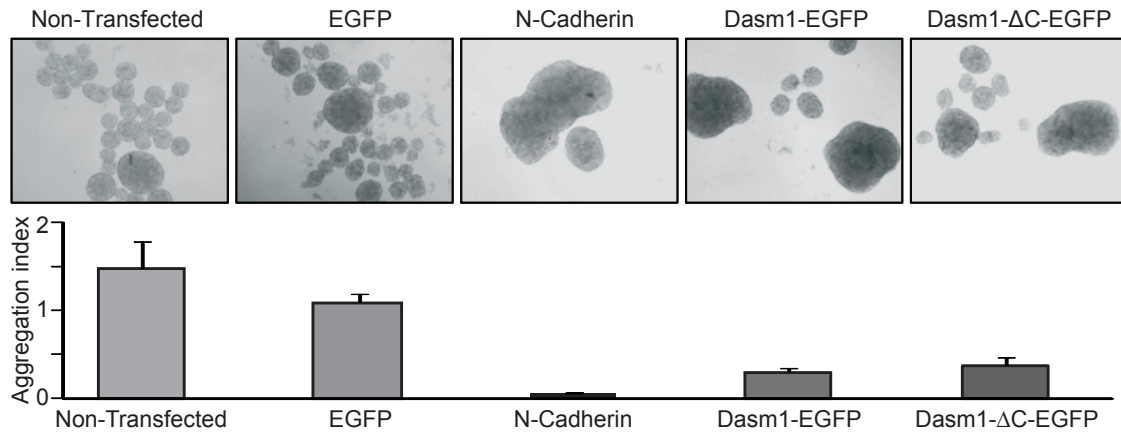


**Figure 6.15: Dasm1-EGFP as well as Dasm1-ΔC-EGFP are capable of homotypic adhesion in a cell aggregation assay.** Cell aggregation assay data suggests that Dasm1 is a cell adhesion molecule acting in a homotypic manner. Like N-Cadherin, Dasm1-EGFP as well as Dasm1-ΔC-EGFP form cell aggregates, whereas the controls (non-transfected and transfected with EGFP) do not form big clusters of cells. Aggregation index: number of aggregates divided by the size of the biggest aggregate. Lower index number represents more adhesive properties. Experiments were performed by A. Mishra.

6.15). Experiments were performed by A. Mishra.

#### 6.4.8 Evoked inhibitory postsynaptic currents (eIPSCs) in P15-20 mice

The reduced frequency in both spontaneous and miniature IPSCs most likely originates from the same effect, which is the spontaneous non-activity driven fusion of presynaptic GABA vesicles. Consequently I tested by evoking IPSCs, whether also coordinated vesicle release upon electrical activity is altered. Inhibitory inputs to CA1 neurons lack the highly organized structure as the bundle of Schaffer collateral axons. Therefore, IPSCs were evoked close to the soma as described in the methods section.

Neither the input-output curve, nor the decay time constant of evoked IPSCs were different in *Dasm1*<sup>-/-</sup> mice compared to *Dasm1*<sup>+/+</sup> mice (see Figure 6.16), suggesting that action potential-driven release is unaltered.

#### 6.4.9 Paired pulse ratio (PPR) of evoked IPSCs in P15-20 mice

As the observed reduced frequencies of both miniature and spontaneous IPSCs could arise from either fewer synapses, or altered presynaptic release properties, the inhibitory presynapse was tested with the paired pulse paradigm.

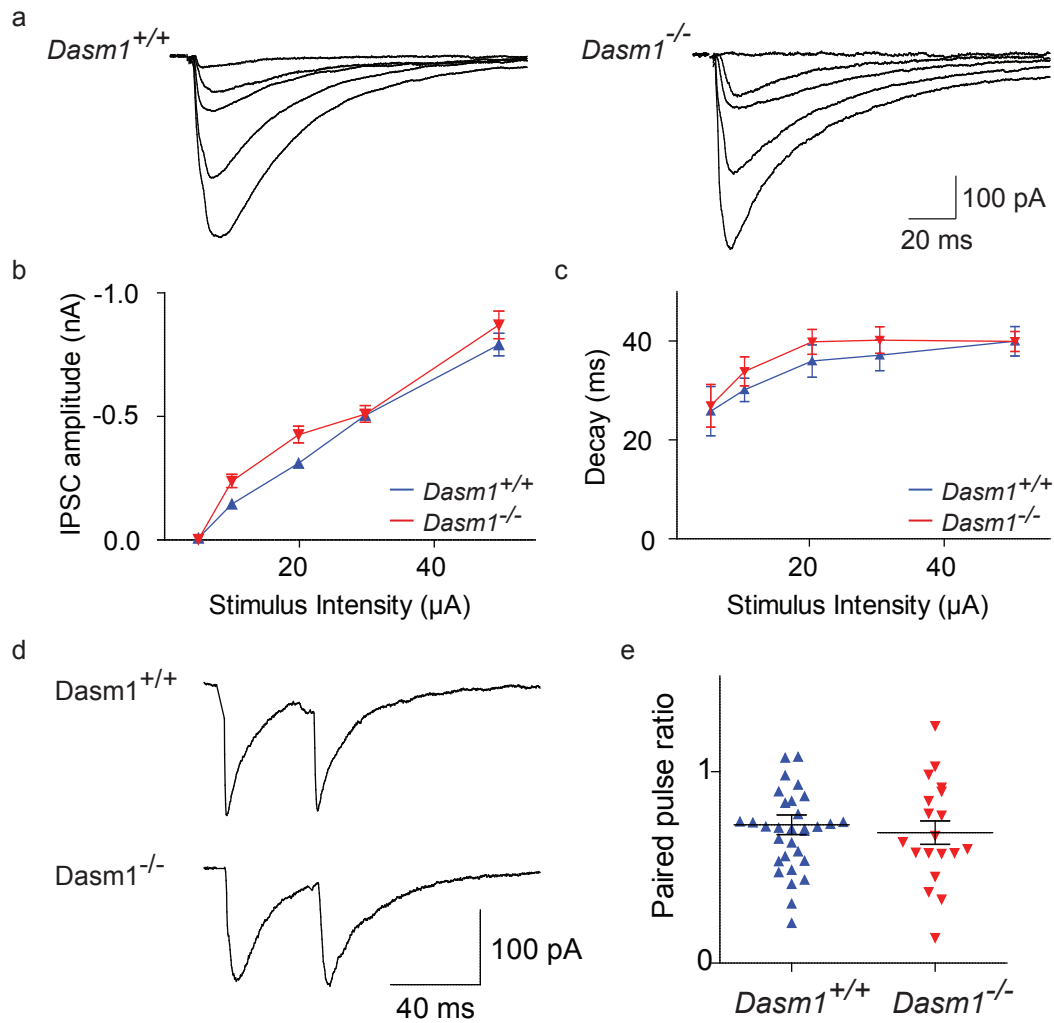


**Figure 6.16: Evoked inhibitory postsynaptic currents are not altered in *Dasm1*<sup>-/-</sup> mice.** (a) Example traces of eIPSCs of P15-20 mice. (b) Input-output curve of eIPSCs were not significantly different (*Dasm1*<sup>+/+</sup>  $n = 11$  and *Dasm1*<sup>-/-</sup>  $n = 11$ , only cells with all five stimulus intensities were evaluated). (c) Decay time constant of eIPSCs. (d) Example traces of eIPSCs paired pulse stimulation of P15-20 mice. (e) Paired pulse ratios of eIPSCs with a stimulus intensity of 10  $\mu\text{A}$  were not different (*Dasm1*<sup>+/+</sup>:  $0.7 \pm 0.1$ ,  $n = 32$ ; *Dasm1*<sup>-/-</sup>:  $0.7 \pm 0.1$ ,  $n = 19$ ,  $p > 0.5$ ). Error bars represent SEM in all graphs.

No difference could be observed in the presynaptic release properties with the applied settings (10  $\mu\text{A}$  stimulus intensity and 40 ms inter stimulus interval, see Figure 6.16) when comparing the PPR of *Dasm1*<sup>+/+</sup> mice ( $0.7 \pm 0.1$ ,  $n = 32$ ) with *Dasm1*<sup>-/-</sup> mice ( $0.7 \pm 0.1$ ,  $n = 19$ ,  $p > 0.5$ ). This suggests, that the GABAergic presynapse is functionally not impaired in *Dasm1*<sup>-/-</sup> mice.

## 6.5 EPSP-spike (E-S) coupling

Disturbing the balanced system of excitation to inhibition can alter the excitability of neurons. I asked whether as a consequence of reduced inhibition, the excitability of CA1 neurons is increased in *Dasm1*<sup>-/-</sup> mice compared to *Dasm1*<sup>+/+</sup> mice. Excitability of CA1 neurons was evaluated by recording the field excitatory postsynaptic potential (fEPSP) in stratum radiatum, and simultaneously recording the excitability of CA1 neurons with a second electrode placed next to their somas in stratum pyramidale (see Figure 5.1 in Material and Methods section). Following stronger stimulation of Schaffer collateral axons, fEPSPs as well as spike heights typically increase. fEPSP to spike (E-S) coupling is usually visualized by plotting the slope of the fEPSP (input) to the spike height (output).

Before starting to record E-S coupling in *Dasm1*<sup>+/+</sup> and *Dasm1*<sup>-/-</sup> mice, I tested, whether reducing inhibition increases excitability of CA1 neurons. Mean frequency of mIPSCs in P15-20 mice is reduced by roughly one fifth in *Dasm1*<sup>-/-</sup> mice compared to *Dasm1*<sup>+/+</sup> mice. First of all, the necessary concentration of the GABA receptor blocker PTX to mimick the effect of reduced inhibitory inputs was evaluated. To estimate this concentration, IPSCs in wildtype slices were evoked and the slice was perfused with increasing concentrations of PTX. A nonlinear regression was fitted to the dose-response-relationship and the PTX concentration needed to block half of the eIPSCs amplitude was calculated (see Figure 6.17a, the IC<sub>50</sub> value was 7.1 μM PTX). Then a concentration blocking roughly 20 percent of the inhibition (approximately 3 μM PTX) was tested whether it is able to alter the E-S relationship. In fact I could show, that the spike size was massively increased in the presence of 3 μM PTX (see Figure 6.17b, red traces), whereas neither the amplitude of the fiber volley (green traces), nor the slope of the fEPSP (black traces) were significantly changed. This demonstrates, that inhibition has a major impact on CA1 excitability. Reducing inhibition by roughly one fifth increases excitability of CA1 neurons dramatically. I therefore recorded E-S-coupling in *Dasm1*<sup>+/+</sup> and *Dasm1*<sup>-/-</sup> mice (see Figure 6.17c).

Interestingly, no difference in E-S-coupling could be observed (see Figure 6.17d), suggesting that the overall excitability of CA1 neurons is not changed in *Dasm1*<sup>-/-</sup> mice compared to *Dasm1*<sup>+/+</sup> mice. A potential explanation could be, that in the previous simulation experiments with PTX, not only synaptic GABA receptors, but also extrasynaptic receptors

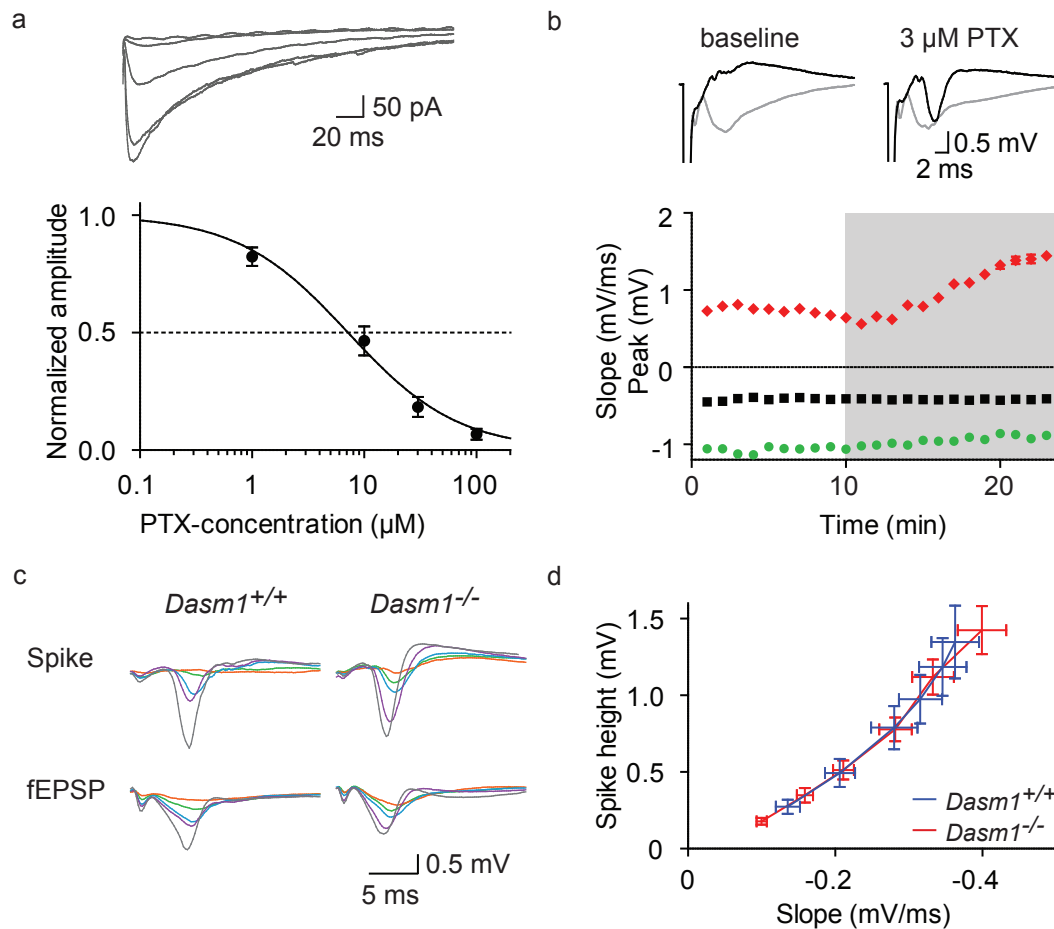


**Figure 6.17: EPSP-spike (E-S) coupling is not altered in mice lacking *Dasm1*.** (a) Example traces and dose response curve of blocking evoked IPSCs with different concentrations of picrotoxin (PTX). The IC<sub>50</sub> value was 7.1 μM PTX ( $n = 5$ ). (b) Example traces and quantification of the effect of 3 μM PTX on spike height (black traces and red dots), fEPSP slope (gray traces and black dots) and fiber volley (gray traces and green dots). PTX application started after 10 minutes. (c) Example traces of fEPSPs recorded in stratum radiatum (lower traces) and the corresponding spikes at the CA1 somas in stratum pyramidale (upper traces) in *Dasm1*<sup>+/+</sup> and *Dasm1*<sup>-/-</sup> mice. Same colors represent same stimulus intensities. (d) Quantification of the E-S-coupling in *Dasm1*<sup>+/+</sup> and *Dasm1*<sup>-/-</sup> mice. Plotted is the slope of the fEPSP against the spike height (*Dasm1*<sup>+/+</sup>  $n = 22$  and *Dasm1*<sup>-/-</sup>  $n = 26$ ). Error bars represent SEM in all graphs.

were blocked. Therefore a differentiation between phasic (synaptic) and tonic (extrasynaptic) inhibition was not possible.

## 6.6 Giant depolarizing potentials (GDPs)

Reducing inhibitory inputs changes the balance of excitation to inhibition and can thus lead to altered network activity patterns. As the biggest reduction of the miniature and spontaneous

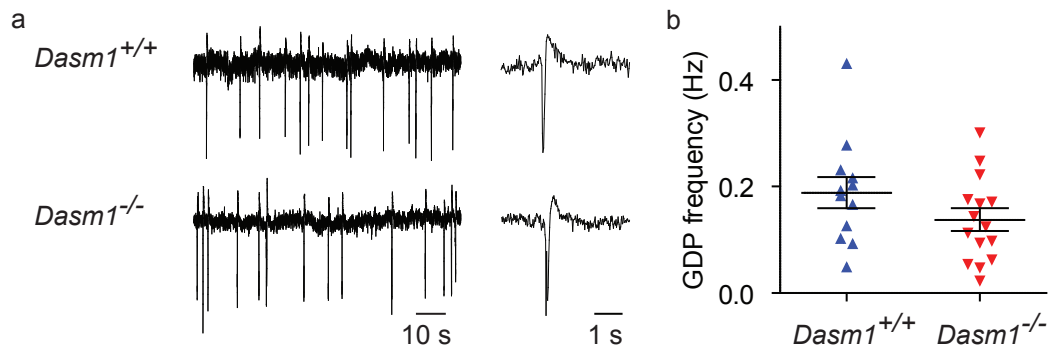


**Figure 6.18: Giant depolarizing potentials are not altered in *Dasm1*<sup>-/-</sup> mice.** (a) Example traces of giant depolarizing potentials in *Dasm1*<sup>+/+</sup> and *Dasm1*<sup>-/-</sup> mice. Note the different time scale. (b) Quantification of the frequencies of GDPs. GDPs were recorded with slices of littermate at the same day. The recording chamber was heated to 32°C and to increase excitability, KCl was elevated to 4.5 mM. Minutes 20 to 30 of the recording were used for analysis. Error bars represent SEM.

IPSCs frequency was observed in young mice, I questioned, whether early network activity is affected in *Dasm1*<sup>-/-</sup> mice. The earliest network activity patterns are the giant depolarizing potentials, which are spontaneous GABAergic currents, traveling through the hippocampus without having a point of origin (Ben-Ari et al., 2007). GDPs were recorded at 32°C with an ACSF containing an elevated potassium concentration (4.5 mM KCl instead of 2.5 mM KCl) to increase excitability. The extracellular recording electrode was placed into the stratum pyramidale of the CA3 region (see Figure 6.18a).

Frequency of GDPs in acute slices of P6-8 *Dasm1*<sup>+/+</sup> and *Dasm1*<sup>-/-</sup> littermates were not significantly different (*Dasm1*<sup>+/+</sup> 0.19 Hz ± 0.03 Hz, *n* = 12 and *Dasm1*<sup>-/-</sup> 0.14 Hz ± 0.02 Hz, *n* = 15; t-test, *p* > 0.05; see Figure 6.18b). This suggests that although loss of Dasm1 affects miniature and spontaneous inhibitory postsynaptic currents, this protein is not required for early network activity patterns.

## 7 Discussion

The present study suggests that the protein Dasm1 (Dendrite arborization and synapse maturation 1) acts on the number of inhibitory synapses in the hippocampus. A significant reduction of frequencies of miniature and spontaneous inhibitory postsynaptic currents in CA1 neurons of *Dasm1*<sup>-/-</sup> mice points to fewer inhibitory synapses. Accordingly, cultured hippocampal neurons of *Dasm1*<sup>-/-</sup> mice display less gephyrin puncta suggesting reduced numbers of inhibitory synapses. Adhesive properties of the extracellular N-terminal part of Dasm1 indicate that Dasm1 is a cell adhesion molecule.

### 7.1 Dasm1 in dendrite arborization and synaptic transmission

The immunoglobulin superfamily member 9 (IgSF9) was identified in a genetic screen as the protein most closely related to the protein turtle in *Drosophila melanogaster* (Doudney et al., 2002). Based on the observed phenotype upon RNAi knockdown, it was named Dendrite arborization and synapse maturation 1 (Dasm1, Shi et al., 2004b). These authors assessed the role of Dasm1 using virus-based RNAi mediated knockdown. Their data from organotypic hippocampal slice cultures suggest a role for Dasm1 in excitatory synapse maturation. Suppression of Dasm1 expression decreased AMPA- but not NMDA receptor mediated synaptic transmission. The AMPA/NMDA ratio was significantly reduced in Dasm1-RNAi infected CA1 neurons compared to uninfected control neurons. Cells infected with a putative dominant negative Dasm1 construct, lacking only the intracellular C-terminus, had also a reduced AMPA/NMDA ratio as well as decreased amplitudes of miniature excitatory postsynaptic currents (mEPSCs). According to Shi et al., the C-terminus of Dasm1 has a crucial role in excitatory synapse maturation (Shi et al., 2004b).

Contrary to these results, I observed an increased AMPA/NMDA ratio and no alterations in amplitudes and frequencies of AMPA receptor mediated miniature EPSCs, suggesting that the elevated ratio is caused by alterations of NMDA receptor mediated synaptic transmission in *Dasm1*<sup>-/-</sup> mice. Furthermore, mice lacking only the intracellular C-terminus of Dasm1

(*Dasm1*<sup>ΔC/ΔC</sup>) did not show alterations in the AMPA/NMDA ratio, indicating that the N-terminus, rather than the C-terminus, is crucial for Dasm1 function in synaptic transmission. In addition, amplitudes and frequencies of miniature EPSCs were not altered in *Dasm1*<sup>-/-</sup> mice, which again is in opposition to the RNAi study (Shi et al., 2004b).

Different systematic approaches might underly the observed discrepancies between the RNAi study (Shi et al., 2004b) and my knockout study. Both knockdown with RNAi and over-expression of a putative dominant-negative Dasm1-ΔC construct are acting acutely on the expression level of the proteins, whereas knockout mice never express the protein and might induce compensatory mechanisms. In our knockout animal model, the function of Dasm1 could be compensated by the closely related protein IgSF9b and thus occlude potential effects of an acute knockdown. Similar discrepancies between transient knockdown and knockout experiments are known from other proteins such as PSD-95 (postsynaptic density-95) and neuroligins. PSD-95 is a member of the membrane-associated guanylate kinase (MAGUK) family and is a scaffolding protein in excitatory synapses. Acute RNAi knockdown of PSD-95 strongly decreased AMPA receptor mediated currents in a subset of synapses while PSD-95 knockout mice show functional compensation, hence no impaired AMPA receptor mediated synaptic transmission (Elias et al., 2006). Also acute knockdown of a single neuroligin resulted in strongly reduced number of synapses in cultured neurons *in vitro* (Chih et al., 2005), whereas knockout of all neuroligins has no effect on synapse numbers in cultured neurons *in vitro* or in the intact brain *in vivo* (Varoqueaux et al., 2006).

While knockout studies are jeopardized by endogenous compensatory mechanisms, RNAi studies also have their caveat - if the constructs used are not highly specific, off-target effects may arise. For the PSD-95 study, the specificity of the used RNAi constructs was nicely proven by demonstrating that they do not elicit the observed effects in PSD-95 knockout mice (Elias et al., 2006).

The RNAi constructs used for the publication assessing a role of Dasm1 in synaptic transmission (Shi et al., 2004b) were also used to study the morphology of hippocampal neurons (Shi et al., 2004a). Therefore, cultured neurons were transfected with the RNAi constructs to suppress expression levels of Dasm1. We confirmed that dendrite branch length as well as complexity of dendrite arborization were impaired in RNAi transfected neurons, suggesting a role of Dasm1 in dendrite development.

However, in our knockout model, A. Mishra could not observe any morphological alterations in CA1 pyramidal neurons when comparing *Dasm1*<sup>-/-</sup> to *Dasm1*<sup>+/+</sup> mice (Mishra et al., 2008). Also dissociated hippocampal neurons displayed normal dendrite organization *in vitro*, as shown by analysis of total dendrite length, number of free ends, and Sholl analysis (Mishra et al., 2008). Strikingly, the RNAi used by Shi and colleagues impaired dendrite arborization not only of *Dasm1*<sup>+/+</sup> neurons, but also of *Dasm1*<sup>-/-</sup> neurons, strongly suggesting an off-target effect. Their constructs could also impair the function of other proteins and thus lead to the reduced complexity of dendrite arborization. Two potential off-target proteins could be synaptojanin (Synj1, NM\_001164483) and Catechol-O-methyltransferase 1 (Comt1, NM\_007744), both having only three non-matching bases in the flanking region of the used RNAi. Synaptojanin is involved in synaptic vesicle recovery at presynaptic terminals. During endocytosis, synaptojanin recruits clathrin to the newly forming vesicles. Comt1, located in postsynaptic neurons, is an enzyme which inactivates catecholamine neurotransmitters (dopamine, epinephrine, and norepinephrine) by transferring a methyl group. Interestingly, both potential off-target proteins are involved in synaptic transmission. But as the RNAi used by Shi and colleagues has various potential targets including *Dasm1*, any conclusion based on the reported phenotype would be purely speculative. Proper controls would have been necessary to test the specificity of the used RNAi constructs. Point mutations in the used RNAi constructs for instance should have abolished the effect and proven specificity of the used constructs.

The most closely related gene to murine *Dasm1* in *Drosophila melanogaster* is *tut1*. *Tut1* mutants show inabilities in executing coordinated motor output: They can not fly in adulthood and - like a turtle - are unable to regain an upright position when inverted (Bodily et al., 2001). *Dasm1*<sup>-/-</sup> mice do not show any impairment in coordinated motor control and behavior. Different aspects of brain function in *Dasm1*<sup>-/-</sup> mice were tested with behavioral paradigms. Spatial learning and memory was tested with the Morris water navigation task (Morris, 1984). *Dasm1*<sup>-/-</sup> mice did not have altered abilities in this task when compared to *Dasm1*<sup>+/+</sup> littermates. Object memory was analyzed with the novel object recognition task (Ennaceur and Delacour, 1988). Here, a novel object is placed in a familiar environment and the interest of the animal in the novel object versus familiar objects is compared. *Dasm1*<sup>-/-</sup> mice spent significantly less time with novel objects compared to their *Dasm1*<sup>+/+</sup> littermates,

indicating that exploratory behavior is reduced in mice lacking Dasm1 (A. Mishra, unpublished observations).

Based on the high expression profile in hippocampus as well as the described functions of the homologous protein turtle in *Drosophila melanogaster* (Bodily et al., 2001), I started to examine a potential role of Dasm1 in synaptic transmission with electrophysiological recordings.

## 7.2 Excitatory currents

I first focused on excitatory synaptic transmission at the CA3–CA1 synapse in hippocampus, as Shi and colleagues reported effects of Dasm1 on glutamatergic currents at this synapse based on RNAi experiments (Shi et al., 2004a,b). Unfortunately, interpretation of the RNAi experiments is challenging, caused by the fact that the used RNAi might not be specific enough (Mishra et al., 2008).

The AMPA/NMDA ratio was significantly elevated in *Dasm1*<sup>-/-</sup> mice, which is caused either by elevated AMPA receptor mediated currents, or decreased NMDA receptor mediated synaptic transmission. AMPA receptor mediated currents were assessed by recording miniature excitatory postsynaptic currents (mEPSCs) in conditions, where only AMPA but not NMDA receptors are active. AMPA receptor mediated mEPSCs were not altered in *Dasm1*<sup>-/-</sup> mice compared to *Dasm1*<sup>+/+</sup> mice, suggesting alterations of NMDA receptor mediated synaptic transmission as the cause for the elevated AMPA/NMDA ratio. I examined NMDA receptor mediated currents in more detail and recorded field excitatory postsynaptic potentials (fEPSPs) in the presence of NBQX to block AMPA receptors and in the presence of low magnesium concentration to remove the magnesium block from the NMDA receptors. Synaptic transmission under these recording conditions is then mediated only by NMDA receptors. Field recordings of isolated NMDA receptor mediated synaptic transmission were not different in *Dasm1*<sup>-/-</sup> mice compared to *Dasm1*<sup>+/+</sup> mice, which might be the consequence of limited resolution in this assay. I next isolated NMDA receptor mediated currents in whole cell recordings. I could not observe alterations in kinetics and current-voltage relationship, suggesting that receptor composition and properties are unaltered. The elevated AMPA/NMDA ratio in *Dasm1*<sup>-/-</sup> mice could arise from the presence of more NMDA receptors at excitatory synapses. Number of synapses and quantity of receptors per synapse is assessed

by mEPSCs frequencies and amplitudes, respectively. For AMPA receptors, being active at the resting membrane potential of -70 mV, these recordings are a feasible approach. For NMDA receptors, however, discriminating and quantifying single mEPSCs is not possible. As NMDA receptors need to be depolarized to relieve the voltage-dependent magnesium block, recordings would have to be performed at a membrane potential of +40 mV. Whole cell recordings at this potential are noisy, and together with the long decay time constant of NMDA receptors, makes quantification unreliable. Therefore, the number of NMDA receptors in *Dasm1*<sup>-/-</sup> neurons has to be assessed by different methods. A staining with an NMDA receptor antibody unfortunately was not specific enough to quantify NMDA receptor content (A. Mishra, personal communication). Hence, the underlying mechanism for the observed change in AMPA/NMDA ratio in *Dasm1*<sup>-/-</sup> mice is currently not known. However, the postulated changes in NMDA receptor mediated signaling is in contradiction to the study by Shi et al., which suggests that AMPA receptor mediated synaptic transmission is impaired (Shi et al., 2004b). The aforementioned unspecificity of the used RNAi constructs in this study might be causative for their observed effects.

The NMDA receptor has a conductivity for calcium, which makes this receptor a key player of synaptic plasticity. Depending on the pattern of synaptic stimulation, synapses can undergo long lasting changes which are either long term depression (LTD) or long term potentiation (LTP). Based on the hypothesis that the AMPA/NMDA ratio is elevated due to alterations of NMDA receptor mediated signaling, I assessed long term potentiation with the tetanic stimulation protocol. I observed no difference in *Dasm1*<sup>-/-</sup> mice compared to *Dasm1*<sup>+/+</sup> mice, suggesting normal plasticity properties. However, the tetanic stimulation protocol is a rather strong protocol for LTP induction. Upon stimulation, postsynaptic cells are depolarized and therefore the NMDA receptors are activated. Depending on the calcium influx different signaling cascades lead to the addition or removal of AMPA receptors from the postsynaptic membrane. Weaker stimulation protocols for LTP or LTD experiments could perhaps unravel altered NMDA receptor properties in *Dasm1*<sup>-/-</sup> mice.

Calcium imaging tools could be used to discriminate differences in NMDA receptor dependent calcium conductivity of *Dasm1*<sup>-/-</sup> mice compared to *Dasm1*<sup>+/+</sup> mice. However, as one has to compare *Dasm1*<sup>-/-</sup> to *Dasm1*<sup>+/+</sup>, the problem arises how to compare calcium signals of different specimens. Calcium signals can easily be compared within the same slice, but as

signal strength not only depends on software and filtering settings, but also on loading with fluorescent calcium dyes, it is difficult to compare different specimens. However, I postulate that *Dasm1*<sup>-/-</sup> mice have reduced NMDA receptor mediated currents, as this seems to be the only explanation for the elevated AMPA/NMDA ratio.

### 7.3 Inhibitory currents

Balanced excitation and inhibition is necessary for a properly working brain, hence, after examining excitatory synapses, I next focused on inhibitory synaptic currents.

Surprisingly, miniature inhibitory postsynaptic currents (mIPSCs) of *Dasm1*<sup>-/-</sup> mice showed unaltered amplitudes but significantly reduced frequencies when compared to *Dasm1*<sup>+/+</sup> littermates. Western blot data demonstrates that protein levels of Dasm1 decline during postnatal brain maturation. Consequently I tested, whether in young mice with higher endogenous Dasm1 protein levels the observed phenotype is more pronounced. Indeed, I could show that frequencies were even more reduced in younger mice. Miniature IPSCs are recorded in the presence of TTX to suppress action potential-driven events. To confirm the effect of reduced mIPSCs frequencies, I also recorded spontaneous IPSCs (sIPSCs), which in contrast to mIPSCs also include action potential-driven events. Indeed, I could confirm that also frequencies but not amplitudes of sIPSCs were significantly reduced in a developmental manner. Spontaneous IPSCs include large events elicited by the fusion of presynaptic vesicles upon activity. Large events were not observed less frequently in *Dasm1*<sup>-/-</sup> neurons, hence, the reduced frequency of sIPSCs arises most likely from the non-activity driven fusion of neurotransmitter-filled vesicles. For *Dasm1*<sup>-/-</sup> mice, decreased sIPSC frequency represents the same alteration as observed in mIPSCs.

Alterations in the frequency of spontaneous IPSCs in *Dasm1*<sup>-/-</sup> mice compared to *Dasm1*<sup>+/+</sup> mice could be caused by alterations in either GABA release probability, number of release sites, or activity of presynaptic interneurons. Changes in miniature IPSCs, recorded in conditions with suppressed activity, can only be accounted for by the first two possibilities. Therefore, reduced frequencies of sIPSCs as well as mIPSCs in *Dasm1*<sup>-/-</sup> mice are suggestive for either altered presynaptic GABA release or reduced number of synapses. I assessed presynaptic GABA release probability with paired pulse stimulation of evoked IPSCs in *Dasm1*<sup>-/-</sup> mice and their *Dasm1*<sup>+/+</sup> littermates. I observed no difference in the paired pulse

ratio, suggesting unaltered GABA release properties in *Dasm1*<sup>-/-</sup> mice compared to *Dasm1*<sup>+/+</sup> mice. Reduced frequencies of mIPSCs and sIPSCs observed in *Dasm1*<sup>-/-</sup> mice therefore most likely result from fewer inhibitory synapses. The hypothesis of reduced number of inhibitory synapses was confirmed by gephyrin staining of dissociated hippocampal neurons. Fewer inhibitory synapses were detected in *Dasm1*<sup>-/-</sup> neurons compared to *Dasm1*<sup>+/+</sup> neurons with a staining against gephyrin, a marker for inhibitory synapses.

Fewer GABAergic synapses could result in smaller currents when evoking IPSCs, if the numbers of receptors per synapse and activated vesicle pool are not altered. However, I did not observe alterations of currents and decay parameters of evoked IPSCs when comparing *Dasm1*<sup>-/-</sup> with *Dasm1*<sup>+/+</sup> mice. Inhibitory projections to CA1 neurons lack the highly organized laminar structure which excitatory projections have, and thus the elicited currents upon stimulation are variable. Although highly standardized stimulation and analysis patterns were used, I could not detect differences in amplitudes and decay kinetics of eIPSCs when comparing *Dasm1*<sup>-/-</sup> mice with *Dasm1*<sup>+/+</sup> mice. Either a potential effect was not resolved as a consequence of the interneuron specific projection pattern, or *Dasm1* interferes specifically with the protein machinery necessary for miniature but not for evoked IPSCs.

A similar phenotype has already been reported in the neuroligin-deficient mice. Here, alterations of miniature IPSCs but not evoked IPSCs were found (Varoqueaux et al., 2006). Frequencies, but not amplitudes, of miniature IPSCs were reduced in neuroligin double knockout mice, a response even greater in triple knockout mice. However, evoked IPSCs were only reduced in triple knockout mice but not in double and single knockout mice. Some of the neuroligin functions seemed to be compensated whereas others are not (Varoqueaux et al., 2006). IgSF9b, having high homology to *Dasm1* in the extracellular part, could also compensate for some of *Dasm1* functions.

Another explanation for the observed alterations of miniature, but not evoked IPSCs is that different pools for different kinds of vesicle release might exist. Miniature postsynaptic currents were first described at the neuromuscular junction by Fatt and Katz (1952) and reflect the randomly occurring spontaneous exocytosis of vesicles in the absence of action potentials. The classical view is that the same vesicles do not only release their content stochastically, but also in a synchronized manner upon action potentials (Lou et al., 2005; Groemer and Klingauf, 2007; Prange and Murphy, 1999). However, recent findings suggest

that miniature postsynaptic currents might be related to a special pool of vesicles which differs from the pool responsible for evoked transmission (Sara et al., 2005; Virmani et al., 2005; Fredj and Burrone, 2009; Mathew et al., 2008; Hablitz et al., 2009). If clearly separated vesicle pools for miniature and evoked release do exist, impaired miniature but not evoked IPSCs in *Dasm1*<sup>-/-</sup> mice could be caused by a specific effect of *Dasm1* on the miniature vesicle pool.

Different pools were not only postulated for presynaptic vesicles, but also for postsynaptic receptors. The assumption that spontaneous and action potential-driven neurotransmitter release activates the same set of postsynaptic receptors was challenged by studies of the Kavalali group, who demonstrated the existence of two pools of postsynaptic NMDA receptors (Atasoy et al., 2008). Briefly, NMDA-mEPSCs were decreased with the use-dependent blocker MK-801 ((+)-5-methyl-10,11-dihydro-5H-dibenzo [a,d] cyclohepten-5,10-imine maleate), which did not affect evoked NMDA-eEPSCs. The reverse experiment of depressing only evoked NMDA-eEPSCs also did not affect spontaneous NMDA-mEPSCs, suggesting distinct postsynaptic NMDA receptor pools. Decreased frequencies of mIPSCs and sIPSCs but no alterations of eIPSCs in *Dasm1*<sup>-/-</sup> mice could also be caused by different postsynaptic receptor pools. The GABA<sub>A</sub> receptor pool responsible for mIPSCs might be a different pool as the pool mediating eIPSCs. Lack of a specific use-dependent antagonist for GABA<sub>A</sub> receptors, renders the investigation of different GABA<sub>A</sub> receptor pools for different kinds of vesicle release impossible.

#### **7.4 GABA during development**

As GABAergic synaptic transmission is impaired in *Dasm1*<sup>-/-</sup> mice in a developmental manner, it is indispensable to emphasize the importance of GABA during development. GABA is the main inhibitory neurotransmitter in the adult mammalian central nervous system and it is also the key player during embryonic maturation and postnatal development. During these processes, neurons follow a genetic program which alters the current fluxes through the membrane in different ways – for example, the ionic driving forces and the properties of receptors are massively changed, with the most prominent paradigm being the GABA receptors. Early in postnatal development, the intracellular concentration of chloride is high, caused by the high expression level of the sodium-potassium-chloride cotransporter

NKCC1 (Hubner et al., 2001a; Pfeffer et al., 2009; Blaesse et al., 2009). Activation of GABA receptors during early brain maturation leads to an outward current of chloride, resulting in a depolarization of the cell up to action potential firing. Depolarization of the cell is able to remove the voltage-dependent magnesium block from NMDA receptors, which can then conduct for the second messenger calcium. Calcium signals can then trigger the insertion of AMPA receptors into the postsynaptic density (Hall et al., 2007; Ben-Ari et al., 1997), as well as start signaling cascades up to the activation of specific transcription factors. The property of high intracellular chloride during early postnatal development seems to be conserved throughout evolution, and makes GABA the key player of balanced maturation of inhibitory and excitatory connections (Wang and Kriegstein, 2008).

During the first week after birth, intracellular chloride levels are reduced by the developmental upregulation of the potassium-chloride cotransporter KCC2 (see Stein et al., 2004; Hubner et al., 2001b; Rivera et al., 2005), which causes GABA to act hyperpolarizing. Extensive modifications have to take place during development, and in all animal species and brain structures studied so far, the adult brain never had the same properties compared to an immature brain, in other words: a young brain is not just a small adult brain. In many brain regions, GABA synapses are the first synapses to occur, followed later by glutamatergic synapses (Akerman and Cline, 2006). Some studies suggest that this is a common principle, which also holds true for adult neurogenesis. Newly formed neurons in adult hippocampus receive depolarizing synaptic GABAergic input prior to glutamatergic inputs (Ge et al., 2006; Overstreet Wadiche et al., 2005).

Developmental changes might also underly the declining phenotype of reduced mIPSCs frequencies in *Dasm1*<sup>-/-</sup> mice during maturation. Delayed maturation was also observed in mice lacking the NKCC1 cotransporter: amplitudes of mIPSCs were only reduced at P7, whereas they were unchanged at P15 (Pfeffer et al., 2009). If the elevated AMPA/NMDA ratio in *Dasm1*<sup>-/-</sup> mice is not a direct effect of *Dasm1* on excitatory synaptic transmission, it could also be the consequence of disturbed GABA signaling during early postnatal maturation. A delayed GABAergic maturation affects most likely also the balance of excitation to inhibition. In addition, GABA acts not only on GABA<sub>A</sub> receptors, but also on metabotropic GABA<sub>B</sub> receptors. GABA<sub>B</sub> receptors are G-protein coupled receptors that release upon activation their G<sub>α</sub> and G<sub>βγ</sub> subunits. Many downstream targets including inwardly rectifying potassium

channels, voltage-sensitive calcium channels, and adenylyl cyclase are influenced by these signaling molecules (Misgeld et al., 1995). GABA<sub>B</sub> receptors influence synaptic transmission through inhibiting neurotransmitter release or attenuating postsynaptic excitability. These receptors can also strongly inhibit NMDA receptor calcium signals via PKA (Chalifoux and Carter, 2010). Reduced miniature and spontaneous inhibitory postsynaptic currents in *Dasm1*<sup>-/-</sup> also imply that fewer metabotropic GABA<sub>B</sub> receptors are activated. Downstream signaling cascades of GABA<sub>B</sub> receptors could also influence the maturation of the excitatory network.

## 7.5 Extracellular versus intracellular domains of Dasm1

The extracellular part of Dasm1 consists of five Ig domains followed by two FN domains. On the intracellular side, Dasm1 has a putative PDZ motif. Shi and colleagues suggest a prominent role for the intracellular C-terminus, as overexpression of the putative dominant negative protein Dasm1- $\Delta$ C resulted in reduced complexity of dendrite arborization, reduced AMPA/NMDA ratio, and reduced mEPSCs amplitudes (Shi et al., 2004a,b). However, proper subcellular localization of overexpressed Dasm1- $\Delta$ C was not assessed and the reported effect might also arise from dislocated protein.

Turtle, the most closely related protein to Dasm1 in *Drosophila melanogaster*, has the same extracellular domain structure as Dasm1. Long and colleagues discovered that turtle controls dendrite branching, and could also show that the cytoplasmic tail of turtle is dispensable (Long et al., 2009). Overexpression of full length turtle as well as of turtle lacking the intracellular C-terminus rescued branching and morphology defects in *tut1* mutants, suggesting that the C-terminus is not required for the *tut1* mutant phenotype.

To address the question, whether the intracellular C-terminus of Dasm1 containing a PDZ signaling motif is important, I analyzed mice lacking the C-terminus (*Dasm1* <sup>$\Delta$ C/ $\Delta$ C</sup>). Miniature and spontaneous IPSCs revealed no difference in amplitudes and frequencies of *Dasm1* <sup>$\Delta$ C/ $\Delta$ C</sup> and *Dasm1*<sup>+/+</sup>, suggesting that the C-terminus is dispensable for inhibitory synaptic transmission. In addition, the AMPA/NMDA ratio was also not altered, indicating that the C-terminus does not mediate this effect. The ecto- and transmembrane domains of Dasm1 are thus necessary and sufficient to rescue the phenotypes observed in *Dasm1*<sup>-/-</sup> mice.

## 7.6 Interneurons in hippocampus

Reduced frequencies of mIPSCs as well as sIPSCs together with lower numbers of gephyrin puncta in cultured neurons suggest that the numbers of inhibitory synapses in the hippocampus of *Dasm1*<sup>-/-</sup> mice are reduced. A prerequisite for synapse formation is the presence of pre- and postsynaptic partners. Therefore, the numbers of interneurons in hippocampus of *Dasm1*<sup>-/-</sup> mice could also be reduced. Possible scenarios leading to such a phenotype would be defects in interneuron migration, differentiation, neurogenesis, or apoptosis (see Figure 7.1). In contrast to pyramidal cells, interneurons do not arise from the germinal ventricular zone, but they originate in the ganglionic eminence of the ventral telencephalon. Starting at the site of their last mitotic division, they follow two main tangential migratory routes to the cortex, where they integrate into specific brain circuits (Marin and Rubenstein, 2001).

Other members of the immunoglobulin superfamily play a role in interneuron development such as migration, differentiation, and neurogenesis. The adhesion molecule TAG-1 for instance, is important for interneuron migration (Denaxa et al., 2001). NCAM-mutant mice display retarded tangential migration of olfactory bulb interneurons (Hu et al., 1996; Cremer et al., 1994). NCAM also influences proliferation and differentiation of neural progenitor cells *in vitro* (Amoureux et al., 2000; Kim et al., 2005). Overexpression of the NCAM isoform 140 in radial glia induced an increase in cell proliferation *in vivo* (Boutin et al., 2009). Integrins are cell adhesion molecules that are involved in integration of cells in networks through their interaction with the extracellular matrix as well as with other cells (Janik et al., 2010). Deletion of the protocadherin  $\gamma$  cluster results in a dramatic loss of interneurons in spinal cord (Wang et al., 2002). Spinal interneurons died at late stages of embryogenesis in mutant mice lacking all 22 *Pcdhn*- $\gamma$  genes, although they differentiated and formed synapses (Wang et al., 2002). This implies that  $\gamma$ -protocadherins do not induce synapse formation in this specific subclass of spinal neurons but are necessary for survival of these neurons.

Thus, cell adhesion molecules are not only involved in the establishment of cell contacts and synapses, but they also play a role in migration, differentiation, neurogenesis, and apoptosis. Neurons are usually generated at sites distinct from their destination place, which implies that they have to migrate before they integrate into networks. Glutamatergic pyramidal neurons are believed to originate in the ventricular zone of the pallium and migrate radially,

whereas GABAergic neurons originate in the ventricular zone of the subpallium and migrate tangentially to their final position. Reduced mIPSCs and sIPSCs in *Dasm1*<sup>-/-</sup> mice could arise from deficits in the generation or migration of interneurons.

Ongoing studies in our lab address the question, whether the number of interneurons present in hippocampus is affected by loss of *Dasm1*.

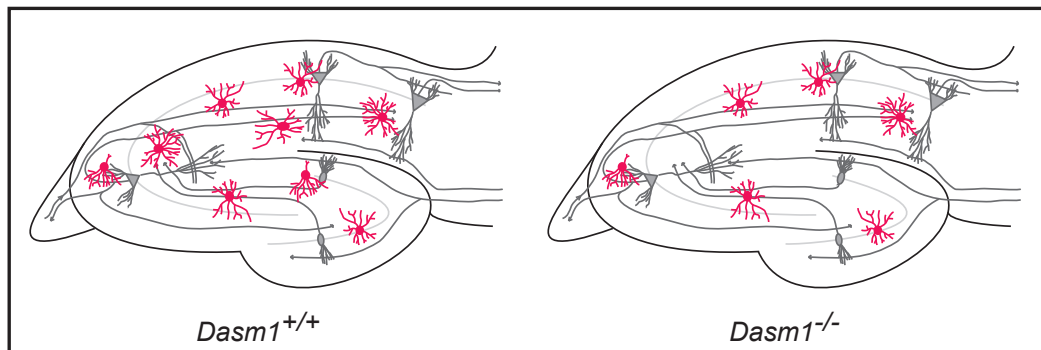


**Figure 7.1: Fewer interneurons might be present in *Dasm1*<sup>-/-</sup> mice.** Altered migration, differentiation, neurogenesis, or apoptosis could reduce number of interneurons (in red) in hippocampus of *Dasm1*<sup>-/-</sup> mice.

## 7.7 Synapse formation and network development

The finding that the frequency of mIPSCs is more reduced in young mice compared to old mice implies that *Dasm1* is involved in the formation of synapses. Synapse formation is a process that occurs in two stages: after an initial adhesive contact has formed, the synapse matures. Other members of the Ig superfamily were shown to induce synapse formation *in vitro* (Fogel et al., 2007) through either homo- or heterophilic adhesion. We therefore addressed the adhesive properties of *Dasm1* with a cell adhesion assay. Aggregation assay data suggests that *Dasm1* as well as *Dasm1*- $\Delta$ C have adhesive properties, mediated through the extracellular part of the protein. Adhesive properties are a requirement for synaptogenic proteins, but are not sufficient for synapse formation. Multiple steps are needed to form functional synaptic contacts, and each of these steps could be affected in *Dasm1*<sup>-/-</sup> mice. In mice, hundreds of different proteins are involved in the establishment and maintenance of the presynapse, and approximately 1500 proteins have been identified as being part of the postsynaptic proteome (Bayes and Grant, 2009; Collins et al., 2006). The postsynaptic protein machinery consisting of neurotransmitter receptors, signaling molecules, and scaffolding proteins, has to assemble

in a coordinated manner. Some cell adhesion molecules are able to form initial adhesive contacts, which then induce the assembly of functional presynaptic boutons (Lucido et al., 2009; Ziv and Garner, 2004). Presynaptically expressed neurexin induces the differentiation of postsynaptic receptors (Graf et al., 2004) and overexpression of different isoforms of neuroligins increases excitatory and inhibitory synaptic responses (Chubykin et al., 2007; Chih et al., 2005).

Only a couple of proteins inducing synapse formation have been shown so far, for example neuroligins (Scheiffele et al., 2000; Woo et al., 2009), neurexins (Graf et al., 2004), SynCAMs (Biederer et al., 2002), EphBs and ephrinBs (Aoto et al., 2007; Kayser et al., 2006), SALMs (Mah et al., 2010), LRRTM (Linhoff et al., 2009), and netrin G ligands (Kim et al., 2006). The majority of them acts on excitatory glutamatergic synapses for different reasons: (1) roughly 85% of synaptic connections within the gray matter of neocortex are excitatory (Douglas et al., 1995), (2) excitatory neurons predominantly project onto other excitatory neurons (Douglas et al., 1995), (3) the most studied synapse in the brain is the CA3–CA1-synapse in hippocampus, which is excitatory, and (4) postsynaptic receptors of excitatory synapses are constituted of few subunits, making them relatively easy to reconstitute in heterologous systems which are used to study functional synapse formation in non-neuronal cells.

For obvious reasons, pre- and postsynaptic partners of inhibitory synapses also need to establish contacts, but only few proteins that specifically act on the development of GABAergic synapses are known to date, for example gephyrin, dystrophin, semaphorin 4 D, and neuroligin-2 (Fritschy and Brunig, 2003; Paradis et al., 2007; Chubykin et al., 2007; Dong et al., 2007). Possible reasons for the lack of knowledge for these molecules are (1) there is a great diversity of interneurons (for review see Klausberger and Somogyi, 2008 and McBain and Fisahn, 2001), (2) they are low in number and interspersed throughout the hippocampus, (3) they do not have standard projections, as for example, the excitatory laminar CA3–CA1-pathway does, (4) pentameric GABA receptors are heterogeneously assembled (Mohler, 2006), which complicates reconstitution in heterologous systems, and (5) pre- and postsynaptic partners are predominantly not the same type of neurons.

First results of a co-culture assay suggest that Dasm1 might induce inhibitory synapse formation. For that purpose, Cos-7 cells were transfected with Dasm1 and co-cultured with hippocampal neurons. Stainings with an antibody against the vesicular GABA transporter

(VGAT), an inhibitory specific presynaptic marker, provide first evidence that the axons of neurons contacting *Dasm1* transfected cells establish presynaptic structures (A. Mishra, unpublished observations). Further experiments will be performed to test which extracellular domains are needed and whether only inhibitory or also excitatory synapses are induced. The interesting question, whether *Dasm1* acts via a homo- or heterophilic mechanism could be addressed by modifying the synapse induction assay. Co-culturing *Dasm1*<sup>-/-</sup> neurons with *Dasm1* transfected non-neuronal cells should still induce synapse formation, if the effect is mediated by heterophilic interactions.

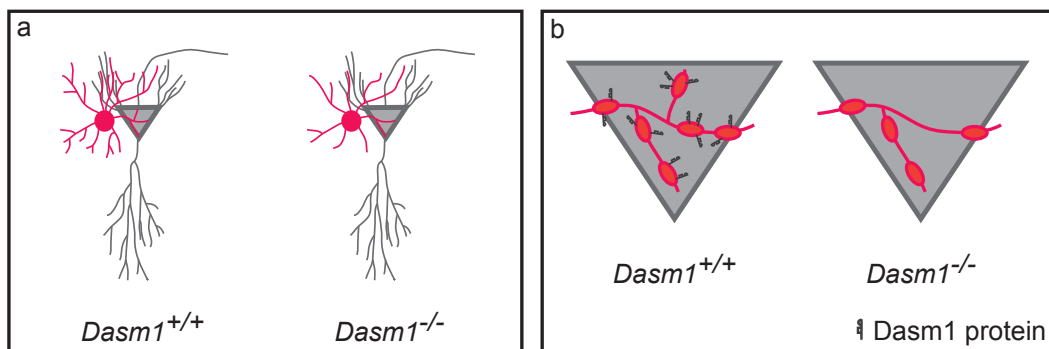


**Figure 7.2: Excitatory neurons receive fewer inhibitory synapses in *Dasm1*<sup>-/-</sup> mice.** (a) Fewer inhibitory synapses might be established due to impaired target recognition and synapse formation. *Dasm1* could be a synaptogenic molecule acting on the number of inhibitory synapses. (b) Magnification of the model shown in (a).

Further analysis of a potential function of *Dasm1* in synapse formation will help to understand how GABAergic connections are formed. Is there a unitary mechanism of synapse formation for all classes of interneurons contacting excitatory neurons or do subclasses of interneurons have specific mechanisms to prevent wrong or excess connections? The majority of interneurons project locally and innervate nearby cells, whereas pyramidal cells predominantly project over long distances. Although interneurons probably do not need highly elaborated axon guidance cues, as projection neurons for proper wiring over long distances (Sanes and Yamagata, 2009), they still require mechanisms for specific target recognition. Major molecule classes implicated in target recognition are cadherins, as well as immunoglobulin superfamilies (Shapiro et al., 2007; Takeichi, 2007). Recently, Fazzari and colleagues described that connectivity of specific GABA-containing interneurons is regulated by neuregulin 1 (*Nrg1*) and its receptor ErbB4 (Fazzari et al., 2010). ErbB4-*Nrg1* signalling is required for

proper axo-axonic inhibitory synapse development from chandelier cells onto pyramidal cells. Dasm1 might also be involved in the wiring of GABA mediated circuits - decreased frequencies of miniature IPSCs might arise from deficits in the connectivity pattern of interneurons with pyramidal cells during maturation. Synaptogenic properties of Dasm1 might be necessary for interneurons in general, or for a subset of interneurons, to establish inhibitory contacts onto pyramidal cells (see Figure 7.2).

Understanding how balanced networks, consisting of excitatory and inhibitory neurons are wired during brain maturation is one of the most fascinating questions in neuroscience. Neuropsychiatric disorders such as autism spectrum disorders, schizophrenia, and Tourette's syndrome are often linked to insufficient wiring, which is the main task of cell adhesion molecules (Jamain et al., 2003; Walsh et al., 2008; Yan et al., 2005). Understanding how the great abundance of cell adhesion molecules acts in an orchestrated manner is necessary to develop strategies for the treatment of the aforementioned disorders. Only few cell adhesion molecules acting exclusively on inhibitory synapses are known, a fact that makes Dasm1 even more interesting.



## 8 Outlook

Reduced frequencies of miniature and spontaneous inhibitory postsynaptic currents, as well as reduced gephyrin puncta in dissociated hippocampal neurons suggest a reduced number of inhibitory synapses in *Dasm1*<sup>-/-</sup> mice compared to *Dasm1*<sup>+/+</sup> littermates. Cell aggregation assay data together with preliminary data of a co-culture assay indicate that Dasm1 has synaptogenic properties.

The way Dasm1 specifically reduces inhibitory synapses in a developmental manner remains to be elucidated. Up to now, it is not clear which cells express Dasm1. In situ hybridizations and RT-PCRs on interneurons indicate that Dasm1 is present in excitatory and at least in a subset of inhibitory neurons in hippocampus. Taking advantage of a GENSAT reporter mouse line (Gong et al., 2003), which expresses EGFP under the IgSF9 promoter, will help to show which cells express Dasm1. Co-stainings with specific antibodies for subclasses of interneurons (see chapter 4.3.3) will help to discriminate whether all or only a subset of interneurons express Dasm1. It will also be important to figure out the subcellular location of Dasm1. Most likely, Dasm1 is located at or near inhibitory synapses, as this is their site of action. Unfortunately, all attempts to produce a specific antibody against Dasm1 failed so far (A. Mishra, unpublished results). As only the number of inhibitory synapses of a subset of interneurons may be decreased, whereas other interneuron classes are unaffected by loss of Dasm1, it is important to investigate whether numbers and classes of interneurons present in *Dasm1*<sup>-/-</sup> hippocampus are altered or not. If Dasm1 acts only on a subset of inhibitory synapses, specific mechanisms for shaping inhibitory connections could be identified.

Detailed analysis of the IgSF9b knockout mice could unravel shared mechanisms with Dasm1, as well as compensatory actions of these closely related proteins. Double knockout mice lacking Dasm1 and IgSF9b could show even more impaired synapse formation. For neuroligins, it was reported that in brainstem respiratory centers frequencies, but not amplitudes of spontaneous and miniature inhibitory postsynaptic currents, were significantly reduced in double and even more in triple knockout mice compared to single knockout mice (Varoquaux

et al., 2006).

An interesting experiment would be to overexpress Dasm1 in interneurons and/or in pyramidal CA1 neurons of wildtype mice and test whether Dasm1 induces inhibitory synapses *in vitro* or even *in vivo* in wildtype mice. The frequency of mIPSCs would then even be higher in cells overexpressing Dasm1 compared to control neurons provided that Dasm1 acts in a homophilic manner. I started recently to establish the method of *in utero* electroporation. I will address the potential synaptogenic properties of Dasm1 *in vivo* by overexpression of a Dasm1 full length construct together with the EGFP reporter in CA1 pyramidal neurons of wildtype mice.

## 9 Other projects during PhD

During my time at the Max-Planck-Institute of Neurobiology I did not only work on my Ph.D. thesis project about Dasm1, but also contributed to other research projects, which I will mention in the following paragraphs.

### 9.1 Serine phosphorylation of ephrinB2 regulates trafficking of synaptic AMPA receptors

EphrinB ligands are involved in spine morphogenesis, synapse formation and synaptic plasticity and are the ligands of EphB receptors. In this study we could show that ephrinB2 is critical for stabilization of AMPA receptors at the cellular membrane. Using dissociated hippocampal neurons, we could demonstrate that upon EphB4-FC stimulation the internalization of AMPA receptors is higher in ephrinB2 knockout neurons compared to wildtype neurons. Miniature excitatory postsynaptic currents (mEPSCs) were significantly decreased in ephrinB2 knockout neurons compared to littermate neurons, suggesting a role for ephrinB2 in stabilizing AMPA receptors at synapses.

In 2008, this study was published in Nature Neuroscience:

Essmann C.L., Martinez E., Geiger J.C., Zimmer M., **Traut M.H.**, Stein V., Klein R., and Acker-Palmer A. Serine phosphorylation of ephrinb2 regulates trafficking of synaptic AMPA receptors. *Nature Neuroscience* 2008 Sep;11(9):1035-43.

### 9.2 Electrical activity suppresses axon growth through Ca<sub>v</sub>1.2 channels in adult primary sensory neurons

Dorsal root ganglion (DRG) cells are sensory neurons that display axon growth competence after lesions. In this study, we assessed whether electrical activity is involved in axon regrowth. We could show that cessation of electrical activity after lesion contributes to regeneration. Freshly isolated DRG neurons start firing action potentials upon depolarization with 40

mM KCl and shift membrane potentials from -56 mV to -9 mV (n=14). Also DRG neurons cultured for 3 DIV in normal medium shift the membrane potential from -54 mV to -13 mV (n=13), suggesting that DRG neurons do not alter their membrane potential upon cultivation. DRG neurons cultured in 40 mM KCl for 3 DIV, remain depolarized (-17 mV) throughout the whole time and hyperpolarize upon K<sup>+</sup> washout to a membrane potential of -53 mV (n=8). This nicely demonstrates, that DRG neurons do not adapt their membrane potential during long periods of depolarization.

In 2010, this study was published in *Current Biology*:

Enes J., Langwieser N., Ruschel J., Carballosa-Gonzalez M.M., Klug A., **Traut M.H.**, Ylera B., Tahirovic S., Hofmann F., Stein, V., Moosmang S., Hentall I.D., Bradke F. Electrical activity suppresses axon growth through Ca<sub>v</sub>1.2 channels in adult primary sensory neurons. *Current Biology* 2010 Jul 13; 20(13):1154-1164.

## Bibliography

- Akerman, C. J. and Cline, H. T. (2006). Depolarizing GABAergic conductances regulate the balance of excitation to inhibition in the developing retinotectal circuit in vivo. *J Neurosci*, 26(19):5117–30.
- Al-Anzi, B. and Wyman, R. J. (2009). The *Drosophila* immunoglobulin gene turtle encodes guidance molecules involved in axon pathfinding. *Neural Dev*, 4:31.
- Amoureux, M. C., Cunningham, B. A., Edelman, G. M., and Crossin, K. L. (2000). N-CAM binding inhibits the proliferation of hippocampal progenitor cells and promotes their differentiation to a neuronal phenotype. *J Neurosci*, 20(10):3631–40.
- Anderson, P., Bliss, T. V., and Skrede, K. K. (1971). Lamellar organization of hippocampal pathways. *Exp Brain Res*, 13(2):222–38.
- Aoto, J., Ting, P., Maghsoodi, B., Xu, N., Henkemeyer, M., and Chen, L. (2007). Postsynaptic ephrinB3 promotes shaft glutamatergic synapse formation. *J Neurosci*, 27(28):7508–19.
- Arnaut, M. A., Mahalingam, B., and Xiong, J. P. (2005). Integrin structure, allostery, and bidirectional signaling. *Annu Rev Cell Dev Biol*, 21:381–410.
- Atasoy, D., Ertunc, M., Moulder, K. L., Blackwell, J., Chung, C., Su, J., and Kavalali, E. T. (2008). Spontaneous and evoked glutamate release activates two populations of NMDA receptors with limited overlap. *J Neurosci*, 28(40):10151–66.
- Barclay, A. N. (2003). Membrane proteins with immunoglobulin-like domains—a master superfamily of interaction molecules. *Semin Immunol*, 15(4):215–23.
- Barry, P. H. and Lynch, J. W. (1991). Liquid junction potentials and small cell effects in patch-clamp analysis. *J Membr Biol*, 121(2):101–17.
- Bayes, A. and Grant, S. G. (2009). Neuroproteomics: understanding the molecular organization and complexity of the brain. *Nat Rev Neurosci*, 10(9):635–46.
- Bear, M. F., Connors, B. W., and Paradiso, M. A. (2001). Neuroscience - Exploring The Brain. *Lippincott Williams and Wilkins*.
- Becker, C. G., Artola, A., Gerardy-Schahn, R., Becker, T., Welzl, H., and Schachner, M. (1996). The polysialic acid modification of the neural cell adhesion molecule is involved in spatial learning and hippocampal long-term potentiation. *J Neurosci Res*, 45(2):143–52.
- Ben-Ari, Y. (2002). Excitatory actions of gaba during development: the nature of the nurture. *Nat Rev Neurosci*, 3(9):728–39.
- Ben-Ari, Y., Cherubini, E., Corradetti, R., and Gaiarsa, J. L. (1989). Giant synaptic potentials in immature rat CA3 hippocampal neurones. *J Physiol*, 416:303–25.
- Ben-Ari, Y., Gaiarsa, J. L., Tyzio, R., and Khazipov, R. (2007). GABA: a pioneer transmitter that excites immature neurons and generates primitive oscillations. *Physiol Rev*, 87(4):1215–84.
- Ben-Ari, Y., Khazipov, R., Leinekugel, X., Cailhard, O., and Gaiarsa, J. L. (1997). GABAA, NMDA and AMPA receptors: a developmentally regulated 'menage a trois'. *Trends Neurosci*, 20(11):523–9.
- Benes, F. M. and Berretta, S. (2001). GABAergic interneurons: implications for understanding schizophrenia and bipolar disorder. *Neuropsychopharmacology*, 25(1):1–27.
- Benson, D. L. and Tanaka, H. (1998). N-cadherin redistribution during synaptogenesis in hippocampal neurons. *J Neurosci*, 18(17):6892–904.
- Biederer, T., Sara, Y., Mozhayeva, M., Atasoy, D., Liu, X., Kavalali, E. T., and Sudhof, T. C. (2002). SynCAM, a synaptic adhesion molecule that drives synapse assembly. *Science*, 297(5586):1525–31.

- Blaesse, P., Airaksinen, M. S., Rivera, C., and Kaila, K. (2009). Cation-chloride cotransporters and neuronal function. *Neuron*, 61(6):820–38.
- Bliss, T. V. and Gardner-Medwin, A. R. (1973). Long-lasting potentiation of synaptic transmission in the dentate area of the unanaesthetized rabbit following stimulation of the perforant path. *J Physiol*, 232(2):357–74.
- Blum, B. P. and Mann, J. J. (2002). The GABAergic system in schizophrenia. *Int J Neuropsychopharmacol*, 5(2):159–79.
- Bodily, K. D., Morrison, C. M., Renden, R. B., and Broadie, K. (2001). A novel member of the Ig superfamily, turtle, is a CNS-specific protein required for coordinated motor control. *J Neurosci*, 21(9):3113–25.
- Borst, J. G., Lodder, J. C., and Kits, K. S. (1994). Large amplitude variability of GABAergic IPSCs in melanotropes from *Xenopus laevis*: evidence that quantal size differs between synapses. *J Neurophysiol*, 71(2):639–55.
- Boutin, C., Schmitz, B., Cremer, H., and Diestel, S. (2009). NCAM expression induces neurogenesis in vivo. *Eur J Neurosci*, 30(7):1209–18.
- Carter, A. G. and Regehr, W. G. (2002). Quantal events shape cerebellar interneuron firing. *Nat Neurosci*, 5(12):1309–18.
- Cathala, L., Holderith, N. B., Nusser, Z., DiGregorio, D. A., and Cull-Candy, S. G. (2005). Changes in synaptic structure underlie the developmental speeding of AMPA receptor-mediated EPSCs. *Nat Neurosci*, 8(10):1310–8.
- Chalifoux, J. R. and Carter, A. G. (2010). GABAB receptors modulate NMDA receptor calcium signals in dendritic spines. *Neuron*, 66(1):101–13.
- Chevalyere, V. and Siegelbaum, S. A. (2010). Strong CA2 pyramidal neuron synapses define a powerful disinaptic cortico-hippocampal loop. *Neuron*, 66(4):560–72.
- Chih, B., Engelman, H., and Scheiffele, P. (2005). Control of excitatory and inhibitory synapse formation by neuroligins. *Science*, 307(5713):1324–8.
- Chubykin, A. A., Atasoy, D., Etherton, M. R., Brose, N., Kavalali, E. T., Gibson, J. R., and Sudhof, T. C. (2007). Activity-dependent validation of excitatory versus inhibitory synapses by neuroligin-1 versus neuroligin-2. *Neuron*, 54(6):919–31.
- Claiborne, B. J., Amaral, D. G., and Cowan, W. M. (1990). Quantitative, three-dimensional analysis of granule cell dendrites in the rat dentate gyrus. *J Comp Neurol*, 302(2):206–19.
- Collingridge, G. L., Olsen, R. W., Peters, J., and Spedding, M. (2009). A nomenclature for ligand-gated ion channels. *Neuropharmacology*, 56(1):2–5.
- Collins, M. O., Husi, H., Yu, L., Brandon, J. M., Anderson, C. N., Blackstock, W. P., Choudhary, J. S., and Grant, S. G. (2006). Molecular characterization and comparison of the components and multiprotein complexes in the postsynaptic proteome. *J Neurochem*, 97 Suppl 1:16–23.
- Cremer, H., Lange, R., Christoph, A., Plomann, M., Vopper, G., Roes, J., Brown, R., Baldwin, S., Kraemer, P., Scheff, S., and et al. (1994). Inactivation of the N-CAM gene in mice results in size reduction of the olfactory bulb and deficits in spatial learning. *Nature*, 367(6462):455–9.
- Dalva, M. B., McClelland, A. C., and Kayser, M. S. (2007). Cell adhesion molecules: signalling functions at the synapse. *Nat Rev Neurosci*, 8(3):206–20.
- De Koninck, Y. and Mody, I. (1994). Noise analysis of miniature IPSCs in adult rat brain slices: properties and modulation of synaptic GABAA receptor channels. *J Neurophysiol*, 71(4):1318–35.
- Denaxa, M., Chan, C. H., Schachner, M., Parnavelas, J. G., and Karagogeos, D. (2001). The adhesion molecule TAG-1 mediates the migration of cortical interneurons from the ganglionic eminence along the corticofugal fiber system. *Development*, 128(22):4635–44.
- Dong, N., Qi, J., and Chen, G. (2007). Molecular reconstitution of functional GABAergic synapses with expression of neuroligin-2 and GABAA receptors. *Mol Cell Neurosci*, 35(1):14–23.

- Doudney, K., Murdoch, J. N., Braybrook, C., Paternotte, C., Bentley, L., Copp, A. J., and Stanier, P. (2002). Cloning and characterization of Igsf9 in mouse and human: a new member of the immunoglobulin superfamily expressed in the developing nervous system. *Genomics*, 79(5):663–70.
- Douglas, R. J., Koch, C., Mahowald, M., Martin, K. A., and Suarez, H. H. (1995). Recurrent excitation in neocortical circuits. *Science*, 269(5226):981–5.
- Doyle, J. P. and Colman, D. R. (1993). Glial-neuron interactions and the regulation of myelin formation. *Curr Opin Cell Biol*, 5(5):779–85.
- Elias, G. M., Funke, L., Stein, V., Grant, S. G., Brecht, D. S., and Nicoll, R. A. (2006). Synapse-specific and developmentally regulated targeting of AMPA receptors by a family of MAGUK scaffolding proteins. *Neuron*, 52(2):307–20.
- Ennaceur, A. and Delacour, J. (1988). A new one-trial test for neurobiological studies of memory in rats. 1: Behavioral data. *Behav Brain Res*, 31(1):47–59.
- Farrant, M. and Nusser, Z. (2005). Variations on an inhibitory theme: phasic and tonic activation of GABA(A) receptors. *Nat Rev Neurosci*, 6(3):215–29.
- Fatt, P. and Katz, B. (1952). Spontaneous sub-threshold activity at motor nerve endings. *J Physiol*, 117(1):109–28.
- Fazzari, P., Paternain, A. V., Valiente, M., Pla, R., Lujan, R., Lloyd, K., Lerma, J., Marin, O., and Rico, B. (2010). Control of cortical GABA circuitry development by Nrg1 and ErbB4 signalling. *Nature*.
- Ferguson, K., Long, H., Cameron, S., Chang, W. T., and Rao, Y. (2009). The conserved Ig superfamily member turtle mediates axonal tiling in *Drosophila*. *J Neurosci*, 29(45):14151–9.
- Fogel, A. I., Akins, M. R., Krupp, A. J., Stagi, M., Stein, V., and Biederer, T. (2007). SynCAMs organize synapses through heterophilic adhesion. *J Neurosci*, 27(46):12516–30.
- Foster, K. A. and Regehr, W. G. (2004). Variance-mean analysis in the presence of a rapid antagonist indicates vesicle depletion underlies depression at the climbing fiber synapse. *Neuron*, 43(1):119–31.
- Frank, C. A., Kennedy, M. J., Goold, C. P., Marek, K. W., and Davis, G. W. (2006). Mechanisms underlying the rapid induction and sustained expression of synaptic homeostasis. *Neuron*, 52(4):663–77.
- Fredj, N. B. and Burrone, J. (2009). A resting pool of vesicles is responsible for spontaneous vesicle fusion at the synapse. *Nat Neurosci*.
- Frerking, M., Borges, S., and Wilson, M. (1995). Variation in GABA mini amplitude is the consequence of variation in transmitter concentration. *Neuron*, 15(4):885–95.
- Fritschy, J. M. and Brunig, I. (2003). Formation and plasticity of GABAergic synapses: physiological mechanisms and pathophysiological implications. *Pharmacol Ther*, 98(3):299–323.
- Fuerst, P. G., Koizumi, A., Masland, R. H., and Burgess, R. W. (2008). Neurite arborization and mosaic spacing in the mouse retina require DSCAM. *Nature*, 451(7177):470–4.
- Garaschuk, O., Hanse, E., and Konnerth, A. (1998). Developmental profile and synaptic origin of early network oscillations in the CA1 region of rat neonatal hippocampus. *J Physiol*, 507 ( Pt 1):219–36.
- Ge, S., Goh, E. L., Sailor, K. A., Kitabatake, Y., Ming, G. L., and Song, H. (2006). GABA regulates synaptic integration of newly generated neurons in the adult brain. *Nature*, 439(7076):589–93.
- Gong, S. C., Zheng, C., Doughty, M. L., Losos, K., Didkovsky, N., Schambra, U. B., Nowak, N. J., Joyner, A., Leblanc, G., Hatten, M. E., and Heintz, N. (2003). A gene expression atlas of the central nervous system based on bacterial artificial chromosomes. *Nature*, 425(6961):917–925.
- Graf, E. R., Zhang, X., Jin, S. X., Linhoff, M. W., and Craig, A. M. (2004). Neurexins induce

- differentiation of GABA and glutamate postsynaptic specializations via neuroligins. *Cell*, 119(7):1013–26.
- Groemer, T. W. and Klingauf, J. (2007). Synaptic vesicles recycling spontaneously and during activity belong to the same vesicle pool. *Nat Neurosci*, 10(2):145–7.
- Hablitz, J. J., Mathew, S. S., and Pozzo-Miller, L. (2009). GABA vesicles at synapses: are there 2 distinct pools? *Neuroscientist*, 15(3):218–24.
- Hall, B. J., Ripley, B., and Ghosh, A. (2007). NR2B signaling regulates the development of synaptic AMPA receptor current. *J Neurosci*, 27(49):13446–56.
- Hashimoto, T., Maekawa, S., and Miyata, S. (2009). IgLON cell adhesion molecules regulate synaptogenesis in hippocampal neurons. *Cell Biochem Funct*, 27(7):496–8.
- Hu, H., Tomasiewicz, H., Magnuson, T., and Rutishauser, U. (1996). The role of polysialic acid in migration of olfactory bulb interneuron precursors in the subventricular zone. *Neuron*, 16(4):735–43.
- Hubner, C. A., Lorke, D. E., and Hermans-Borgmeyer, I. (2001a). Expression of the Na-K-2Cl-cotransporter NKCC1 during mouse development. *Mech Dev*, 102(1-2):267–9.
- Hubner, C. A., Stein, V., Hermans-Borgmeyer, I., Meyer, T., Ballanyi, K., and Jentsch, T. J. (2001b). Disruption of KCC2 reveals an essential role of K-Cl cotransport already in early synaptic inhibition. *Neuron*, 30(2):515–24.
- Hynes, R. O. (2002). Integrins: bidirectional, allosteric signaling machines. *Cell*, 110(6):673–87.
- Ichtchenko, K., Hata, Y., Nguyen, T., Ullrich, B., Missler, M., Moomaw, C., and Sudhof, T. C. (1995). Neuroligin 1: a splice site-specific ligand for beta-neurexins. *Cell*, 81(3):435–43.
- Jamain, S., Quach, H., Betancur, C., Rastam, M., Colineaux, C., Gillberg, I. C., Soderstrom, H., Giros, B., Leboyer, M., Gillberg, C., and Bourgeron, T. (2003). Mutations of the X-linked genes encoding neuroligins NLGN3 and NLGN4 are associated with autism. *Nat Genet*, 34(1):27–9.
- Janik, M. E., Litynska, A., and Vereecken, P. (2010). Cell migration-The role of integrin glycosylation. *Biochim Biophys Acta*.
- Jentsch, T. J., Stein, V., Weinreich, F., and Zdebik, A. A. (2002). Molecular structure and physiological function of chloride channels. *Physiol Rev*, 82(2):503–68.
- Jungling, K., Eulenburg, V., Moore, R., Kemler, R., Lessmann, V., and Gottmann, K. (2006). N-cadherin transsynaptically regulates short-term plasticity at glutamatergic synapses in embryonic stem cell-derived neurons. *J Neurosci*, 26(26):6968–78.
- Katz, B. and Miledi, R. (1968). The role of calcium in neuromuscular facilitation. *J Physiol*, 195(2):481–92.
- Kaufmann, N., DeProto, J., Ranjan, R., Wan, H., and Van Vactor, D. (2002). Drosophila liprin-alpha and the receptor phosphatase Dlar control synapse morphogenesis. *Neuron*, 34(1):27–38.
- Kayser, M. S., McClelland, A. C., Hughes, E. G., and Dalva, M. B. (2006). Intracellular and transsynaptic regulation of glutamatergic synaptogenesis by EphB receptors. *J Neurosci*, 26(47):12152–64.
- Kessels, H. W. and Malinow, R. (2009). Synaptic AMPA receptor plasticity and behavior. *Neuron*, 61(3):340–50.
- Khazipov, R., Khalilov, I., Tyzio, R., Morozova, E., Ben-Ari, Y., and Holmes, G. L. (2004). Developmental changes in GABAergic actions and seizure susceptibility in the rat hippocampus. *Eur J Neurosci*, 19(3):590–600.
- Kim, J. H., Lee, J. H., Park, J. Y., Park, C. H., Yun, C. O., Lee, S. H., Lee, Y. S., and Son, H. (2005). Retrovirally transduced NCAM140 facilitates neuronal fate choice of hippocampal progenitor cells. *J Neurochem*, 94(2):417–24.
- Kim, S., Burette, A., Chung, H. S., Kwon, S. K., Woo, J., Lee, H. W., Kim, K., Kim, H., Weinberg, R. J., and Kim, E. (2006). NGL family PSD-95-interacting adhesion molecules regulate

- excitatory synapse formation. *Nat Neurosci*, 9(10):1294–301.
- Klausberger, T. and Somogyi, P. (2008). Neuronal diversity and temporal dynamics: the unity of hippocampal circuit operations. *Science*, 321(5885):53–7.
- Kneussel, M., Brandstatter, J. H., Laube, B., Stahl, S., Muller, U., and Betz, H. (1999). Loss of postsynaptic GABA(A) receptor clustering in gephyrin-deficient mice. *J Neurosci*, 19(21):9289–97.
- Kochlamazashvili, G., Senkov, O., Grebenyuk, S., Robinson, C., Xiao, M. F., Stummeyer, K., Gerardy-Schahn, R., Engel, A. K., Feig, L., Semyanov, A., Suppiramaniam, V., Schachner, M., and Dityatev, A. (2010). Neural cell adhesion molecule-associated polysialic acid regulates synaptic plasticity and learning by restraining the signaling through GluN2B-containing NMDA receptors. *J Neurosci*, 30(11):4171–83.
- Koike-Tani, M., Kanda, T., Saitoh, N., Yamashita, T., and Takahashi, T. (2008). Involvement of AMPA receptor desensitization in short-term synaptic depression at the calyx of Held in developing rats. *J Physiol*, 586(9):2263–75.
- Lewis, D. A. (2000). GABAergic local circuit neurons and prefrontal cortical dysfunction in schizophrenia. *Brain Res Brain Res Rev*, 31(2-3):270–6.
- Linhoff, M. W., Lauren, J., Cassidy, R. M., Dobie, F. A., Takahashi, H., Nygaard, H. B., Airaksinen, M. S., Strittmatter, S. M., and Craig, A. M. (2009). An unbiased expression screen for synaptogenic proteins identifies the LRRTM protein family as synaptic organizers. *Neuron*, 61(5):734–49.
- Long, H., Ou, Y., Rao, Y., and van Meyel, D. J. (2009). Dendrite branching and self-avoidance are controlled by Turtle, a conserved IgSF protein in *Drosophila*. *Development*, 136(20):3475–84.
- Lopez-Bendito, G., Sturgess, K., Erdelyi, F., Szabo, G., Molnar, Z., and Paulsen, O. (2004). Preferential origin and layer destination of GAD65-GFP cortical interneurons. *Cereb Cortex*, 14(10):1122–33.
- Lou, X., Scheuss, V., and Schneggenburger, R. (2005). Allosteric modulation of the presynaptic Ca<sup>2+</sup> sensor for vesicle fusion. *Nature*, 435(7041):497–501.
- Lucido, A. L., Suarez Sanchez, F., Thostrup, P., Kwiatkowski, A. V., Leal-Ortiz, S., Gopalakrishnan, G., Liazoghli, D., Belkaid, W., Lennox, R. B., Grutter, P., Garner, C. C., and Colman, D. R. (2009). Rapid assembly of functional presynaptic boutons triggered by adhesive contacts. *J Neurosci*, 29(40):12449–66.
- Luthi, A., Laurent, J. P., Figuero, A., Muller, D., and Schachner, M. (1994). Hippocampal long-term potentiation and neural cell adhesion molecules L1 and NCAM. *Nature*, 372(6508):777–9.
- Lynch, G. S., Dunwiddie, T., and Gribkoff, V. (1977). Heterosynaptic depression: a postsynaptic correlate of long-term potentiation. *Nature*, 266(5604):737–9.
- Mah, W., Ko, J., Nam, J., Han, K., Chung, W. S., and Kim, E. (2010). Selected SALM (synaptic adhesion-like molecule) family proteins regulate synapse formation. *J Neurosci*, 30(16):5559–68.
- Malenka, R. C. and Bear, M. F. (2004). LTP and LTD: an embarrassment of riches. *Neuron*, 44(1):5–21.
- Malinow, R. and Malenka, R. C. (2002). AMPA receptor trafficking and synaptic plasticity. *Annu Rev Neurosci*, 25:103–26.
- Marin, O. and Rubenstein, J. L. (2001). A long, remarkable journey: tangential migration in the telencephalon. *Nat Rev Neurosci*, 2(11):780–90.
- Mathew, S. S., Pozzo-Miller, L., and Hablitz, J. J. (2008). Kainate modulates presynaptic GABA release from two vesicle pools. *J Neurosci*, 28(3):725–31.
- Matsunaga, M., Hatta, K., and Takeichi, M. (1988). Role of N-cadherin cell adhesion molecules in the histogenesis of neural retina. *Neuron*, 1(4):289–95.
- McBain, C. J. and Fisahn, A. (2001). Interneurons unbound. *Nat Rev Neurosci*, 2(1):11–23.

- McKinney, R. A., Capogna, M., Durr, R., Gahwiler, B. H., and Thompson, S. M. (1999). Miniature synaptic events maintain dendritic spines via AMPA receptor activation. *Nat Neurosci*, 2(1):44–9.
- Mi, Z. P., Jiang, P., Weng, W. L., Lindberg, F. P., Narayanan, V., and Lagenaur, C. F. (2000). Expression of a synapse-associated membrane protein, P84/SHPS-1, and its ligand, IAP/CD47, in mouse retina. *J Comp Neurol*, 416(3):335–44.
- Misgeld, U., Bijak, M., and Jarolimek, W. (1995). A physiological role for GABAB receptors and the effects of baclofen in the mammalian central nervous system. *Prog Neurobiol*, 46(4):423–62.
- Mishra, A., Knerr, B., Paixao, S., Kramer, E. R., and Klein, R. (2008). The protein dendrite arborization and synapse maturation 1 (Dasm-1) is dispensable for dendrite arborization. *Mol Cell Biol*, 28(8):2782–91.
- Miyata, S., Matsumoto, N., and Maekawa, S. (2003). Polarized targeting of IgLON cell adhesion molecule OBCAM to dendrites in cultured neurons. *Brain Res*, 979(1-2):129–36.
- Mizoguchi, A., Nakanishi, H., Kimura, K., Matsumura, K., Ozaki-Kuroda, K., Katata, T., Honda, T., Kiyohara, Y., Heo, K., Higashi, M., Tsutsumi, T., Sonoda, S., Ide, C., and Takai, Y. (2002). Nectin: an adhesion molecule involved in formation of synapses. *J Cell Biol*, 156(3):555–65.
- Mohler, H. (2006). GABA(A) receptor diversity and pharmacology. *Cell Tissue Res*, 326(2):505–16.
- Morris, R. (1984). Developments of a water-maze procedure for studying spatial learning in the rat. *J Neurosci Methods*, 11(1):47–60.
- Muller, M., Goutman, J. D., Kochubey, O., and Schneggenburger, R. (2010). Interaction between facilitation and depression at a large CNS synapse reveals mechanisms of short-term plasticity. *J Neurosci*, 30(6):2007–16.
- Murai, K. K., Misner, D., and Ranscht, B. (2002). Contactin supports synaptic plasticity associated with hippocampal long-term depression but not potentiation. *Curr Biol*, 12(3):181–90.
- Neher, E. and Sakaba, T. (2008). Multiple roles of calcium ions in the regulation of neurotransmitter release. *Neuron*, 59(6):861–72.
- Nicoll, R. A. and Schmitz, D. (2005). Synaptic plasticity at hippocampal mossy fibre synapses. *Nat Rev Neurosci*, 6(11):863–76.
- Nusser, Z., Cull-Candy, S., and Farrant, M. (1997). Differences in synaptic GABA(A) receptor number underlie variation in GABA mini amplitude. *Neuron*, 19(3):697–709.
- Oliet, S. H., Malenka, R. C., and Nicoll, R. A. (1997). Two distinct forms of long-term depression coexist in CA1 hippocampal pyramidal cells. *Neuron*, 18(6):969–82.
- Overstreet Wadiche, L., Bromberg, D. A., Bensen, A. L., and Westbrook, G. L. (2005). GABAergic signaling to newborn neurons in dentate gyrus. *J Neurophysiol*, 94(6):4528–32.
- Paradis, S., Harrar, D. B., Lin, Y., Koon, A. C., Hauser, J. L., Griffith, E. C., Zhu, L., Brass, L. F., Chen, C., and Greenberg, M. E. (2007). An RNAi-Based Approach Identifies Molecules Required for Glutamatergic and GABAergic Synapse Development. *Neuron*, 53(2):217–32.
- Parra, P., Gulyas, A. I., and Miles, R. (1998). How many subtypes of inhibitory cells in the hippocampus? *Neuron*, 20(5):983–93.
- Pfeffer, C. K., Stein, V., Keating, D. J., Maier, H., Rinke, I., Rudhard, Y., Hentschke, M., Rune, G. M., Jentsch, T. J., and Hubner, C. A. (2009). NKCC1-dependent GABAergic excitation drives synaptic network maturation during early hippocampal development. *J Neurosci*, 29(11):3419–30.
- Piccolino, M., Strettoi, E., and Laurenzi, E. (1989). Santiago Ramon y Cajal, the retina and the neuron theory. *Doc Ophthalmol*, 71(2):123–41.
- Prange, O. and Murphy, T. H. (1999). Correlation of miniature synaptic activity and evoked release probability in cultures of cortical neurons. *J Neurosci*, 19(15):6427–38.
- Redies, C. (2000). Cadherins in the central nervous system. *Prog Neurobiol*, 61(6):611–48.

- Reyes, A. A., Schulte, S. V., Small, S., and Akeson, R. (1993). Distinct NCAM splicing events are differentially regulated during rat brain development. *Brain Res Mol Brain Res*, 17(3-4):201–11.
- Rivera, C., Voipio, J., and Kaila, K. (2005). Two developmental switches in GABAergic signalling: the K<sup>+</sup>-Cl<sup>-</sup> cotransporter KCC2 and carbonic anhydrase CAVII. *J Physiol*, 562(Pt 1):27–36.
- Ropert, N., Miles, R., and Korn, H. (1990). Characteristics of miniature inhibitory postsynaptic currents in CA1 pyramidal neurones of rat hippocampus. *J Physiol*, 428:707–22.
- Rougon, G. and Hobert, O. (2003). New insights into the diversity and function of neuronal immunoglobulin superfamily molecules. *Annu Rev Neurosci*, 26:207–38.
- Rubenstein, J. L. and Merzenich, M. M. (2003). Model of autism: increased ratio of excitation/inhibition in key neural systems. *Genes Brain Behav*, 2(5):255–67.
- Saghatelian, A. K., Nikonenko, A. G., Sun, M., Rolf, B., Putthoff, P., Kutsche, M., Bartsch, U., Dityatev, A., and Schachner, M. (2004). Reduced GABAergic transmission and number of hippocampal perisomatic inhibitory synapses in juvenile mice deficient in the neural cell adhesion molecule L1. *Mol Cell Neurosci*, 26(1):191–203.
- Sanes, J. R. and Yamagata, M. (2009). Many paths to synaptic specificity. *Annu Rev Cell Dev Biol*, 25:161–95.
- Sara, Y., Virmani, T., Deak, F., Liu, X., and Kavalali, E. T. (2005). An isolated pool of vesicles recycles at rest and drives spontaneous neurotransmission. *Neuron*, 45(4):563–73.
- Scheiffele, P., Fan, J., Choih, J., Fetter, R., and Serafini, T. (2000). Neuroligin expressed in non-neuronal cells triggers presynaptic development in contacting axons. *Cell*, 101(6):657–69.
- Scoville, W. B. and Milner, B. (1957). Loss of recent memory after bilateral hippocampal lesions. *J Neurol Neurosurg Psychiatry*, 20(1):11–21.
- Senkov, O., Sun, M., Weinhold, B., Gerardy-Schahn, R., Schachner, M., and Dityatev, A. (2006). Polysialylated neural cell adhesion molecule is involved in induction of long-term potentiation and memory acquisition and consolidation in a fear-conditioning paradigm. *J Neurosci*, 26(42):10888–10989.
- Shapiro, L., Doyle, J. P., Hensley, P., Colman, D. R., and Hendrickson, W. A. (1996). Crystal structure of the extracellular domain from P0, the major structural protein of peripheral nerve myelin. *Neuron*, 17(3):435–49.
- Shapiro, L., Love, J., and Colman, D. R. (2007). Adhesion molecules in the nervous system: structural insights into function and diversity. *Annu Rev Neurosci*, 30:451–74.
- Shi, S. H., Cheng, T., Jan, L. Y., and Jan, Y. N. (2004a). The immunoglobulin family member dendrite arborization and synapse maturation 1 (Dasm1) controls excitatory synapse maturation. *Proc Natl Acad Sci U S A*, 101(36):13346–51.
- Shi, S. H., Cox, D. N., Wang, D., Jan, L. Y., and Jan, Y. N. (2004b). Control of dendrite arborization by an Ig family member, dendrite arborization and synapse maturation 1 (Dasm1). *Proc Natl Acad Sci U S A*, 101(36):13341–5.
- Silletti, S., Mei, F., Sheppard, D., and Montgomery, A. M. (2000). Plasmin-sensitive dibasic sequences in the third fibronectin-like domain of L1-cell adhesion molecule (CAM) facilitate homomultimerization and concomitant integrin recruitment. *J Cell Biol*, 149(7):1485–502.
- Sperry, R. W. (1963). Chemoaffinity in the Orderly Growth of Nerve Fiber Patterns and Connections. *Proc Natl Acad Sci U S A*, 50:703–10.
- Stein, V., Hermans-Borgmeyer, I., Jentsch, T. J., and Hubner, C. A. (2004). Expression of the KCl cotransporter KCC2 parallels neuronal maturation and the emergence of low intracellular chloride. *J Comp Neurol*, 468(1):57–64.
- Stoenica, L., Senkov, O., Gerardy-Schahn, R., Weinhold, B., Schachner, M., and Dityatev, A. (2006). In vivo synaptic plasticity in the dentate gyrus of mice deficient in the neural cell adhesion molecule NCAM or its polysialic acid. *Eur J Neurosci*, 23(9):2255–64.

- Sudhof, T. C. (2008). Neuroligins and neurexins link synaptic function to cognitive disease. *Nature*, 455(7215):903–11.
- Sutton, M. A., Wall, N. R., Aakalu, G. N., and Schuman, E. M. (2004). Regulation of dendritic protein synthesis by miniature synaptic events. *Science*, 304(5679):1979–83.
- Tabuchi, K. and Sudhof, T. C. (2002). Structure and evolution of neurexin genes: insight into the mechanism of alternative splicing. *Genomics*, 79(6):849–59.
- Takeichi, M. (2007). The cadherin superfamily in neuronal connections and interactions. *Nat Rev Neurosci*, 8(1):11–20.
- Taniguchi, H., Gollan, L., Scholl, F. G., Mahadomrongkul, V., Dobler, E., Limthong, N., Peck, M., Aoki, C., and Scheiffele, P. (2007). Silencing of neuroligin function by postsynaptic neurexins. *J Neurosci*, 27(11):2815–24.
- Thomson, A. M. (1990). Glycine is a coagonist at the NMDA receptor/channel complex. *Prog Neurobiol*, 35(1):53–74.
- Turrigiano, G. G. (2008). The self-tuning neuron: synaptic scaling of excitatory synapses. *Cell*, 135(3):422–35.
- Turrigiano, G. G. and Nelson, S. B. (2004). Homeostatic plasticity in the developing nervous system. *Nat Rev Neurosci*, 5(2):97–107.
- Ullrich, B., Ushkaryov, Y. A., and Sudhof, T. C. (1995). Cartography of neurexins: more than 1000 isoforms generated by alternative splicing and expressed in distinct subsets of neurons. *Neuron*, 14(3):497–507.
- Ushkaryov, Y. A., Petrenko, A. G., Geppert, M., and Sudhof, T. C. (1992). Neurexins: synaptic cell surface proteins related to the alpha-latrotoxin receptor and laminin. *Science*, 257(5066):50–6.
- Varoqueaux, F., Aramuni, G., Rawson, R. L., Mohrmann, R., Missler, M., Gottmann, K., Zhang, W., Sudhof, T. C., and Brose, N. (2006). Neuroligins determine synapse maturation and function. *Neuron*, 51(6):741–54.
- Virmani, T., Ertunc, M., Sara, Y., Mozhayeva, M., and Kavalali, E. T. (2005). Phorbol esters target the activity-dependent recycling pool and spare spontaneous vesicle recycling. *J Neurosci*, 25(47):10922–9.
- Walsh, T., McClellan, J. M., McCarthy, S. E., Addington, A. M., Pierce, S. B., Cooper, G. M., Nord, A. S., Kusenda, M., Malhotra, D., Bhandari, A., Stray, S. M., Rippey, C. F., Roccanova, P., Makarov, V., Lakshmi, B., Findling, R. L., Sikich, L., Stromberg, T., Merriman, B., Gogtay, N., Butler, P., Eckstrand, K., Noory, L., Gochman, P., Long, R., Chen, Z., Davis, S., Baker, C., Eichler, E. E., Meltzer, P. S., Nelson, S. F., Singleton, A. B., Lee, M. K., Rapoport, J. L., King, M. C., and Sebat, J. (2008). Rare structural variants disrupt multiple genes in neurodevelopmental pathways in schizophrenia. *Science*, 320(5875):539–43.
- Wang, D. D. and Kriegstein, A. R. (2008). GABA regulates excitatory synapse formation in the neocortex via NMDA receptor activation. *J Neurosci*, 28(21):5547–58.
- Wang, X., Weiner, J. A., Levi, S., Craig, A. M., Bradley, A., and Sanes, J. R. (2002). Gamma protocadherins are required for survival of spinal interneurons. *Neuron*, 36(5):843–54.
- Woo, J., Kwon, S. K., Choi, S., Kim, S., Lee, J. R., Dunah, A. W., Sheng, M., and Kim, E. (2009). Trans-synaptic adhesion between NGL-3 and LAR regulates the formation of excitatory synapses. *Nat Neurosci*, 12(4):428–37.
- Wu, L. G. and Borst, J. G. (1999). The reduced release probability of releasable vesicles during recovery from short-term synaptic depression. *Neuron*, 23(4):821–32.
- Wyszynski, M., Kim, E., Dunah, A. W., Passafaro, M., Valtschanoff, J. G., Serra-Pagez, C., Streuli, M., Weinberg, R. J., and Sheng, M. (2002). Interaction between GRIP and liprin-alpha/SYD2 is required for AMPA receptor targeting. *Neuron*, 34(1):39–52.
- Yamada, S. and Nelson, W. J. (2007). Synapses: sites of cell recognition, adhesion, and functional specification. *Annu Rev Biochem*, 76:267–94.

- Yamagata, M., Sanes, J. R., and Weiner, J. A. (2003). Synaptic adhesion molecules. *Curr Opin Cell Biol*, 15(5):621–32.
- Yamagata, M., Weiner, J. A., and Sanes, J. R. (2002). Sidekicks: synaptic adhesion molecules that promote lamina-specific connectivity in the retina. *Cell*, 110(5):649–60.
- Yamakawa, K., Huot, Y. K., Haendelt, M. A., Hubert, R., Chen, X. N., Lyons, G. E., and Korenberg, J. R. (1998). DSCAM: a novel member of the immunoglobulin superfamily maps in a Down syndrome region and is involved in the development of the nervous system. *Hum Mol Genet*, 7(2):227–37.
- Yan, J., Oliveira, G., Coutinho, A., Yang, C., Feng, J., Katz, C., Sram, J., Bockholt, A., Jones, I. R., Craddock, N., Cook, E. H., J., Vicente, A., and Sommer, S. S. (2005). Analysis of the neuroligin 3 and 4 genes in autism and other neuropsychiatric patients. *Mol Psychiatry*, 10(4):329–32.
- Zhang, C., Atasoy, D., Arac, D., Yang, X., Fucillo, M. V., Robison, A. J., Ko, J., Brunger, A. T., and Sudhof, T. C. (2010). Neurexins Physically and Functionally Interact with GABA(A) Receptors. *Neuron*, 66(3):403–416.
- Ziv, N. E. and Garner, C. C. (2004). Cellular and molecular mechanisms of presynaptic assembly. *Nat Rev Neurosci*, 5(5):385–99.
- Zucker, R. S. and Regehr, W. G. (2002). Short-term synaptic plasticity. *Annu Rev Physiol*, 64:355–405.



## 10 Acknowledgments

I thank my supervisors Dr. Valentin Stein and Prof. Dr. Rüdiger Klein for continued support and helpful scientific discussions. I appreciated having had the possibility to follow my own ideas and the warm atmosphere in their labs. Many thanks to Dr. Volker Scheuss and Prof. Dr. Thomas Misgeld for being excellent members of my thesis advisory committee. I thank Dr. Archana Mishra and Bernadette Antoni for the fruitful collaboration. I thank Prof. Dr. Tobias Bonhoeffer and all the members of his group as well as all members of the Klein department for giving scientific input during progress report series and discussions. Thanks to all members of the Stein lab and also to Volker Staiger for technical troubleshooting as well as scientific discussions. Special thanks to Dr. Barbara Cokic for spreading enthusiasm and philosophical as well as scientific ideas. Many thanks also to Ilka Rinke, Barbara Trattner, Andrea Gruschka, and Alexander Krupp for fruitful scientific discussions as well as non-scientific conversations. Many thanks to Louise Gaitanos and Dr. Tom Gaitanos for proofreading the manuscript. I thank Dr. Alexandra Lepier for helping me to optimize lentiviral constructs. I thank Dr. Damian Refojo and Annette Vogl for introducing me to the technique of in-utero electroporation with the help of which we will try to understand Dasm1 function. Many thanks to the animal husbandry facility - without their help this study would not have been possible. Thanks to the people of IT-group, workshop, and administration who make the Max-Planck-Institute of Neurobiology a great place to work.

All my thanks and love to Anne for her patience and support!

Most importantly, many thanks to Monika, Helmut, and Andreas – without all of you I would not be what I am.



## 11 Curriculum vitae

### PERSONAL DATA

**Name** Matthias H. Traut  
**Date of birth** October 2nd, 1979  
**Place of birth** Ravensburg, Germany  
**Citizenship** German

### EDUCATION

**12/2006-present** Ph.D. research under the supervision of Prof. Dr. Rüdiger Klein and Dr. Valentin Stein, Max Planck Institute of Neurobiology, Martinsried.  
**09/2000-08/2006** Studies of biology (diploma), Ludwig-Maximilians-University, Munich.

### GRANTS

**2004-2005** Associate member of the graduate school “Biology of human diseases” (GRK333) of the German Research Foundation (DFG).

### PUBLICATIONS

- 2008** Essmann C.L., Martinez E., Geiger J.C., Zimmer M., **Traut M.H.**, Stein V., Klein R., and Acker-Palmer A. Serine phosphorylation of ephrinb2 regulates trafficking of synaptic AMPA receptors. *Nature Neuroscience* 2008 Sep;11(9):1035-43.
- 2009** **Traut M.H.**, Berg D., Berg U., Mayerhofer A., and Kunz L. Identification and characterization of Ca<sup>2+</sup> activated K<sup>+</sup> channels in granulosa cells of the human ovary. *Reproductive Biology and Endocrinology* 2009 Apr 8;7:28.
- 2010** Enes J., Langwieser N., Ruschel J., Carballosa-Gonzalez M.M., Klug A., **Traut M.H.**, Ylera B., Tahirovic S., Hofmann F., Stein, V., Moosmang S., Hentall I.D., Bradke F. Electrical activity suppresses axon growth through Cav1.2 channels in adult primary sensory neurons. *Current Biology* 2010 Jul 13; 20(13):1154-1164.